Ref. TH.2072-CERN

DIFFRACTIVE PROCESSES AND THE TRIPLE-POMERON

Hannu I. Miettinen*)

CERN, Geneva, Switzerland

Plenary Session Talk at the
EPS International Conference on High Energy Physics
Palermo, 23-28 June 1975

*) Herman Rosenberg Foundation Fellow. On leave from the Research Institute for Theoretical Physics, University of Helsinki, Finland. Address after 15 August 1975: Stanford Linear Accelerator Center, PO Box 4349, Stanford, California 94305, USA.

Ref. TH.2072
29 August 1975

DIFFRACTIVE PROCESSES AND THE TRIPLE-POMERON

Hannu I. Miettinen*)
CERN, Geneva, Switzerland.

1. INTRODUCTION

Nearly one hundred papers on inelastic diffraction were submitted to this Conference. They represent a wealth of new information and contain many important results. Having such a large amount of material to review I have decided to concentrate on the developments which are entirely new**). Very important but less exciting "bread and butter" results are discussed more briefly. My approach to the subject will be very phenomenological. The more theoretical aspects of diffraction scattering are covered by the talks of B.R. Webber[5], N. Sakai[6] and A. Schwimmer[7].

The material of this my report will be organized as follows:

We begin by briefly discussing in Section 2 the s-channel unitarity relation between diffraction scattering and particle production processes. This provides us with a phenomenological framework in which to organize and interpret the experimental results.

The third section is devoted to a discussion of the production and the decay properties of diffractively excited low-mass systems.

In the past year there has been much progress in the phenomenological understanding of the "absorption" or "rescattering" effects present in inelastic diffraction. This subject is reviewed in Section 4.

The fifth section presents a brief summary of the most recent experimental results on the excitation of large masses and of their phenomenological interpretation.

The sixth section is devoted to a discussion of two rare types of diffractive processes on which new and exciting results are reported at this Conference, namely, double diffractive excitation and double Pomeron exchange processes.

Finally, an attempt is made to suggest some promising directions for future research.

2. THE SHADOW APPROACH

The words "shadow approach" mean the familiar idea that diffraction scattering is the shadow of absorption due to the existence, at high energies, of many open inelastic channels. This idea is illustrated in Fig. 1.

The incoming beam is described by a unit matrix (S = 1) and the effect of the target by a transition matrix T (S = iT). When the target is placed in the beam the incoming and

---

*) Herman Rosenberg Foundation Fellow. On leave from the Research Institute for Theoretical Physics, University of Helsinki, Finland. Address after the 15 August, 1975: Stanford Linear Accelerator Center, P.O. Box 4349, Stanford, California 94305, USA.

**) The reader who wishes to get a more complete view on the subject should refer to the review articles by Leith[1], Mukhin and Tsarev[2], Azimov et al.[3], and Goggi[4].

SHADOW NATURE OF DIFFRACTION

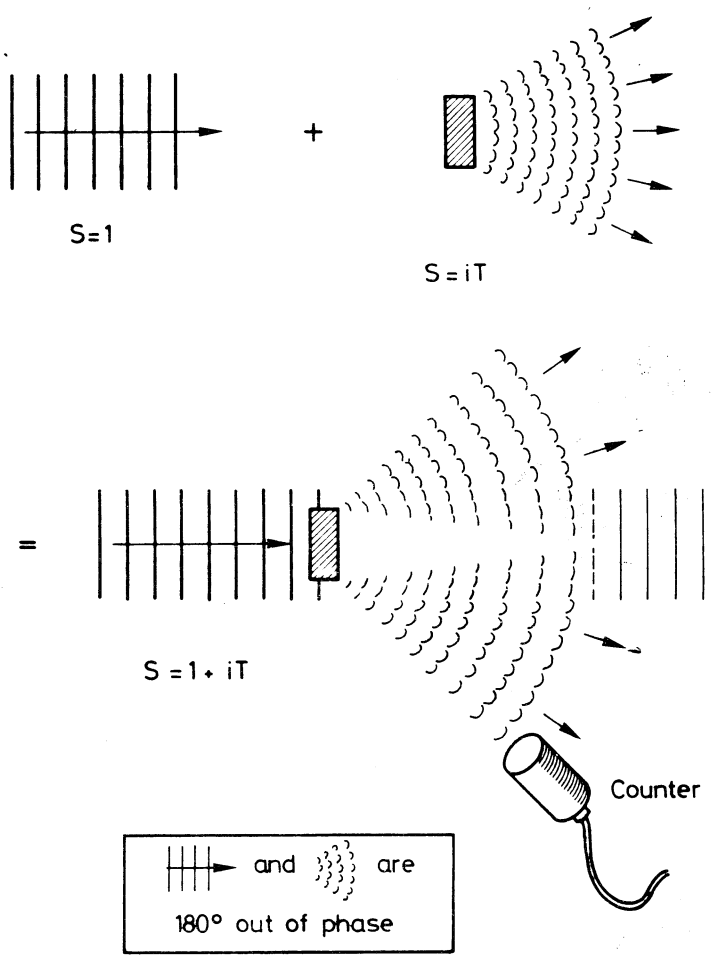

Fig. 1 Illustration of the optical picture of diffraction scattering

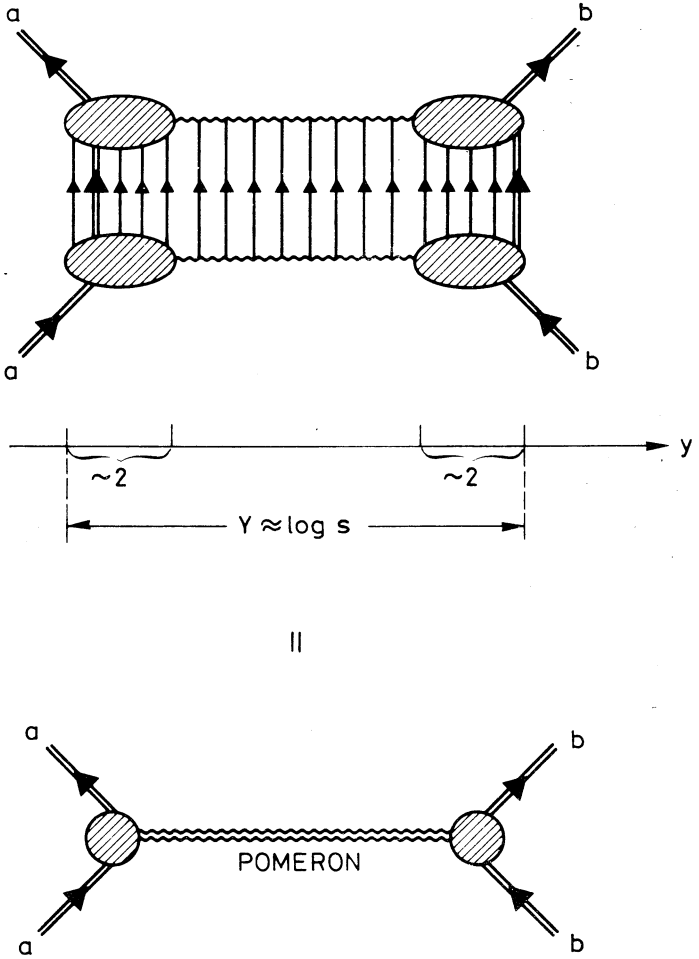

Fig. 2 Illustration of the s-channel unitarity equation for elastic scattering

the scattered waves interfere destructively, producing a "shadow" behind the target. A counter which is placed out of the beam line catches, however, only the scattered wave. One sees immediately that a very "black" (= dense) target gives rise to a strong diffracted wave. A simple analysis shows that the angular distribution of the diffracted wave reflects the size and the shape of the target. A small target gives rise to a flat angular distribution, whereas a large target produces an angular distribution which is strongly concentrated near to the forward direction. A target which has sharp edges gives rise to a rapidly oscillating angular distribution with several minima and maxima ("diffraction pattern").

The above phenomenon, diffraction of matter waves, is closely analogous to that of diffraction of light. It is maybe the most striking manifestation of the wave nature of matter.

2.1 s-channel unitarity

The above optical ideas may be formulated quantitatively in terms of the s-channel unitarity equation[8-10]. It reads:

$$\mathrm{Im}\,\langle f|T|i\rangle = \sum_n \langle f|T^+|n\rangle\,\langle n|T|i\rangle \ . \qquad (2.1)$$

Here, $|i\rangle$ and $|f\rangle$ are the state vectors of the initial and final elastic states, respectively. The equation (2.1) is illustrated below:

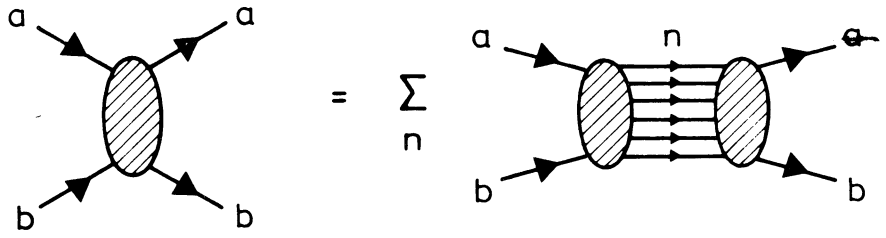

Let me now discuss this equation in some detail, in order to emphasize the similarity of the dynamics that governs elastic scattering and the inelastic diffractive processes which are the subject of this talk.

I shall draw the above unitarity equation "sideways" and place a rapidity scale on the multiparticle side of it. The result is shown in Fig. 2.

In the multiparticle production process, the internal quantum numbers of the incoming beam particle a are carried out by particles whose momenta lie in the "beam fragmentation region", i.e. within approximately two units of rapidity from the left end of the longitudinal phase space. We see from Fig. 2 that the coupling of the Pomeron to the external particle a is built up by the overlap of the particles produced in this region*):

*) For a detailed analysis of how this happens, see the recent article by Białas and Sakai[11].

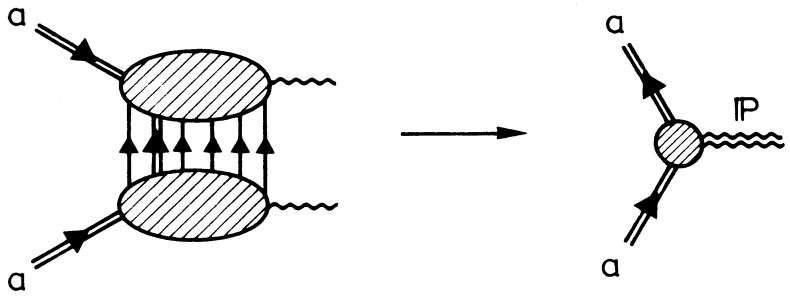

The Pomeranchuk singularity itself is built up by the overlap of the momenta of the particles produced in the central region:

One of the past years' most important discoveries in hadron physics has been the observation that the correlations between the particles produced in the central region are dominantly of a *short-range nature*[*]. The two-particle correlation function defined as

$$C(y_c,y_d) = \rho(y_c,y_d) - \rho(y_c)\,\rho(y_d)\ , \tag{2.2}$$

[$\rho(y_c,y_d)$ and $\rho(y_c)$, $\rho(y_d)$ are the normalized two- and single-particle densities, respectively] is observed to decrease rapidly when the rapidity difference $\Delta y = |y_c - y_d|$ becomes large. A simple parametrization

$$C(y_c,y_d) \sim e^{-1/\lambda|y_c-y_d|} \qquad (|y_c-y_d| \text{ large}) \tag{2.3}$$

fits the data well. The empirical estimates for the correlation length λ vary between 0.7 and two units of rapidity[**].

A well-known result is that any particle production mechanism in which the correlations are of a short-range nature only, gives rise to a Pomeranchuk singularity which is a *simple Regge pole*. Thus the experimental observation that the multiparticle correlations within the central region are dominantly of a short-range nature provides evidence that *the Pomeron singularity is, in the zeroth-order approximation, a simple J-plane pole*. The approximate pole nature of the Pomeranchuk singularity is supported also by the empirical evidence that the diffractive amplitudes factorize[1,4] and by phenomenological analyses of the elastic scattering data[15].

---

*) For the most recent evidence, see the reviews of R. Baier[12] and N. McCubbin[13] in these Proceedings.

**) More complicated correlation functions may indicate long-range effects. In particular, the question of the rapidity dependence of the azimuthal correlations is unsettled[14].

In the past year, an ambitious program has been initiated to derive the properties of the Pomeron pole [the intercept $\alpha(0)$, the slope α', and the couplings] from those of the multiparticle distributions [single-particle densities $\rho_i(y)$, correlation length λ, etc.] in a *model-independent way*[16]. The progress achieved in this very difficult problem is reviewed by Dr. Webber[5]. The unitarity relation has been studied within the framework of specific models by many authors. The results obtained within the multiperipheral and the dual model frameworks are reviewed by B.R. Webber[5] and N. Sakai[6], respectively.

2.2 Inelastic diffraction

Let us now apply the above ideas to the study of the inelastic diffractive processes. We may write a unitarity equation analogous to Eq. (2.1):

$$\mathrm{Im}\,\langle d|T|i\rangle = \sum_n \langle d|T^+|n\rangle\langle n|T|i\rangle \ . \tag{2.4}$$

Here, as previously, $|i\rangle$ is the incoming inelastic state. The state $|d\rangle \equiv |Db\rangle$ is an inelastic diffractive state characterized by a rapidity distribution of the following type*):

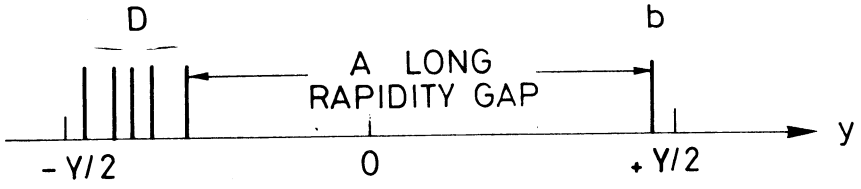

The "off-diagonal" unitarity equation (2.4) is illustrated below:

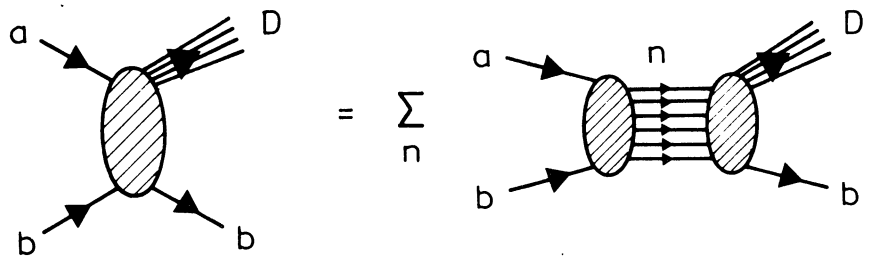

To analyse the contents of this equation let me proceed as previously. I turn it "sideways" and place a rapidity scale on the multiparticle side of it. The result is shown in Fig. 3.

From this figure we immediately see two results:

Firstly, the assumption that the multiparticle correlations are of a short-range nature implies that the particles produced in the central region do not "know" what happens in the

*) In double diffraction dissociation, both the incoming particles dissociate. The produced clusters are separated by a long rapidity gap.

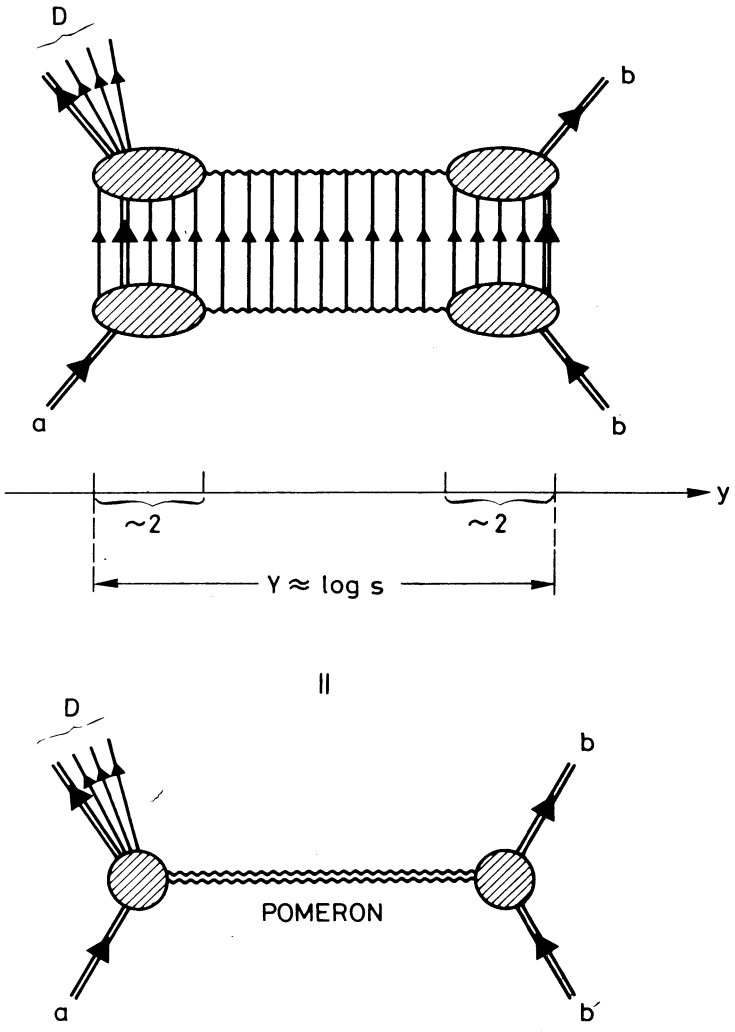

Fig. 3 Illustration of the s-channel unitarity equation for diffraction dissociation

two fragmentation regions. Consequently, the singularity built up by the overlap of the central region particles is the same factorizable J-plane pole that was built up in the elastic scattering.

Secondly, the inelastic aPD vertex is built up by the overlap of the two fragmentation distributions X_f and X_f' produced in

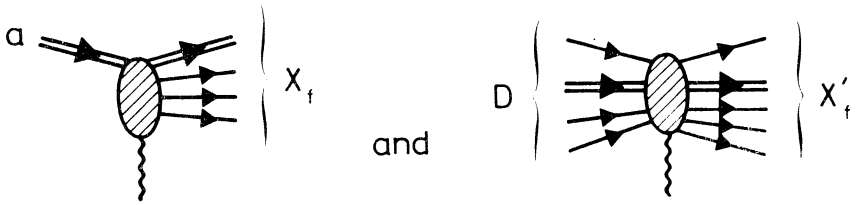

When the system D is very similar to the particle a (such as a low-mass resonance with the same quantum numbers as the particle a) one may expect the two fragmentation region distributions X_f and X_f' to be rather similar and to overlap well. A system D which is very different from the hadron a (such as a system of a mass of 10 GeV and consisting of 7 particles, say), on the other hand, is expected to produce a fragmentation region distribution which is very different from that produced by the particle a. Consequently, for such a system one may expect the aPD coupling to be very small.

The above problem of the m_D dependence of the aPD vertex may be analysed quantitatively using the triple-Regge theory. The result is that the strength of the coupling decreases as an *inverse power* of the mass m_D:

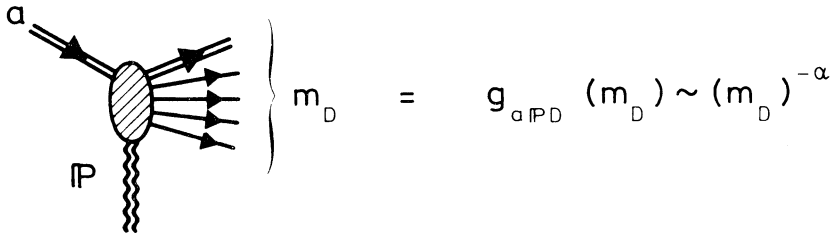

The power α varies between 0.5 and 1.5 depending on the t-value of the collision and the m_D range under study.

2.3 Absorptive corrections

The pole picture of the Pomeron is expected to be approximate only. On very general grounds, one may expect "absorption" or "rescattering" effects to be present and to provide corrections to the pole amplitude. At present, no reliable theory for evaluating their contributions exists, and even their phenomenological understanding is rather vague.

A simple model for calculating the rescattering effects in elastic scattering is provided by the eikonal formula:

$$T_{el}(s,b) = 1 - e^{-\Omega(s,b)} = \Omega(s,b) - \frac{1}{2!}\Omega^2(s,b) + \ldots \qquad (2.6)$$

Here, the amplitude $T_{el}(s,b)$ and the eikonal $\Omega(s,b)$ are written in the impact parameter representation. One may assume the eikonal to be a Regge pole. The rescattering contributions $-\frac{1}{2}\Omega^2(s,b) + \ldots$ then give rise to Regge cuts. They break factorization and modify the energy dependence of the pole amplitude.

The above eikonal expansion has a particularly simple interpretation in the geometrical picture of hadron collisions[17]. The eikonal $\Omega(s,b)$ represents the sum of the elementary probabilities of the constituents of the left-moving hadron to hit those of the right-moving one. If many hits occur in each collision, this term may clearly exceed the unitarity limit. Unitarity is then restored by the rest of the expansion. The physical interpretation of the correction terms is that they represent the effect of the shielding of the back part of the hadron by its front part. This shielding effect is completely analogous to that of the Glauber model description of hadron-nucleus scattering.

A serious drawback of the eikonal formula Eq. (2.6) is that it clearly ignores the existence of diffraction dissociation. It may well happen, however, that the colliding hadrons dissociate in the first scattering and recombine in the second one. Contributions of this type should also be considered, and they may well turn out to be important.

Figure 4 illustrates some of the lowest-order rescattering contributions to elastic and inelastic diffraction. These and other more complicated absorption effects are discussed in Section 4.

We close this section by summarizing the main problems of diffraction scattering, when analysed in the shadow approach:

a) What is the "driving force" amplitude?
b) What are the couplings?
c) What are the absorption corrections?

These three problems are illustrated in Fig. 5.

3. LOW-MASS EXCITATION

3.1 Diffraction dissociation; general features

Let us now turn to a discussion of the new results on exclusive diffraction dissociation processes. The channels that have been studied in most detail are

$$\pi N \to (3\pi)N \tag{3.1a}$$

$$KN \to (K\pi\pi)N \tag{3.1b}$$

$$\left.\begin{aligned} NA &\to (N\pi)A \\ NA &\to (N\pi\pi)A \end{aligned}\right\} A = \pi,\ K,\ N. \tag{3.1c, 3.1d}$$

These processes share many common properties with elastic scattering. Let us list the most important ones, illustrating them by new data.

3.1.1 Weak energy dependence

In the low-energy range ($p_{lab} \leq 30$ GeV/c), the elastic cross-sections decrease slowly with increasing energy. Above 50 GeV/c, they become approximately constant. The elastic proton-proton scattering cross-section rises by $\approx 10\%$ over the ISR energy range.

The cross-sections of the inelastic processes (3.1) show energy dependence very similar to that of elastic scattering. For laboratory momenta below 30 GeV/c, they decrease slowly with increasing momentum. The new data presented at this Conference show that the cross-sections of the processes (3.1c) and (3.1d) are flattening out at the Fermilab energies and maybe even rising at the ISR.

ABSORPTION CORRECTIONS

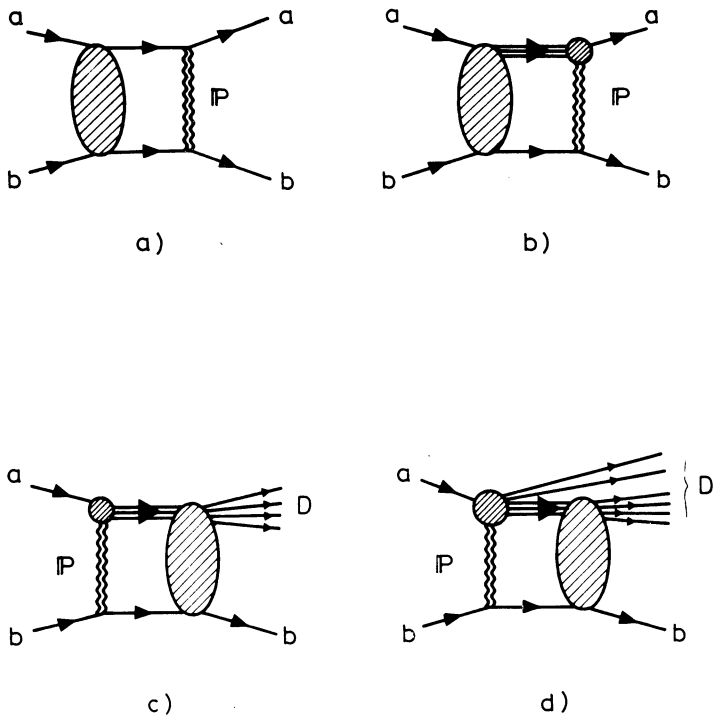

Fig. 4 First-order absorptive corrections to the "driving force" Pomeron P. a) Elastic and b) inelastic initial-state absorptive corrections to elastic scattering; c) and d) Inelastic final-state absorptive corrections to diffraction dissociation.

3 POMERON PROBLEMS :

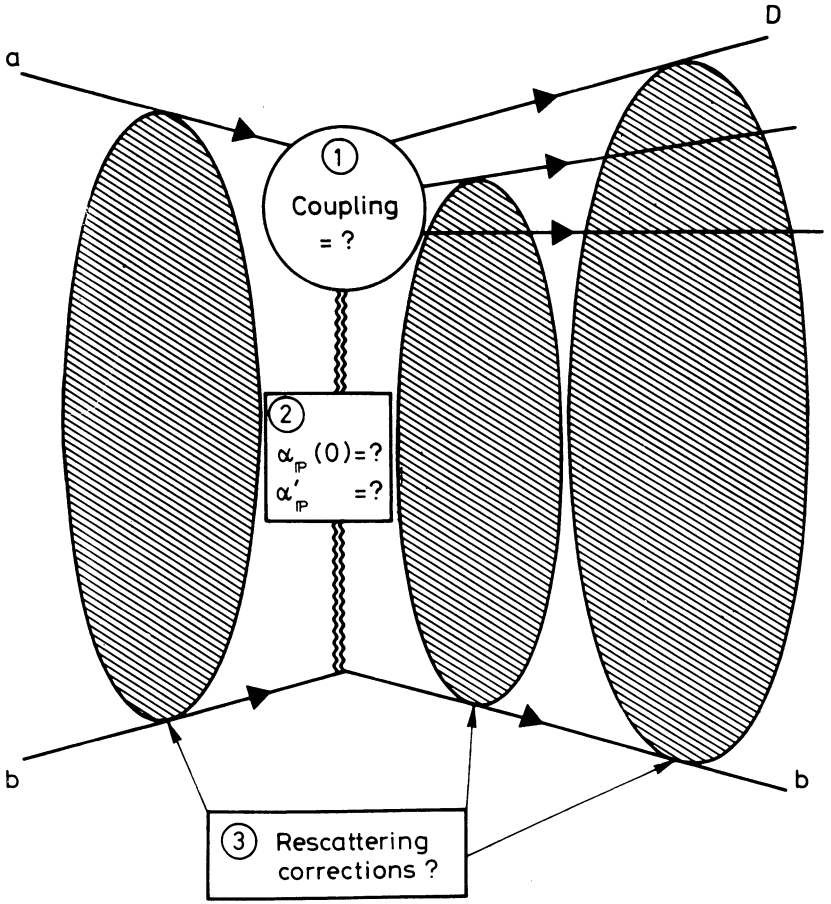

Fig. 5 An illustration of the central problems of diffraction scattering, when analysed in the shadow approach

Figure 6 shows Fermilab data on the neutron dissociation process $np \to (p\pi^-)p$, coming from the FNAL-Northwestern-Rochester-SLAC Collaboration experiment[18]. No energy dependence is visible for energies between 50 and 300 GeV/c.

In Fig. 7, cross-sections are shown for the processes $pp \to p(p\pi^+\pi^-)$, $pp \to p'"N^*(1520)"$, and $pp \to p'"N^*(1688)"$ as a function of incident laboratory momentum[19)*]. It is seen that, for the $N^*(1520)$ and $N^*(1688)$ production, an extrapolation of the $p_{lab} < 30$ GeV/c data badly undershoots the new ISR points. This shows that the cross-sections are flattening out or maybe even rising.

The over-all conclusion to be drawn from the present data is that the energy dependence of low-mass diffraction dissociation is approximately similar to that of elastic scattering[**].

3.1.2 Peripherality of $d\sigma/dt$ and the "mass-slope correlation"

The differential cross-sections of both the elastic and the inelastic diffractive processes are steeply peripheral. They may be roughly described by exponential parametrizations:

$$\frac{d\sigma}{dt} = \frac{d\sigma}{dt}\Big|_{t=0} e^{bt} .$$

In the elastic scattering processes, the logarithmic slope b varies between 8 and 12 $(GeV/c)^{-2}$, depending on the process and on the s- and t-ranges under study. For an up-to-date compilation of data and discussions, see A. Wetherell's talk[22].

In the diffraction dissociation processes, the slope of the differential cross-section varies strongly with the mass of the excited system, being large near the threshold and decreasing rapidly with increasing mass. Figure 9 shows data on this "mass-slope correlation" in the process $np \to (p\pi^-)p$. The data come from the FNAL-Northwestern-Rochester-SLAC Collaboration experiment[18]. The effect is seen to be very strong. At the lowest masses the slope is nearly twice as large as that of elastic proton-proton scattering. At masses 300-400 MeV above the $(p\pi^-)$ threshold it has decreased to a level of approximately half of the elastic slope.

The mass-slope correlation is a general property of all diffraction dissociation processes. Its physics is not fully understood. The old explanation in terms of the pion exchange Deck effect[23] has been known for some time to be inadequate[24]. Some more recent ideas based on the impact parameter picture are discussed in Section 4.

---

*) In this ISR experiment, the nucleon resonance excitation cross-sections were extracted from the data by fitting the mass spectra with a formula describing two Breit-Wigner resonances plus a polynomial background. The fits are shown in Fig. 8. No attempt was made to evaluate if the peaks seen in the mass spectra around 1500 and 1700 MeV really correspond to the $3/2^-(1520)$ and $5/2^+(1688)$ baryon resonances, as the notation used in Ref. 19 and above would indicate.

**) The only evidence against this result comes from the ISR Split-Field Magnet experiment carried out by the CHOV Collaboration[20]. Their cross-section for the process $pp \to p(n\pi^+)$ presented a year ago at the London Conference seems to be very low. The CHOV data are still unpublished and they may have some normalization problems[21]. It seems to me to be best not to draw from these preliminary data any conclusions which are sensitive to the over-all normalization of the data but to wait for the final results of the experiment.

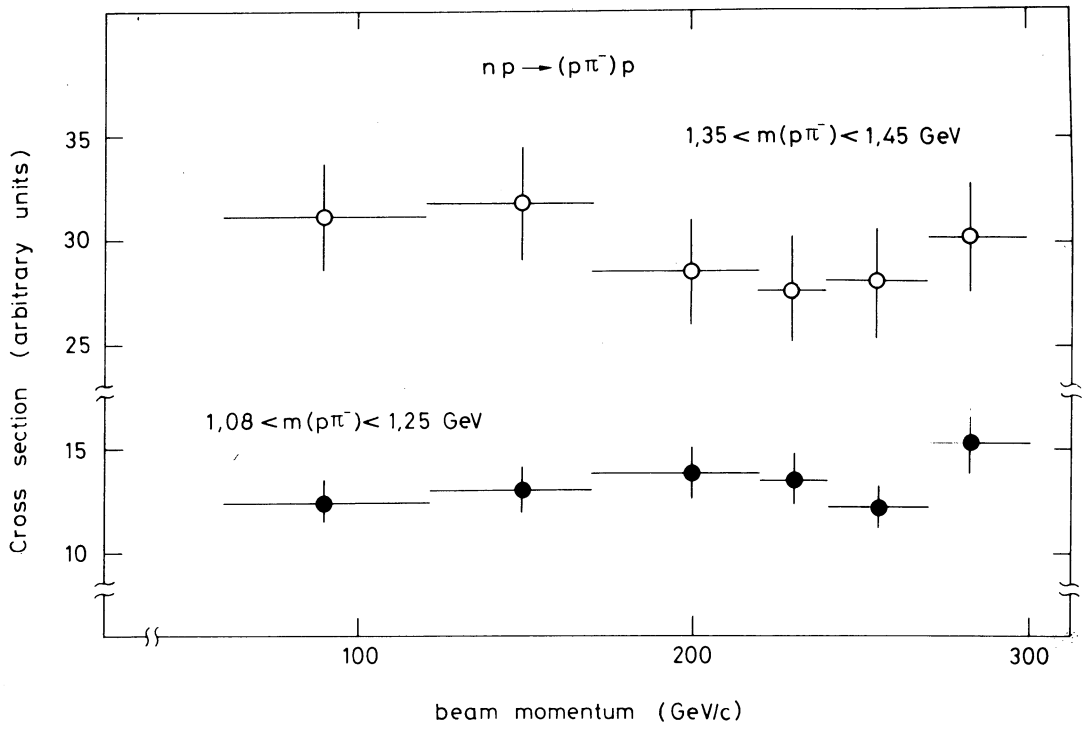

Fig. 6 Energy dependence of the cross-section for neutron dissociation off a hydrogen target. The data have been integrated over t (from Ref. 18).

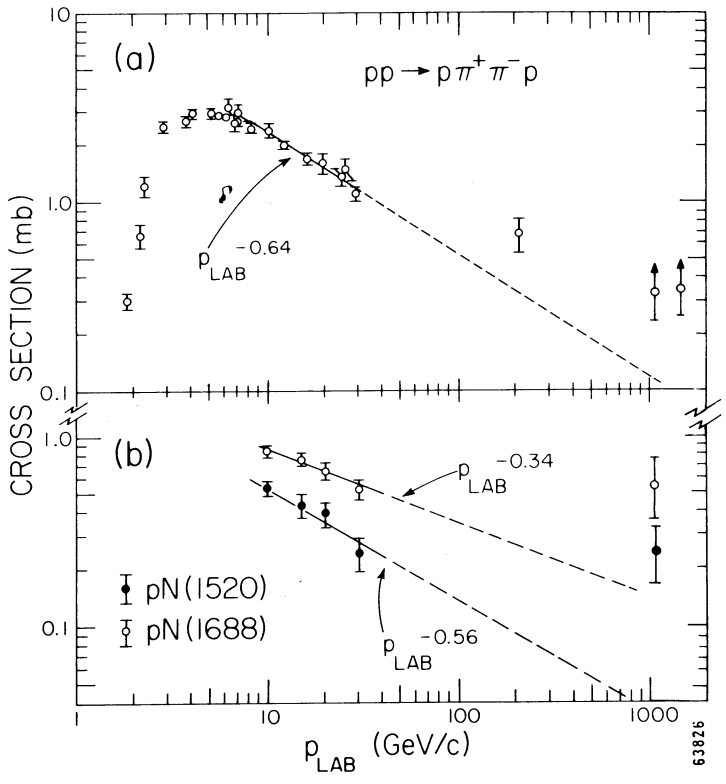

Fig. 7 Cross-sections for a) $pp \to pp\pi^+\pi^-$ and b) $pp \to p"N^*(1520)"$, $p"N^*(1688)"$ as a function of incident laboratory momentum. The points at p_{lab} = 1000 and 1500 GeV/c in (a) are lower limits for $\sigma(pp \to pp\pi^+\pi^-)$ (from Ref. 19).

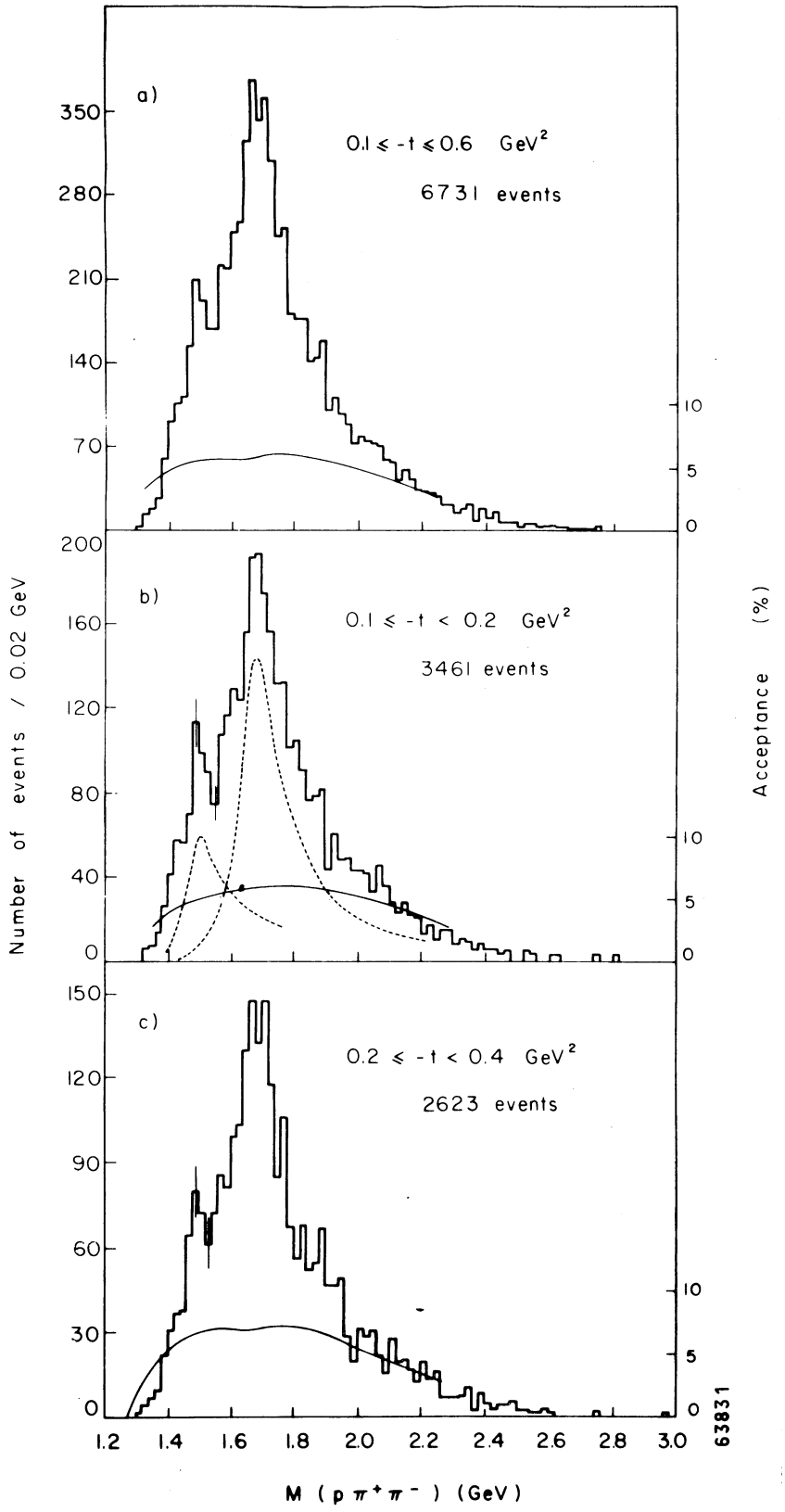

Fig. 8 Experimental distribution in $m(p\pi^+\pi^-)$ for the process $pp \to p(p\pi^+\pi^-)$ at $\sqrt{s}$ = 45 GeV for: a) $0.1 \leq -t \leq 0.6$ GeV^2; b) $0.1 \leq -t \leq 0.2$ GeV^2; c) $0.2 \leq -t \leq 0.4$ GeV^2. The smooth curves are the corresponding acceptances. The broken curves in (b) show the contributions of "N*(1520)" and "N*(1688)" (from Ref. 19).

3.1.3 Shrinkage

The differential cross-sections of both the elastic and the inelastic diffractive processes shrink. The speed of this shrinkage may be described in terms of an "effective" Pomeranchuk trajectory as follows:

$$\left.\frac{d\sigma}{dt}\right|_{s=s_2} = \left.\frac{d\sigma}{dt}\right|_{s=s_1} \left(\frac{s_2}{s_1}\right)^{2\alpha_p(t)-2} .$$

One may extract the trajectory function $\alpha_p(t)$ directly from the data by comparing data at two (or more) energies. In Refs. 25 and 26 the trajectory function has been evaluated from the proton-proton elastic scattering data. In the small-t range, the result may be parametrized by the linear formula $\alpha_p(t) = 1.05 + 0.27\ t$.

The data of the inelastic diffractive processes are much less accurate than those of elastic scattering. While it is clear that the inelastic data shrink too, it is rather difficult to quantitatively evaluate the speed of this shrinkage. A comparison between the slopes of the process $pp \to p(n\pi^+)$ at 24 GeV/c [27] and 1500 GeV/c [20] is shown in Fig. 10. The speed of shrinkage is seen to be roughly the same as in elastic scattering. There may be some indications in the data that the speed of shrinkage depends on the mass of the $n\pi^+$ system. It may be, however, that this effect is caused by the disappearance of the meson exchange contributions which should be present at 24 GeV/c, particularly in the mass region above 1.6 GeV/c.

3.1.4 Vacuum quantum number exchange in the t-channel

The best evidence for the vacuum quantum number (I = 0, C = +1) assignment to the Pomeranchuk singularity is provided by the elastic scattering data. By combining the data using different beams we may extract the cross-sections corresponding to t-channel exchanges with I = 1 and/or C = -1. These cross-sections are seen to decrease as a power of the incident momentum [see Wetherell's talk[22]]. This energy dependence may be contrasted with the approximately constant or rising s-dependence of the I = 0, C = +1 contributions.

While there exists no experimental evidence for a C = -1 component of the Pomeranchuk amplitude, the data do not rule out the possibility that such a component of the size of a few percent of that of the C = +1 component existed. It would be useful to push the experimental upper limit for it further down. The other possibility, namely that such a component were found, would obviously be even more interesting.

In the diffraction dissociation processes, isospin analyses have been carried out by several groups[28]. These analyses allow us to separate the contributions corresponding to the I = 0 and I = +1 t-channel exchanges. The results are in good agreement with the I = 0 assignment of the Pomeranchuk amplitude.

3.1.5 SU(3) nature of the Pomeron

That the difference between the πp and Kp total cross-sections persists at Fermilab energies clearly shows that the Pomeranchuk amplitude has sizeable SU(3) non-singlet contributions. Diffraction dissociation data indicate a similar breaking of the inelastic Pomeranchukon couplings[29].

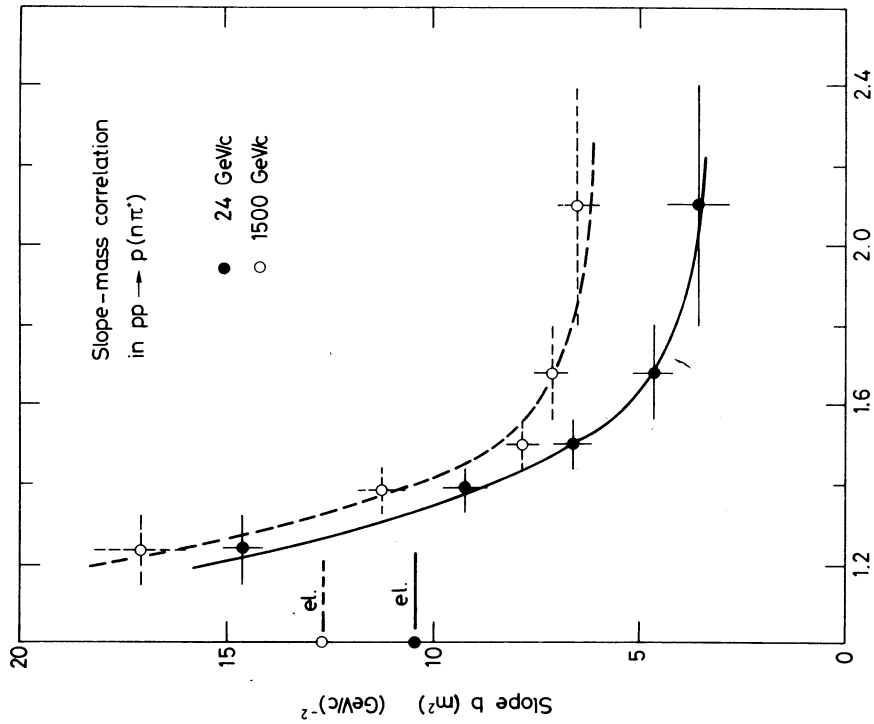

Fig. 10 Variation of the slope parameter b as a function of the invariant mass $m(n\pi^+)$ determined from the 24 GeV/c (Ref. 27) and 1500 GeV/c (Ref. 20) data of the process $pp \to p(n\pi^+)$.

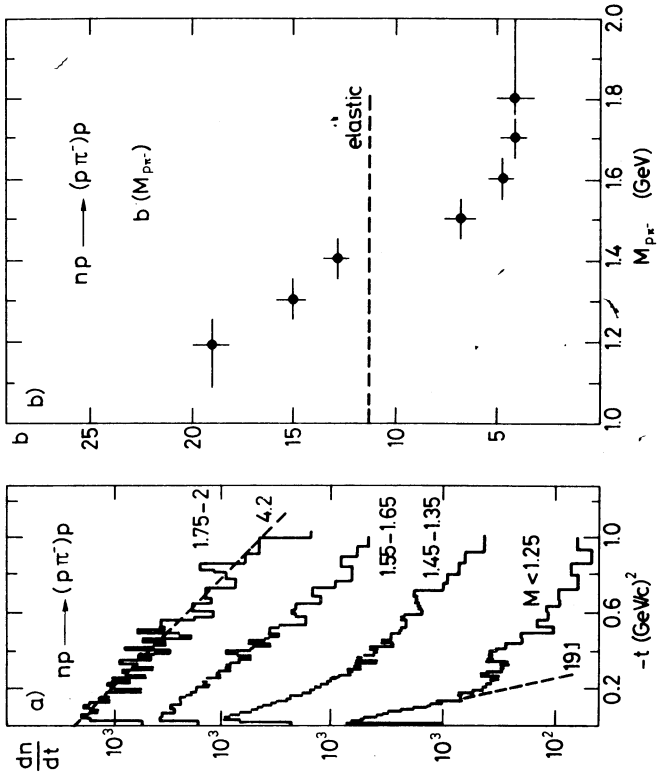

Fig. 9 a) Momentum transfer distributions for various ranges of $(p\pi^-)$ mass, for the reaction $np \to (p\pi^-)p$ at 50-300 GeV/c.
b) Variation of the slope parameter as a function of the invariant mass $m(p\pi^-)$ (from Ref. 18).

A very elegant explanation for the SU(3) breaking of the Pomeron couplings is provided by the "tensor-dominance" scheme of Carlitz, Green and Zee[30]. In this scheme, the breaking of the couplings is directly related to the SU(3) mass-breaking effects. For a summary of some recent applications and tests of this scheme, see the talk of T. Inami[31].

Another scheme has been suggested by Pumplin and Kane[32]. These authors study the contribution of the two-particle cut in the t-channel to the Pomeranchukon amplitude. They show that the two-pion cut provides a large contribution to the total cross-section (typically about 1/4 of σ_{tot}) but its "heavier" SU(3) analogs (the $K\bar{K}$-cut, etc.) are kinematically suppressed. This gives rise to an SU(3) non-singlet component of the Pomeron.

The Pumplin-Kane scheme is similar to the tensor dominance model in the respect that also in it the breaking of the Pomeron couplings is caused by the SU(3) mass-breaking effects. The two schemes differ, however, in their quantitative predictions.

Let us close this section by concluding that, independently of any theoretical considerations, the above results provide strong evidence for the elastic and inelastic diffraction being governed by the same dynamics.

3.2 Mass dependence and spin structure

3.2.1 Low-mass structures in meson dissociation

The mass spectra of the dissociation processes (3.1a) to (3.1d) show all very similar behaviour. They rise rapidly from threshold*), reach a maximum about 250 MeV above the threshold and fall steeply off towards zero. In the peak region, structures are visible. They are caused by resonances and/or by the opening up of new decay channels.

The similarity between pion and kaon dissociation has been known for several years. The (3π) mass spectra of the process (3.1a) shows three major structures: the A_1, A_2, and A_3 peaks. The corresponding structures in the $(K\pi\pi)$ spectra of the process (3.1b) are the Q, $K^*(1420)$, and L peaks. The main properties of these peaks are:

Transition	Peak	Mass (GeV)	J^P	Dominant decay channel
$\pi \to (\pi\pi\pi)$	A_1	1150	1^+	$\rho\pi$
	A_2	1310	2^+	$\rho\pi$
	A_3	1640	2^-	$f\pi$
$K \to (K\pi\pi)$	Q	$\sim$ 1300	1^+	$K^*(890)\pi$
	$K^*(1420)$	1420	2^+	$K^*(890)\pi$
	L	1770	2^-	$K^*(1420)\pi$

The A_2 and the $K^*(1420)$ are "bona fide" resonances whose resonance status is unquestionable. A comparison of the results of the partial-wave analyses carried out at several energies shows that, at high energies, the A_2 meson is diffractively produced[33,34]. The reason

*) By threshold we mean here that of the dominant decay mode.

for the diffractive contribution to its production being much smaller than that to A_1 or A_3 production is that A_2 has the "wrong" parity: a natural parity state produced via natural parity exchange is necessarily produced in a helicity flip state[35] and therefore strongly suppressed in the forward direction.

Since the A_2 meson is diffractively produced, one obviously expects its SU(3) partner, the $K^*(1420)$ meson, to be, too. The data are still inconclusive regarding this question.

It has become clear that the A_1, A_3, Q, and L peaks are not simple, well-defined Breit-Wigner resonances but much more complicated objects. The data do not rule out the possibility, however, that part of these peaks would be due to normal resonances[36]. A popular non-resonant explanation for these peaks is provided by the Deck model[37,38].

The ABBCHLV Collaboration[29] has carried out a detailed comparison between the reactions (3.1a), (3.1b) and their much less studied $K\bar{K}$ production analogs:

$$\pi N \to (\pi K\bar{K})N \tag{3.2a}$$

$$\bar{K}N \to (\bar{K}K\bar{K})N \ . \tag{3.2b}$$

It is interesting to compare the relative magnitudes of the cross-sections of the above four processes to each other and to the elastic cross-sections. At 16 GeV/c, the following cross-section ratios are obtained:

$$\sigma_{\pi^+p}(\text{elastic}):\ \sigma_{(\pi^+\pi^+\pi^-)p}:\ \sigma_{(\pi^+K^+K^-)p} = 100:\ (12.4 \pm 1.4):\ (0.69 \pm 0.09) \tag{3.3}$$

$$\sigma_{K^-p}(\text{elastic}):\ \sigma_{(K^-\pi^+\pi^-)p}:\ \sigma_{(K^-K^+K^-)p} = 100:\ (12.6 \pm 1.5):\ (0.52 \pm 0.09) \tag{3.4}$$

Here, the cross-sections for the three-meson production channels were obtained by applying a cut in the three-meson kinetic energy ($Q_{\text{eff}} \leq 1$ GeV).

From the above results we see that

i) at 16 GeV/c, the pion pair production in the dissociation of the incoming meson ($M \to M\pi\pi$) is about 20 times more probable than kaon pair production ($M \to M\bar{K}K$) and about 8 times less likely than elastic scattering, $M \to M$;

ii) the close similarity between Eqs. (3.3) and (3.4) suggests that the dependence of the three-meson cross-sections on the beam-like meson in the final state may be factorizable, even though this meson is produced in a low-mass three-meson cluster.

The mass spectra of the above four reactions are compared in Fig. 11. Their similarity is seen to be rather striking.

The results concerning the cross-section ratios and the mass spectra are only two particular examples of those obtained in the study of Ref. 29. Many other properties of the dissociated systems were also compared. The results obtained are summarized by P. Schmid[39].

The similarity between the pion and kaon dissociation processes is not unexpected, since the pion and the kaon belong to the same SU(3) multiplet. There exists, however, a more general argument which suggests that not only should the pion and the kaon dissociation processes look alike, but that *all* hadron dissociation processes should be "semi-locally" similar to each other. This argument, which has been called "semi-local" factorization, follows

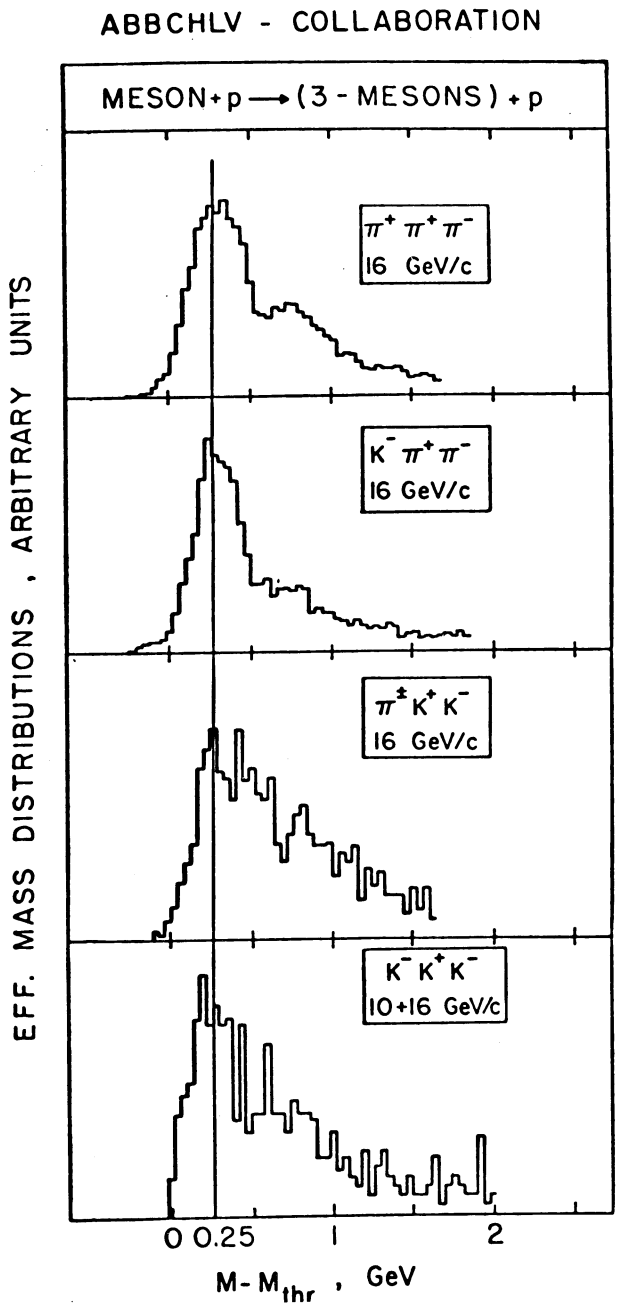

Fig. 11 Effective mass distributions (with arbitrary normalization) for the processes meson + proton → (3 mesons) + proton (from Ref. 29).

from combining factorization with Dolen-Horn-Schmid type semi-local duality[40]. The idea is illustrated in Fig. 12.

Semi-local factorization has been successfully checked so far in diffraction dissociation and in non-diffractive kaon and pion excitation processes[41]. Figure 13 shows one of the tests. It would be very interesting to carry out more detailed comparisons between the meson dissociation processes and the baryon excitation reactions $N \to (N\pi)$ and $N \to (N\pi\pi)$.

3.2.2 Spin structure

The spin and helicity structure of diffraction dissociation has attracted much interest in the past few years. An important boost to this research has been given by the development of a partial-wave analysis program ("Ascoli" program) at the University of Illinois[42,43]. To the eyes of a layman this program appears as follows:

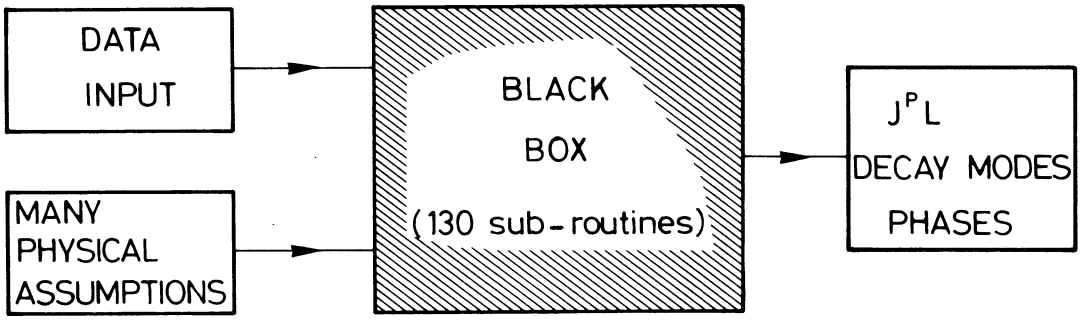

By this sketch I by no means want to belittle the importance of the PWA programs. I fully agree with the opinion which Dr. French expressed in his talk[44] that the development of the PWA programs has been a major contribution to the study of quasi two-body production processes. The reason for drawing the above sketch is that I wish to emphasize that the Ascoli program is a very sophisticated piece of machinery which uses as its input many physical assumptions. Experience has shown that while the main features of the output (such as the dominant partial waves) are relatively insensitive to the assumptions made, the "fine-structures" of the results may depend crucially on these assumptions. This should be kept in mind when drawing conclusions from the PWA results.

The spin structure of meson dissociation processes has been studied in eight papers contributed to this Conference[29,45-51]. Although these works contain much useful and detailed information, their results are in general in good agreement with those of the earlier studies. They rather confirm and sharpen the existing picture than bring qualitatively new features into it. For this reason I shall not discuss these papers in detail*) but focus my attention on three new results which, in my opinion, are particularly interesting.

The first of them concerns the total cross-sections of unstable meson systems on nucleons. The technique for extracting such cross-sections is well known[53]. One measures the coherent production cross-section of, for example, the following process

*) The partial-wave analysis results on meson dissociation are reviewed in detail in a forthcoming paper by A. Eskreys[52].

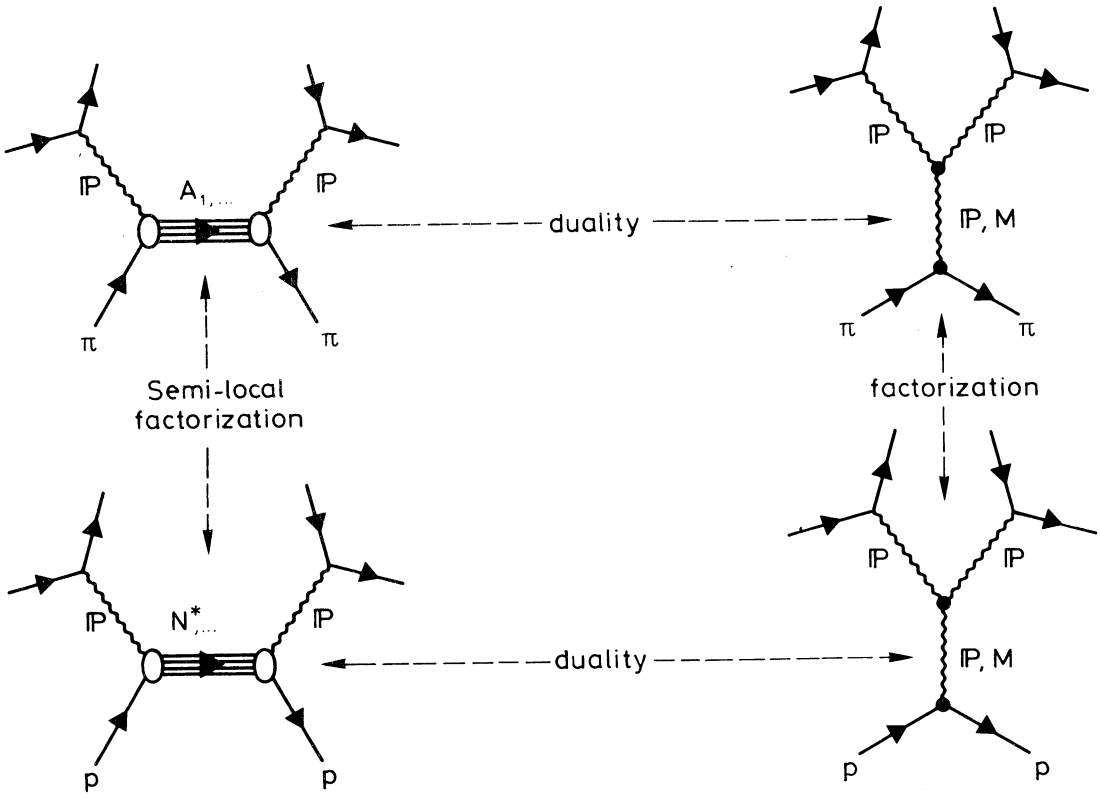

Fig. 12 The idea of "semi-local" factorization

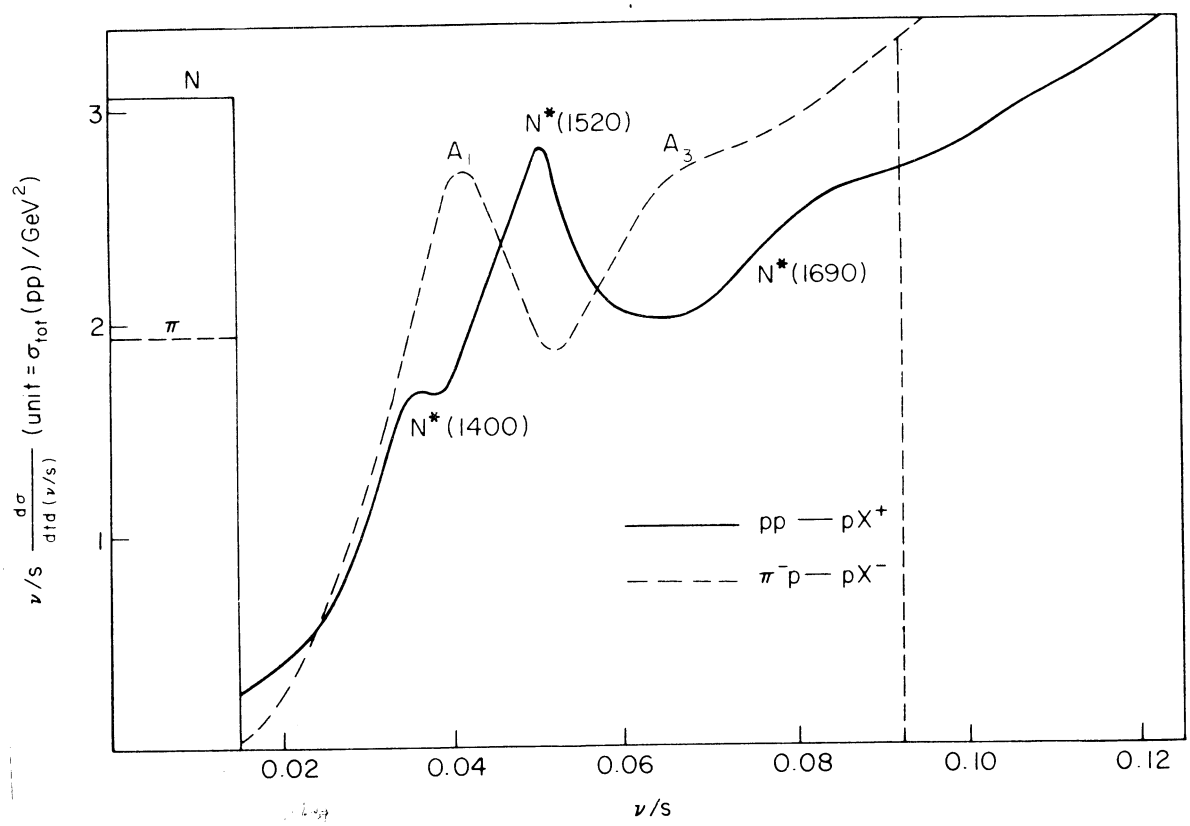

Fig. 13 First moments of cross-sections for $pp \to p + X$ and $\pi^- p \to p + X$ at 24-25 GeV/c and $t = -0.25$ GeV^2, divided by relevant total cross-sections. Dashed vertical line indicates region of equal areas formed by both curves (from Ref. 41).

$$\pi + A \to (\pi\pi\pi) + A \qquad (A = \text{nucleus}) ,$$

for several nuclei. The observed dependence of the cross-section on the atomic weight A of the target nuclei is then fitted by an optical model parametrization which has only one free parameter: the total cross-section of the unstable three-pion system on nucleons. This technique has been previously used to measure the total cross-sections of the low-mass 3π, 5π, $K\pi\pi$, $N\pi$, and $N\pi\pi$ systems on nucleons, with the surprising result that these cross-sections are of the same size as the corresponding particle-particle cross-sections[54]. This result provides very interesting information on the time evolution of the hadronic transitions. Apparently the rescattering in the nucleus happens so soon after the creation of the unstable system that this system has not yet had time to decay. It rather behaves as a "lump" of hadronic material of approximately the same spatial extension and opaqueness as those of the parent particle.

The new result comes from the CERN-ETH (Zurich)-Imperial College-Milano Collaboration experiment[55]. In this experiment, the production cross-section of the process $\pi^+ + A \to \pi^+\pi^-\pi^- + A$ at 15 GeV/c was measured for nine different nuclei ranging from beryllium (A = 8) to lead (A > 200). A partial-wave analysis of the produced 3π system was carried out, and the A-dependence of the cross-sections of the $J^P = 0^-$ and 1^+ states were studied. The result is shown in Fig. 14. By fitting these data by means of the Kölbig-Margolis optical model[53], the authors obtained the following total cross-sections:

$$\sigma_{tot}(\text{"}0^-\text{"}\ N) = 49^{+9}_{-7}\ \text{mb} , \tag{3.5}$$

$$\sigma_{tot}(\text{"}1^+\text{"}\ N) = 15.8^{+1.5}_{-1.3}\ \text{mb} , \tag{3.6}$$

We see that the total cross-section of the $J^P = 0^-$ three-pion state on nucleons is roughly *three times* as large as that of the $J^P = 1^+$ state. This result is totally unexpected and no theoretical explanation for it exists, as far as I know.

The second result to which I wish to draw your attention concerns the helicity conservation properties of diffraction dissociation[56].

It has been known for several years that the transitions $\pi \to (\pi\pi\pi)$ and $K \to (K\pi\pi)$ badly violate s-channel helicity conservation but approximately conserve helicity in the t-channel. Elastic scattering and vector meson photoproduction, on the other hand, conserve helicity in the s-channel in a good approximation. In the nucleon transition $N \to (N\pi)$ neither s- nor t-channel helicity is conserved.

This messy picture is further complicated by the new results, reported by the ABBCHLV Collaboration[45,57]. In Ref. 45, a partial-wave analysis was performed of the $(K\pi\pi)$ system produced in the process $K^-p \to (K^-\pi^-\pi^+)p$ at 10 and 16 GeV/c. In the Q-mass region it was found that the two dominant states, $K^*\pi$ and $K\rho$, both in 1^+S wave, were produced with different polarizations -- helicity being approximately conserved in the t-channel for $K^*\pi$ and in the s-channel for $K\rho$. The s-channel density matrix element $\rho_{00}^{(s)}$ of the $K\rho$ state was measured to have the value $\rho_{00}^{(s)} = 0.95 \pm 0.10$. This result shows that s-channel helicity-conserving inelastic diffractive processes do exist (vector meson photoproduction should probably be classified rather as elastic than as inelastic scattering) and, also, that the Q enhancement is a composite object.

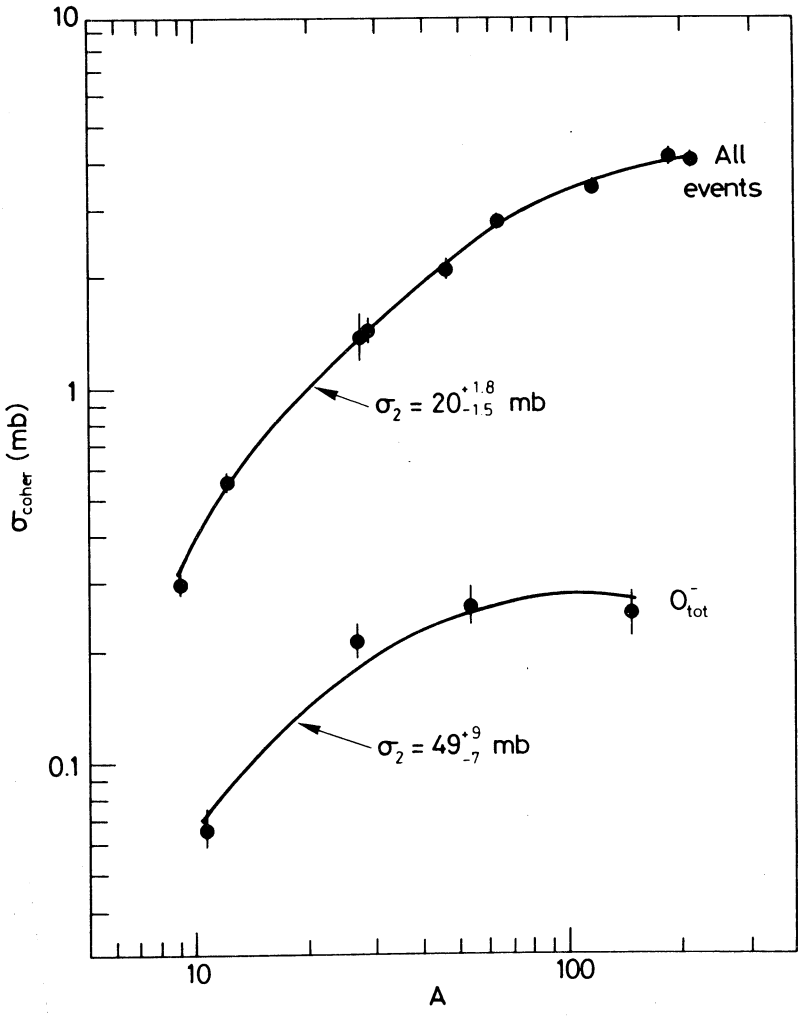

Fig. 14 Production cross-sections of the 3π system and of the 0^- state for different target nuclei at 15.1 GeV/c. Curves correspond to the A dependence as given by the optical model with σ_2 as parameter (from Ref. 55).

In Ref. 57, results were reported on the process $K^- p \to (K^- \omega) p$ at 10 and 16 GeV/c. For low $K\omega$ masses the cross-section was found to be compatible with constant energy dependence, and hence with diffractive production of this system. A study of the density matrix elements of the $J^P = 1^+$ state gives the following results:

$$\rho_{00}^{(s)} = 0.66 \pm 0.07 \qquad \text{(s-channel)} \tag{3.7a}$$

$$\rho_{00}^{(t)} = 0.45 \pm 0.06 \qquad \text{(t-channel)} \; . \tag{3.7b}$$

Thus, also in this process the helicity is closer to be conserved in the s-channel than in the t-channel. Here, however, the s-channel helicity conservation is much more approximate than in the previous process.

The third result concerns the following question: How does the average spin $\langle J \rangle$ of a diffractively produced system depend on the mass of this system? The answer to this problem was provided by the ABBCHLV Collaboration[29], who calculated from their PWA results the function $\langle J \rangle$ versus M for several reactions. Figure 15 shows the spin-mass correlation of the transition $\pi \to (\pi\pi\pi)$. It is seen to be *linear*, with slope of the order of 1.1 $GeV^{-1} \approx$ $\approx$ 0.22 fm. The results for the other channels studied are similar, but the statistics are poorer.

Let me present some very simple impact parameter considerations in order to explain this linear spin-mass correlation[58]. Picture the hadrons as extended objects, built up by constituents of some kind, and assume that the "hit" that causes the $\pi \to (\pi\pi\pi)$ transition happens locally in impact parameter. This is illustrated in Fig. 16. Let me call the small energy-momentum quantum exchanged by the colliding particles the "Pomeron". The t-channel momentum transfer plays the role of the mass of this Pomeron: $m_P^2 = t$.

Consider now the "Pomeron-pion collision" in its c.m. frame. We have the following situation:

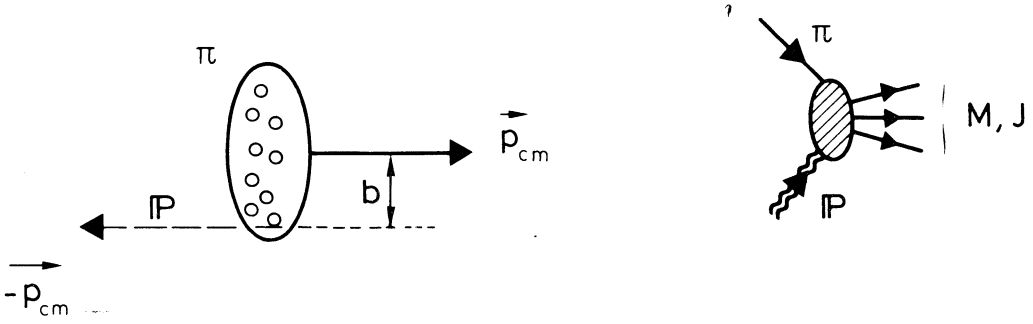

By ignoring the Pomeron spin, we can write for the total angular momentum of the initial Pomeron-pion state

$$J = L = b\, P_{cm} + c \; . \tag{3.8}$$

Here, c is a constant representing some sort of "zero-point angular momentum".

It follows from angular momentum conservation that the total spin of the final state (3π) system is also given by Eq. (3.8).

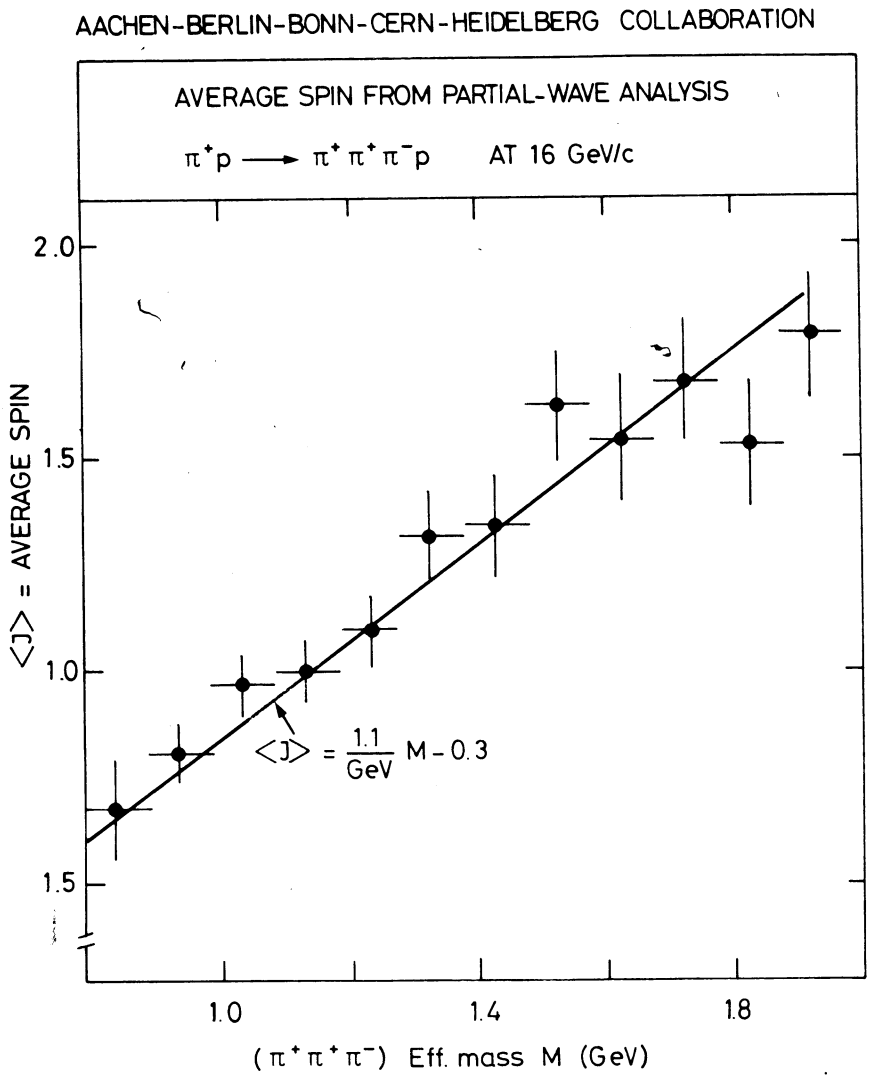

Fig. 15 The average total angular momentum ⟨J⟩ of the three-pion system as a function of $(\pi^+\pi^+\pi^-)$ mass (from Ref. 29)

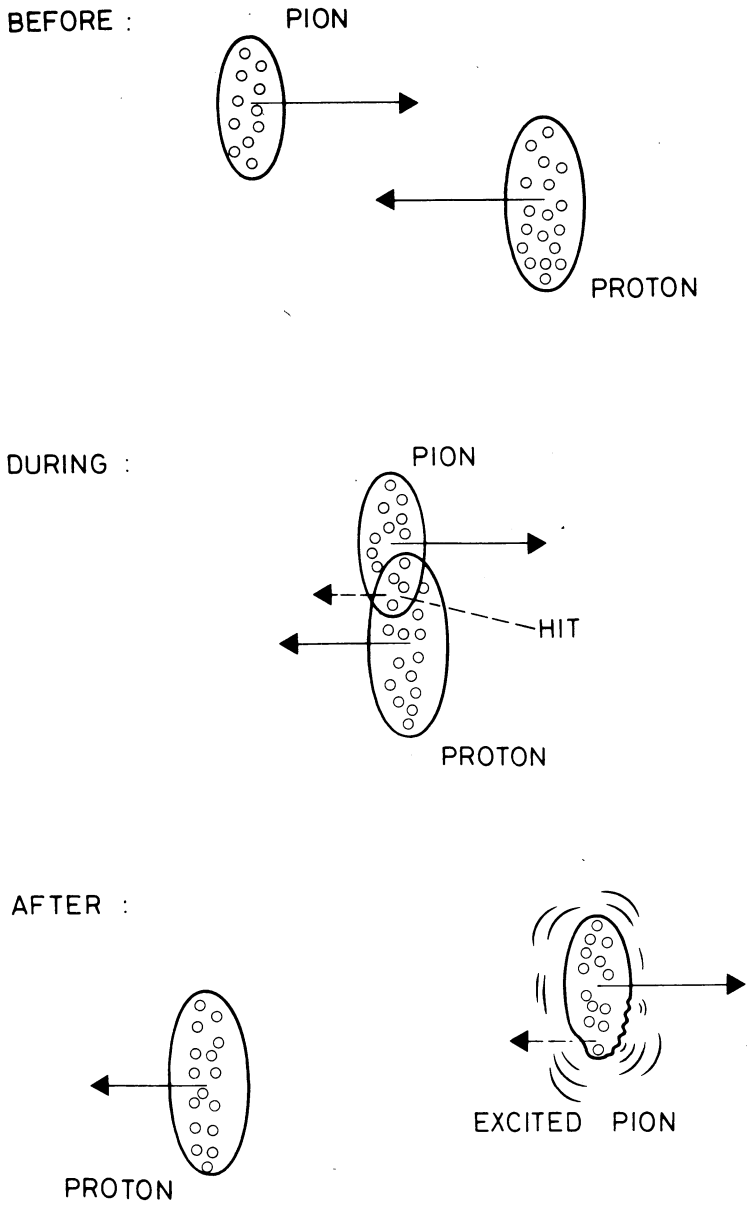

Fig. 16 Geometrical picture of diffraction dissociation

The c.m. momentum of the Pomeron-pion system is given by the formula

$$P_{cm} = \frac{1}{2M}\sqrt{\lambda(M^2, M_\pi^2, M_P^2)} \ . \tag{3.9}$$

Here, M is the total energy of the $P\pi$ collision, $m_P^2 = t$ is the square of the "Pomeron mass", and $\lambda(x,y,z) = (x-y-z)^2 - 4yz$.

Owing to the smallness of the pion and the Pomeron masses ($\langle t\rangle \approx -0.15$ GeV^2), one has in a very good approximation

$$P_{cm} \approx \frac{1}{2} M \ . \tag{3.10}$$

By substituting this result into Eq. (3.8), assuming the impact parameter b to be approximately independent of M and averaging over the impact parameters, one obtains the following result:

$$\langle J\rangle = \frac{1}{2}\langle b\rangle M + c \ . \tag{3.11}$$

A comparison of this formula with the empirical law

$$\langle J\rangle = \lambda M + c \ , \qquad \lambda \approx 1.1 \text{ GeV}^{-1} \ , \tag{3.12}$$

gives us

$$\langle b\rangle \approx 2\lambda \approx 2.2 \text{ GeV}^{-1} \approx 0.45 \text{ fermi} \ . \tag{3.13}$$

One may interpret this value, 0.45 fm, as the *average interaction radius* of the Pomeron-pion collision.

From elastic scattering analyses we know the radius of the proton to be larger than that of the pion and, furthermore, that the radius of the pion is larger than that of the kaon. Consequently, we may expect the spin-mass correlation slope λ to be largest in the baryonic transitions, medium in the pionic transitions, and smallest in the kaonic transitions. The available data are consistent with this prediction but do not provide a stringent test of it.

The above analysis is obviously simplified and I have deliberately presented it in a rather picturesque way. I believe, however, that its physical ideas are essentially correct. The linearity of the spin-mass correlation is due to the spin being "born" in the form of *orbital angular momentum*, and the slope λ of this correlation reflects the radius of the spatial volume in which the transition happens.

3.3 Partial-wave analysis of $pp \to p(p\pi^+\pi^-)$

The first partial-wave analysis of nucleon excitation processes has been reported to this conference by the Bonn-Hamburg-Munich Collaboration[59]. Their results are briefly outlined below.

They have analysed the structure of the $(p\pi^+\pi^-)$ system produced in the proton dissociation process

$$pp \to p(p\pi^+\pi^-) \tag{3.14}$$

at 12 and 24 GeV/c. To increase the statistics, the 12 and 24 GeV/c data were combined. In this energy range and for low $(p\pi^+\pi^-)$ masses, the above process is almost purely diffractive.

The analysis was performed by using a modified version of the Illinois PWA program, due to Kotanski[60].

In Fig. 17 the $(p\pi^+\pi^-)$ mass distribution for the combined 12 and 24 GeV/c data is shown. It displays the two well-known enhancements at $\sim$ 1470 and $\sim$ 1700 MeV. These structures have in the past been studied in great detail[61,62]. From a large compilation of data, Boesebeck et al.[62] have deduced the following "world" averages for the values of the masses and widths of these peaks:

Peak	Mass (MeV)	Width (MeV)
"$N^*(1470)$"	1453 ± 8	80 ± 9
"$N^*(1710)$"	1712 ± 3.4	60 ± 6

The Bonn-Hamburg-Munich Collaboration data are consistent with these values.

In most earlier work, the 1470 and 1710 peaks have been interpreted as being due to the production of the $1/2^+(1470)$ ("Roper") and the $5/2^+(1688)$ isobars, respectively.

The contributions of the different spin-parity states are shown as functions of the $(p\pi^+\pi^-)$ mass in Fig. 18 for $J^P = 1/2^+$, $3/2^-S$ $(\Delta^{++}\pi^-)$, $3/2^-P$ $(p\varepsilon)$, and $5/2^+$ waves. From these plots we may draw the following conclusions:

i) The $J^P = 1/2^+$ contribution does not show any particular structure up to a $(p\pi^+\pi^-)$ mass of 2 GeV.

ii) The $J^P = 3/2^-$ contributions display distinct structure. The S-wave $(\Delta^{++}\pi^-)$ decay contribution peaks at $\sim$ 1470 MeV and that of the P-wave $(p\varepsilon)$ decay at $\sim$ 1680 MeV.

iii) The $5/2^+$ contribution peaks at $\sim$ 1720 MeV.

These results show that the conventional interpretation of the 1470 and 1700 MeV peaks is incorrect. The former peak is not due to the Roper resonance but is due to a $3/2^-$ state. The 1700 MeV peak is mainly due to a $3/2^-$ state but also receives contributions from the $5/2^+$ wave. By counting the events above hand-drawn background curves, we may estimate the ratio of the $3/2^-$ to the $5/2^+$ contributions to be approximately two to one.

We may attempt to identify the observed peaks with the numerous isobar states decaying into $p\pi\pi$ proposed by phase-shift analyses of formation experiments in the 1.4-1.8 GeV mass region[63]. Possible candidates are, for example, the $J^P = 3/2^-$ resonance at 1520 MeV, the claimed $J^P = 3/2^-$ P-wave resonance[64] with a dominant $p\varepsilon$ decay mode at $\sim$ 1700 MeV, and the well-established $J^P = 5/2^+$ resonance at 1688 MeV. The masses and the widths of the peaks seen in Fig. 18 differ considerably from those of the above isobars. This may not, however, altogether rule out the identification, since it is well known that analyses of formation and production experiments may yield different values for resonance masses and widths.

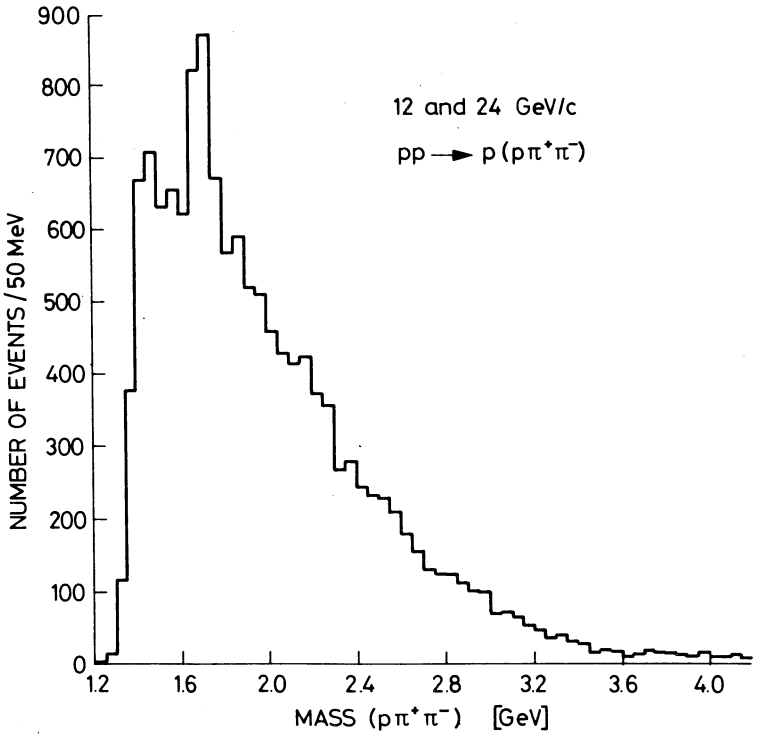

Fig. 17 Combined ($p\pi^+\pi^-$) mass distribution for 12 and 24 GeV/c for the reaction $pp \to p(p\pi^+\pi^-)$ (from Ref. 59)

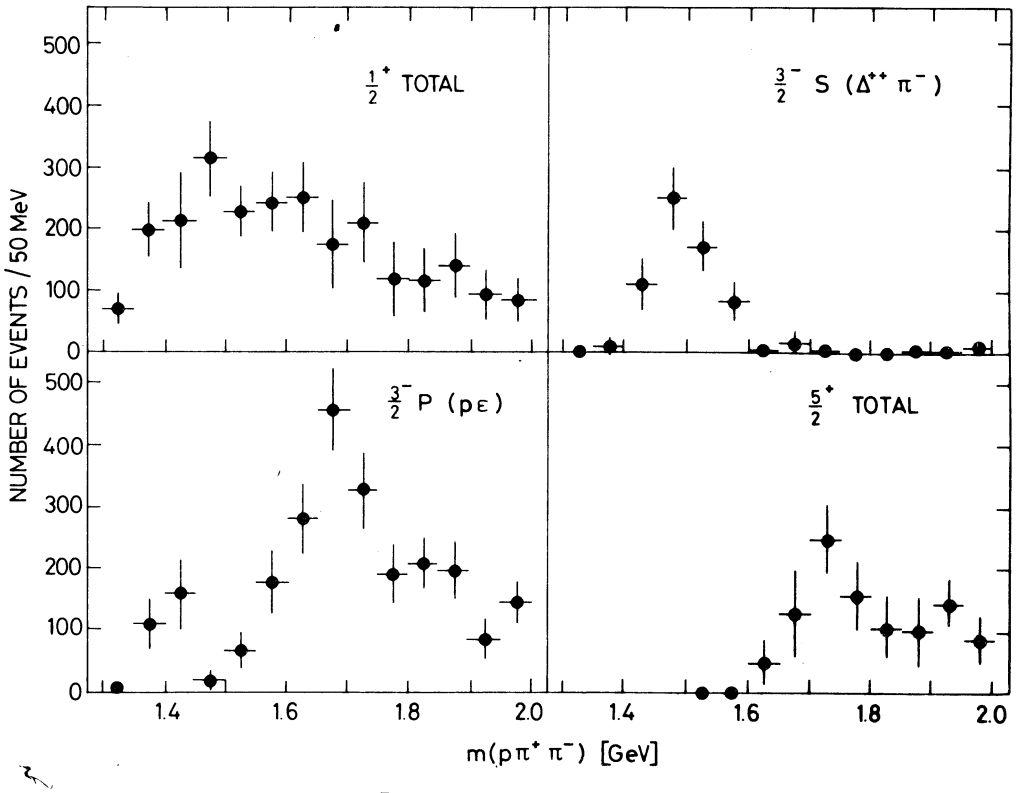

Fig. 18 Dependence of $J^P L$ states on the ($p\pi^+\pi^-$) mass (from Ref. 59)

In order to examine further the nature of these structures, the authors studied the variation of the phases of the different partial waves with the ($p\pi\pi$) mass. Before showing their results, let me briefly remind you of the results which have been previously obtained in the analyses of the pion transition $\pi \to (\pi\pi\pi)$. Figure 19 shows the beautiful Breit-Wigner behaviour of the phase of the 2^+ wave in the A_2 mass region, as deduced in the CERN-IHEP analysis[33]. In this and other experiments[65], the phases of the $1^+(A_1)$ and $2^-(A_3)$ waves were found not to vary (relative to the phase of a smooth "background" wave). This result has been commonly interpreted as strong evidence against the resonance interpretation of the A_1 and A_3 enhancements.

Returning now to the Bonn-Hamburg-Munich experiment, the best state which can be used as reference to measure the phases is the $1/2^+P$ ($\Delta^{++}\pi^-$) state, since it does not display any resonance structure and is sizeable over the whole ($p\pi\pi$) mass region. The phases relative to this state are shown in Fig. 20. One sees that the phase of the $3/2^-S$ wave is not completely inconsistent with a Breit-Wigner behaviour around 1500 MeV. The phases of the $3/2^-P$ and $5/2^+P$ waves, however, do not offer even a hint of such a resonance behaviour in the 1700 MeV mass region! To show how a Breit-Wigner phase variation compares with the data, I have drawn in Fig. 20c a curve corresponding to the A_2 phase shown in Fig. 19.

To close this section, I wish to make the following remarks. Firstly, the above results imply, in my opinion, that the case of the nature of the A_1 and A_3 peaks should be reopened. If the ($p\pi\pi$) peaks are normal resonances but their phases (relative to that of the "background" amplitude) do not vary, it should be obvious that the observed lack of phase variation in the A_1 and A_3 production should not be regarded as evidence against these states being resonances. Secondly, it is important that the results of the Bonn-Hamburg-Munich Collaboration analysis are checked by other independent analyses. Finally, in order to obtain a more complete picture of nucleon dissociation, it would be very useful to carry out partial-wave analyses also of the single-pion production processes $pp \to p(n\pi^+)$ and $np \to (p\pi^-)p$.

3.4 Decay

The Fermilab-Northwestern-Rochester-SLAC Collaboration has presented interesting new data of the diffractive process

$$n\,p \to (p\pi^-)\,p \qquad (3.15)$$

at energies ranging from 50 to 300 GeV/c [18]. Since these data are reviewed by T. Ferbel[18], I shall not discuss them in detail but restrict my remarks to one feature of the data which, in my opinion, provides particularly useful new information.

The decay of the ($p\pi^-$) system in the above process may be described by two decay angles: a polar angle θ and an azimuthal angle ϕ. Usually the analysis is carried out either in the t-channel helicity frame (the Gottfried-Jackson frame) or in the s-channel helicity frame. The two-dimensional $\cos\theta - \phi$ distribution contains much useful information and may be used to isolate different contributing production mechanisms. This is discussed in detail in Refs. 38 and 66.

Before showing the FNRS Collaboration data on the decay distributions, let me make two theoretical predictions.

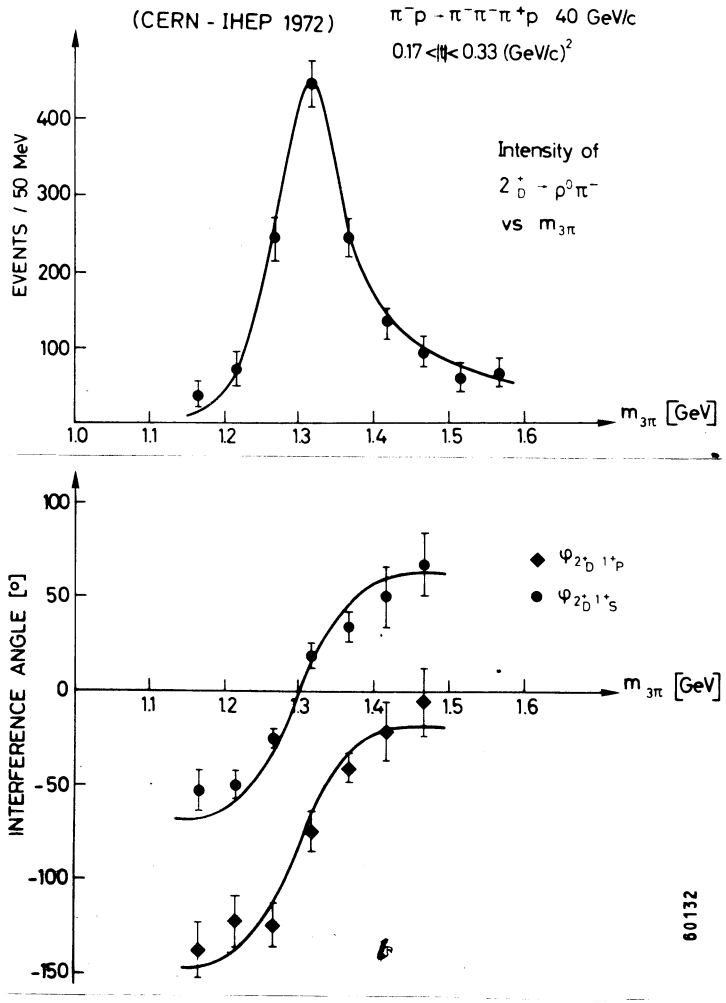

Fig. 19 Results of partial-wave analysis of the process $\pi^- p \to (\pi^-\pi^-\pi^+)p$ at 40 GeV/c. a) Mass dependence of the 2^+D wave. The curve is the fit of a relativistic D-wave Breit-Wigner function without background to the data. b) Interference phase between the 2^+D state and 1^+S and 1^+P wave. The solid curves are calculated from the Breit-Wigner fit of (a) assuming a constant phase for the 1^+S and 1^+P wave and adjusted vertically to fit the data (from Ref. 33).

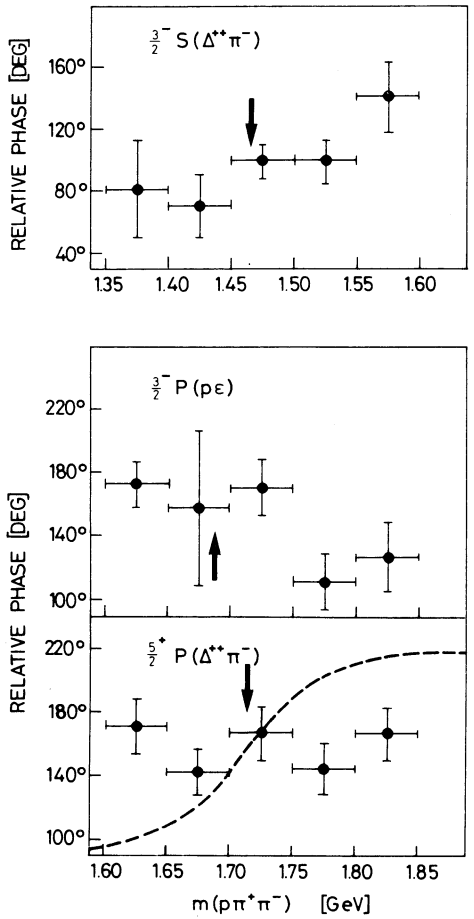

Fig. 20 Interference phases of the $3/2^-S$ $(\Delta^{++}\pi^-)$, $3/2^-P$ $(p\varepsilon)$ and $5/2^+P$ $(\Delta^{++}\pi^-)$ waves relative to the $1/2^+P$ $(\Delta^{++}\pi^-)$ "background" wave. The arrows indicate the positions of the peaks seen in the mass distributions of Fig. 18. The curve in the lowest figure corresponds to the Breit-Wigner phase of Fig. 19 (from Ref. 59).

The first one follows from the assumption of t-channel helicity conservation. Consider the decay in the Gottfried-Jackson frame shown below. Helicity conservation in the t-channel implies that the helicity of the Pomeron is zero. Consequently, the Pomeron is unable to carry any angular information over from the p_A-p'_A-P vertex to the P-p_B-π^--n vertex. The distribution in the Treiman-Yang angle ϕ_{TY} (defined as the angle between the p_A-p'_A-n and p_B-π^--n planes) should then be flat, *irrespective of the value of the polar angle* θ_J. The two-dimensional $\cos\theta_J$ - ϕ_{TY} distribution should appear as follows:

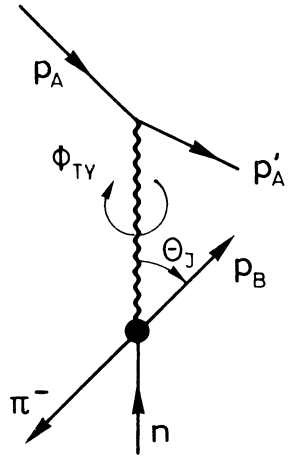

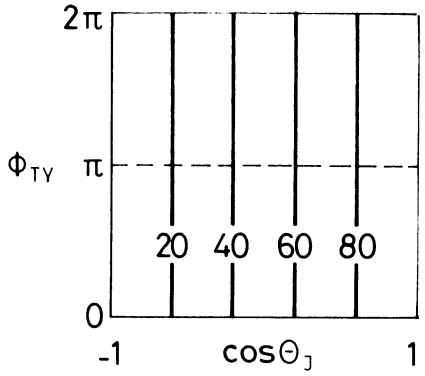

i.e. the isoclines (curves corresponding to constant values of the distribution) should be parallel to the ϕ_{TY} axis.

Let us next work out the prediction of the Deck model. Consider first the pion exchange Deck graph shown below:

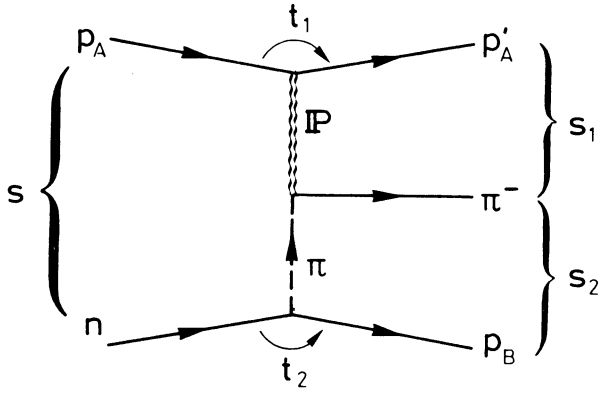

The matrix element corresponding to this graph is the following (the variables are indicated in the figure):

$$|M| = g_1(t_1)\, g_2(t_2)\, (s_1)^{\alpha_P(t_1)}\, (s_2)^{\alpha_\pi(t_2)} \,. \qquad (3.16)$$

Here, $g_1(t_1)$ and $g_2(t_2)$ are peripheral functions of the momentum transfers, and $\alpha_P(t_1) \approx$ $\approx 1 + 0.3\, t_1$ and $\alpha_\pi(t_2) \approx -0.02 + t_2$ are the Pomeron and pion Regge trajectories, respectively. The peripherality of $g_1(t_1)$ is due to the diffractive p_A-p'_A-P vertex and that of $g_2(t_2)$ to the pion propagator $(t_2 - m_\pi^2)^{-1}$.

From the kinematical relationship

$$\frac{s_1\ s_2}{s} \approx \text{constant} \tag{3.17}$$

we see that the Pomeron and the pion exchanges share the available total energy s. The Pomeron exchange, having a higher intercept, wins this competition. Thus the sub-energy s_1 tends to become maximal. This gives rise to a ϕ_{TY} dependence: the pion likes to be aligned in the p_A-p'_A-n plane but to go in a direction opposite to that of the proton p'_A [67]. The qualitative prediction for the $\cos\theta_J$ - ϕ_{TY} distribution is now obvious. This distribution should peak near $\cos\theta_J = +1$ and $\phi_{TY} = 0$:

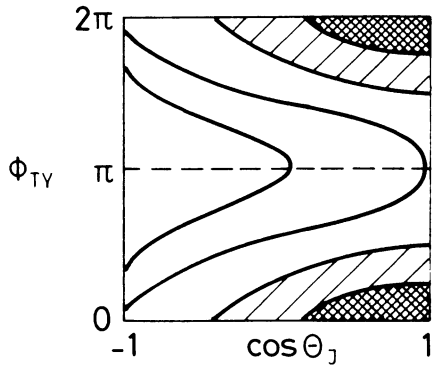

Another possible contribution to the above process is provided by the baryon exchange Deck graph shown below:

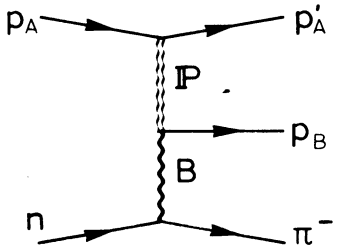

The above considerations apply also to this graph, except that now the roles of the pion and the proton p_B are reversed. We see that this graph should provide a contribution that peaks near $\cos\theta_J = -1$ and $\phi_{TY} = \pi$:

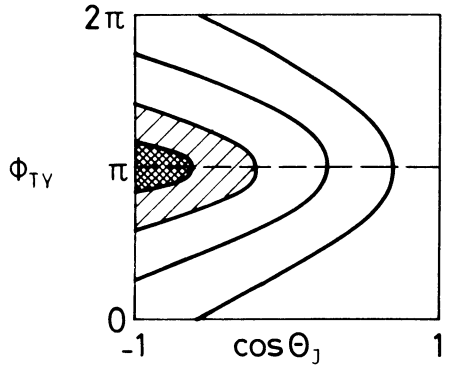

When both mechanisms are present, we expect to see a distribution of the following type*):

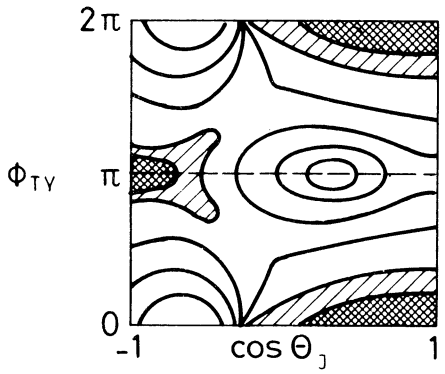

Let us now look at the experimental data. Figure 21 shows the FNRS Collaboration data on the cos θ_J - ϕ_{TY} distribution of the process (3.14), for mass and t-ranges $1.08 \leq M \leq 1.25$ and $0.02 \leq |t| \leq 0.10$. A strong resemblance is seen between the experimental distribution and the qualitative Deck model prediction discussed above.

By integrating the experimental distribution over the cos $\theta_J > 0$ and cos $\theta_J < 0$ regions, we see that these regions contribute an equal amount to the cross-section (the numbers of the data points used to make the plot of Fig. 21 are 1393 for cos $\theta_J > 0$ and 1455 for cos $\theta_J < 0$).

Figure 22 shows the t-distributions for the samples with cos $\theta_J > 0$ and cos $\theta_J < 0$. They are very different. For the forward decay sample, the small-t slope is around $\approx$ 13 $(GeV/c)^{-2}$. For the backward sample it is $\approx$ 20 $(GeV/c)^{-2}$. Both the forward and the backward data show a sudden change of the slope around $t = -0.2$ GeV^2. A simple explanation for this break is that it is due to the non-flip amplitude vanishing at this t-value. This is discussed in detail in the next section.

The above results teach us an important lesson. In the process $np \to (p\pi^-)p$, the regions corresponding to forward and backward decays of the $(p\pi^-)$ system seem to be dominated by different production mechanisms. In the Deck model these are the pion and the baryon exchange mechanisms, respectively. They are seen to contribute with approximately equal strengths. This contradicts past practice and the belief that the baryon exchange mechanism may be ignored in the Deck model. It is important to study whether the proper consideration of the baryon exchange contribution will remove some of the arguments presented against the (pion exchange) Deck model.

3.5 Cross-overs

A novel application of the physical ideas just discussed was suggested by Berger[66] and carried out by the ABBCH Collaboration[68]. It is the following.

Consider the proton dissociation processes

$$\pi^+ p \to \pi^+ (\pi^- \Delta^{++}) , \tag{3.18a}$$

$$\pi^- p \to \pi^- (\pi^- \Delta^{++}) . \tag{3.18b}$$

*) Our sketches are qualitative only; in particular, we neglect the obvious kinematical constraint of isotropy in ϕ_{TY} for cos $\theta_J = \pm 1$. Owing to the limited statistics, this effect is also not visible in the data.

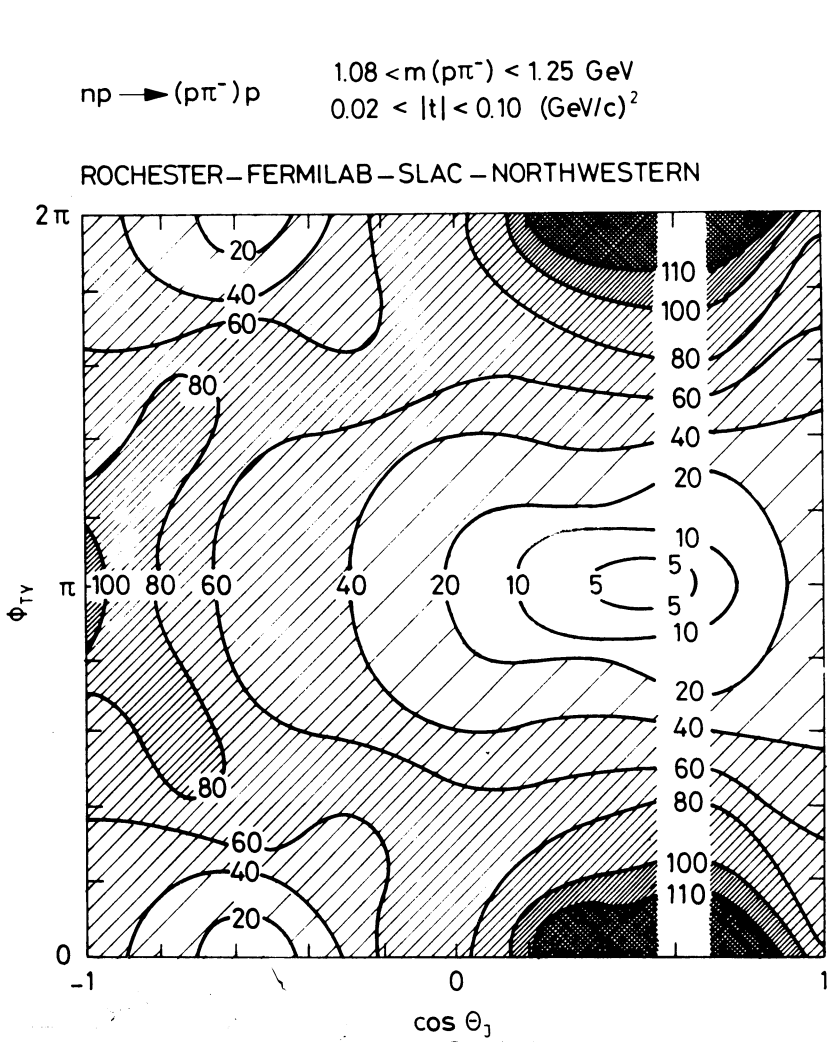

Fig. 21 Correlation between the cos θ_J and ϕ_{TY} of the forward proton for the process np → $(p\pi^-)p$ (from Ref. 18)

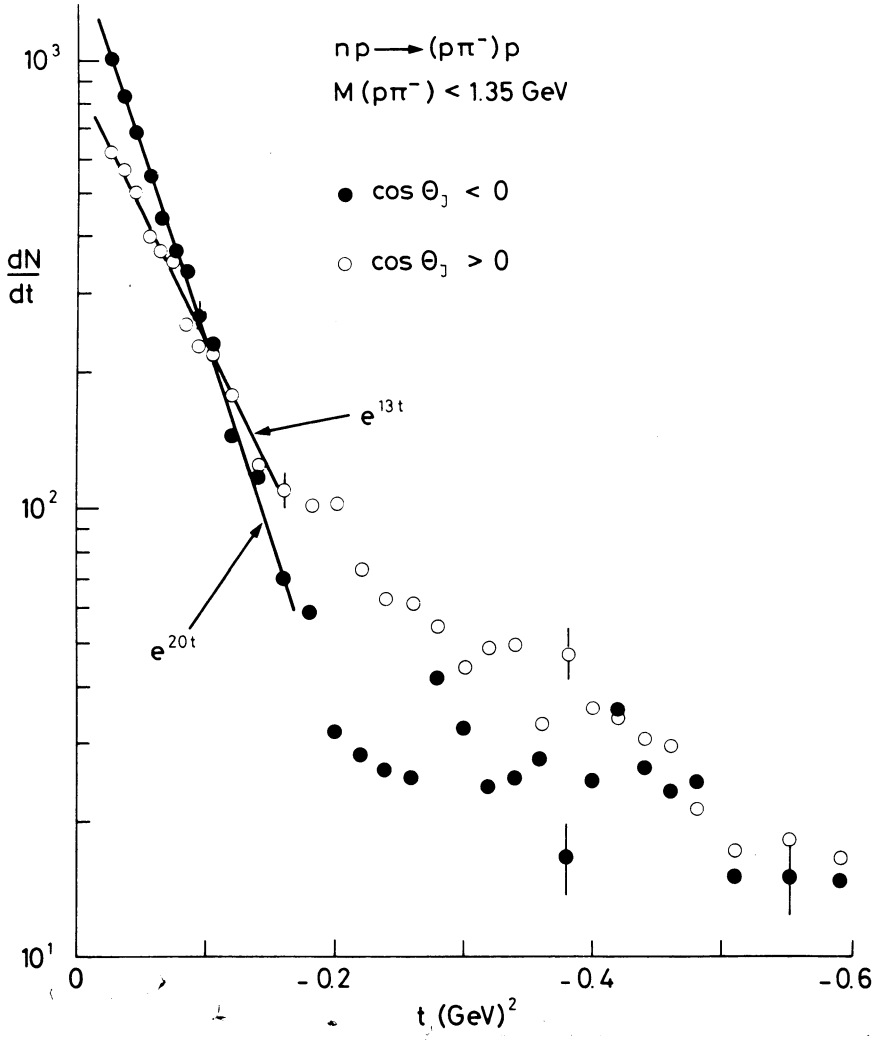

Fig. 22 Differential cross-sections for the process np → $(p\pi^-)p$ for cos θ_J > 0 and cos θ_J < 0 (from Ref. 18)

We may draw the following pion and baryon exchange Deck graphs for these processes:

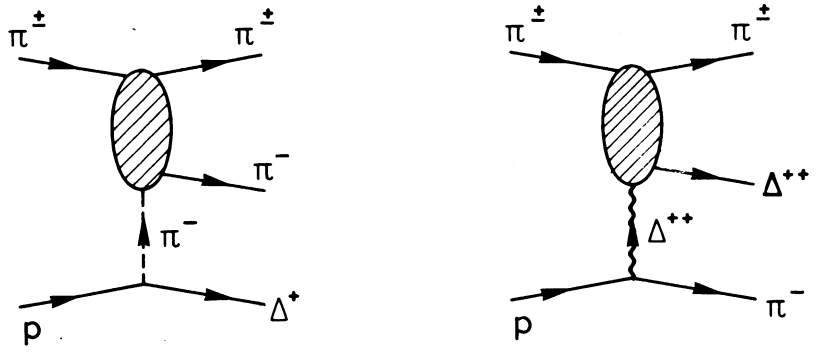

In these graphs, the shadowed blobs represent the full $\pi\pi$ and $\pi\Delta$ elastic scattering amplitudes.

Assume now that $\pi\pi$ and $\pi\Delta$ elastic scattering show the same cross-over systematics that are shown by $\pi^{\pm}p$, $K^{\pm}p$, and $p^{\pm}p$ scattering, i.e. that the cross-sections of the antiparticle-induced processes are larger than those of the corresponding particle-induced processes, and that they cross-over each other somewhere around $t \approx -0.2$ GeV^2. Looking at the above Deck graphs, we immediately see that *the two graphs make opposite predictions for the sign of the cross-over of the differential cross-sections of the processes (3.18).*

By applying cuts in the θ_J - ϕ_{TY} angles we may obtain samples of data with enriched contributions from the pion and baryon exchange mechanisms, respectively. This selection may be performed even better in the s-channel helicity frame*). In this frame, the selections cos $\phi_s > 0$ and cos $\phi_s < 0$ should enhance the pion exchange and the baryon exchange contributions, respectively.

The Deck model predictions may be summarized as follows:

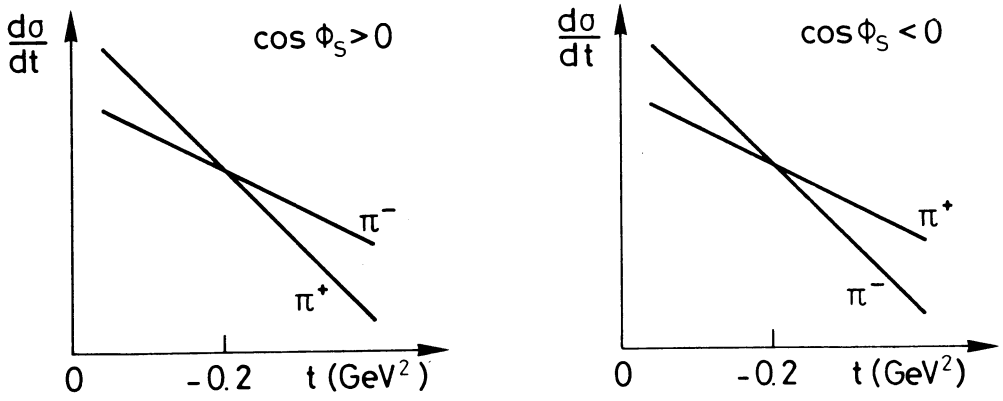

*) The use of the s-channel helicity frame angles has recently been advocated by Berger[38,66]. These angles have many nice properties which make them particularly suitable for the above type of studies[24,38,66].

The experimental differential cross-sections of the processes (3.18) at 16 GeV/c for the samples with $\cos \phi_s > 0$ and $\cos \phi_s < 0$ are shown in Fig. 23. The above theoretical expectations are seen to be borne out by the experiment in a rather striking way. The result in this figure obviously provides strong support for the exchange-model ideas.

The results of this and the previous section clearly show that the *production* and the *decay* of the diffractively excited systems are *not independent but strongly correlated.* It is very important to pursue the study of these correlations further. They may well provide us with much new insight into the dynamics of diffraction dissociation.

4. PROGRESS IN UNDERSTANDING ABSORPTION

A considerable amount of phenomenological and theoretical work on the structure of absorption corrections has been done in the past year. Here we shall discuss some of the phenomenological results. Progress in the "hard" theory is reviewed by A. Schwimmer[7].

4.1 Peripheral picture of diffraction dissociation

In the past year, phenomenological evidence has been mounting for *inelastic diffraction (unlike elastic diffraction) being peripheral in impact parameter space**). In the past, many authors have speculated that this could be so. Their belief has been based partially on intuition, partially on field theoretical model calculations. The new high-energy data provide strong support, although not an indisputable proof, for the peripherality of inelastic diffraction.

Let us begin with a simple model calculation[10,69]. Consider the diffraction dissociation process $pp \to pN^*$, where N^* stands for any low-mass diffractive state, resonant or non-resonant. Denote the mass, spin, and helicity of this state by M, J, and λ, respectively. The momentum space and impact parameter space amplitudes of this process are related by a Fourier-Bessel transform as follows:

$$h^J_{\Delta\lambda}(s,t,M^2) = \int dt\, J_{\Delta\lambda}(b\sqrt{-t})\; h^J_{\Delta\lambda}(s,b,M^2) \; . \tag{4.1}$$

Here, $\Delta\lambda$ is the net s-channel helicity flip of the amplitude.

Let us now assume that the impact parameter profile of the above process is peripheral. In the first-order approximation, we may describe it by a δ-function. Ignoring any dependence on M, J, and $\Delta\lambda$, substituting the δ-peak amplitude in Eq. (4.1), and performing the integration, one obtains

$$h^J_{\Delta\lambda}(s,t,M^2) \sim J_{\Delta\lambda}(R\sqrt{-t}) \; . \tag{4.2}$$

Giving the b-space profile a finite width would modify this result, in the first approximation, by a smooth decreasing "modulating function", such as an exponential:

$$h^J_{\Delta\lambda}(s,t,M^2) \approx e^{at}\, J_{\Delta\lambda}(R\sqrt{-t}) \; . \tag{4.3}$$

---

*) The word "peripheral" is commonly used to describe a process whose t-distribution is steep, as well as one whose impact parameter profile peaks at the edge of the absorption region. We use this word here in the latter meaning only.

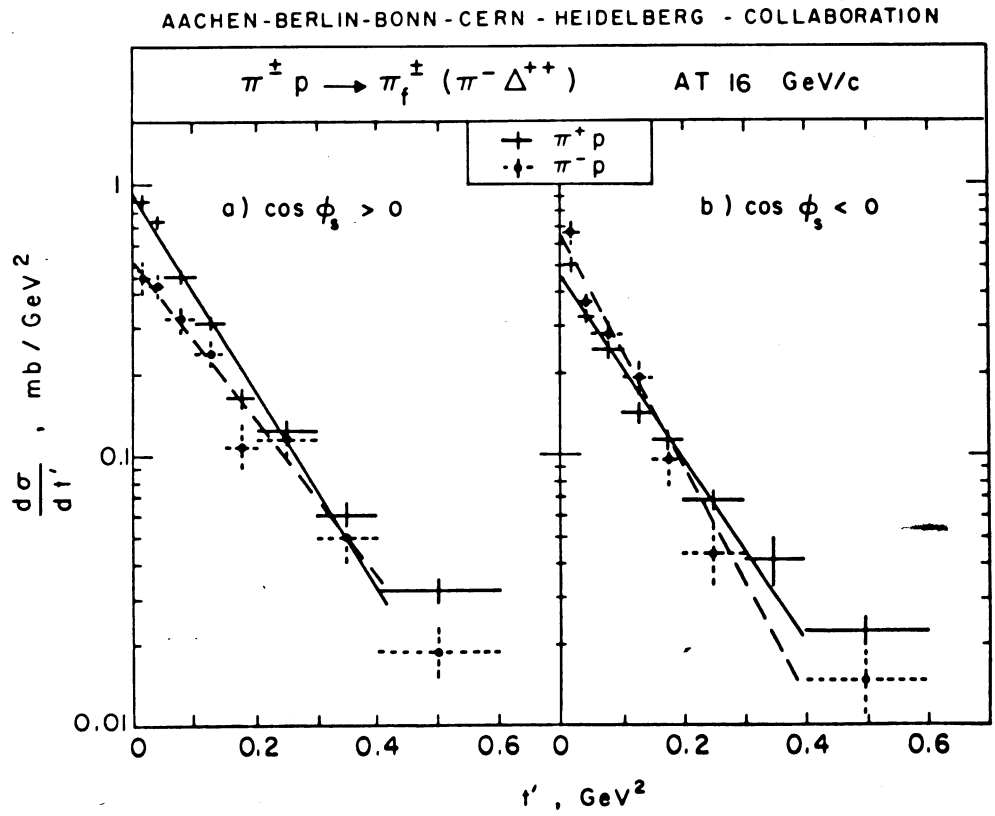

Fig. 23 Momentum transfer distributions for events with a) $\cos \phi_s > 0$; b) $\cos \phi_s < 0$ and $1.3 < m(\pi^- \Delta^{++}) < 1.9$ GeV (from Ref. 68).

The formula for the differential cross-section is given by

$$\frac{d\sigma}{dtdM^2} = \sum_{J,\Delta\lambda} \left| h^J_{\Delta\lambda}(s,t,M^2) \right|^2 \approx \sum_{\Delta\lambda=-J}^{\Delta\lambda=+J} e^{2at} \left| J_{\Delta\lambda}(R\sqrt{-t}) \right|^2 . \tag{4.4}$$

Assume now that only the non-flip amplitude contributes significantly. Then the differential cross-section should behave qualitatively as $\sim |J_0(R\sqrt{-t})|^2$. For $R \approx 1$ fermi, the Bessel function $J_0(R\sqrt{-t})$ has its first zero at $t \approx -0.2$ GeV^2. Consequently, the differential cross-section should exhibit a diffraction minimum at this particular t-value.

Experimentally, the assumption of non-flip dominance in diffraction dissociation is known to be *false*. The results discussed in Section 3 suggest rather the following behaviour. When the mass of the excited system is close to the threshold, its spin $J(M^2)$ is low and the contributions of the helicity flip amplitudes may be small. Thus, in this mass range the Bessel function shape $\sim |J_0(R\sqrt{-t})|^2$ may be visible. Increasing the mass of the excited system, its spin increases rapidly, helicity flip amplitudes get stronger*), and the differential cross-section flattens out. This development is illustrated in Fig. 24.

Let us now look at the experimental data. The results of the Fermilab-Northwestern-Rochester-SLAC Collaboration on the process $np \to (p\pi^-)p$ were shown already in Figs. 9 and 22. In the lowest mass bin, very clear structures at $t \approx -0.2$ GeV^2 are visible, in particular when the cut $\cos\theta_J < 0$ is applied.

Figure 25 shows the ISR Split Field Magnet data of the CHOV Collaboration on the process $pp \to p(n\pi^+)$ at 1500 GeV/c [20]. At masses near the $(n\pi^+)$ threshold, clear structures in the vicinity of $t = -0.2$ GeV^2 are again visible. Indeed, we do not need much imagination to see the Bessel function shape $|J_0(R\sqrt{-t})|^2$ in the data! The curves drawn in the figure are from an impact parameter model calculation of Humble[70].

Similar small-t structures are present also in the 19 GeV/c Scandinavian Collaboration data[71] and the 12 and 24 GeV/c Bonn-Hamburg-Munich Collaboration data[27] on the process $pp \to p(n\pi^+)$.

Finally we show in Fig. 26 data on the double diffraction dissociation process

$$\begin{array}{c} p\,p \to (p\pi^+\pi^-)\ (p\pi^+\pi^-) \\ \qquad\quad \hookrightarrow \text{"}N^*(1470)\text{"} \ . \end{array} \tag{4.5}$$

These data come from the ISR experiment of the Pavia-Princeton Collaboration[72]. The break -- or dip -- seems now to be at somewhat larger t-values, $|t| \approx 0.4 - 0.5$ GeV^2. The curves drawn in the figure were obtained by fitting the formula

$$\frac{d\sigma}{dt} \sim \left| J_0(R\sqrt{-t}) + a\, e^{bt} \right|^2 e^{ct} \tag{4.6}$$

to the data.

---

*) The transitions $\pi \to (\pi\pi\pi)$, $K \to (K\pi\pi)$, and $N \to (N\pi\pi)$ are experimentally known to approximately conserve t-channel helicity. This implies that the s-channel helicity flip amplitudes become stronger when the mass of the excited system increases. For the transition $N \to (N\pi)$ the situation is unclear.

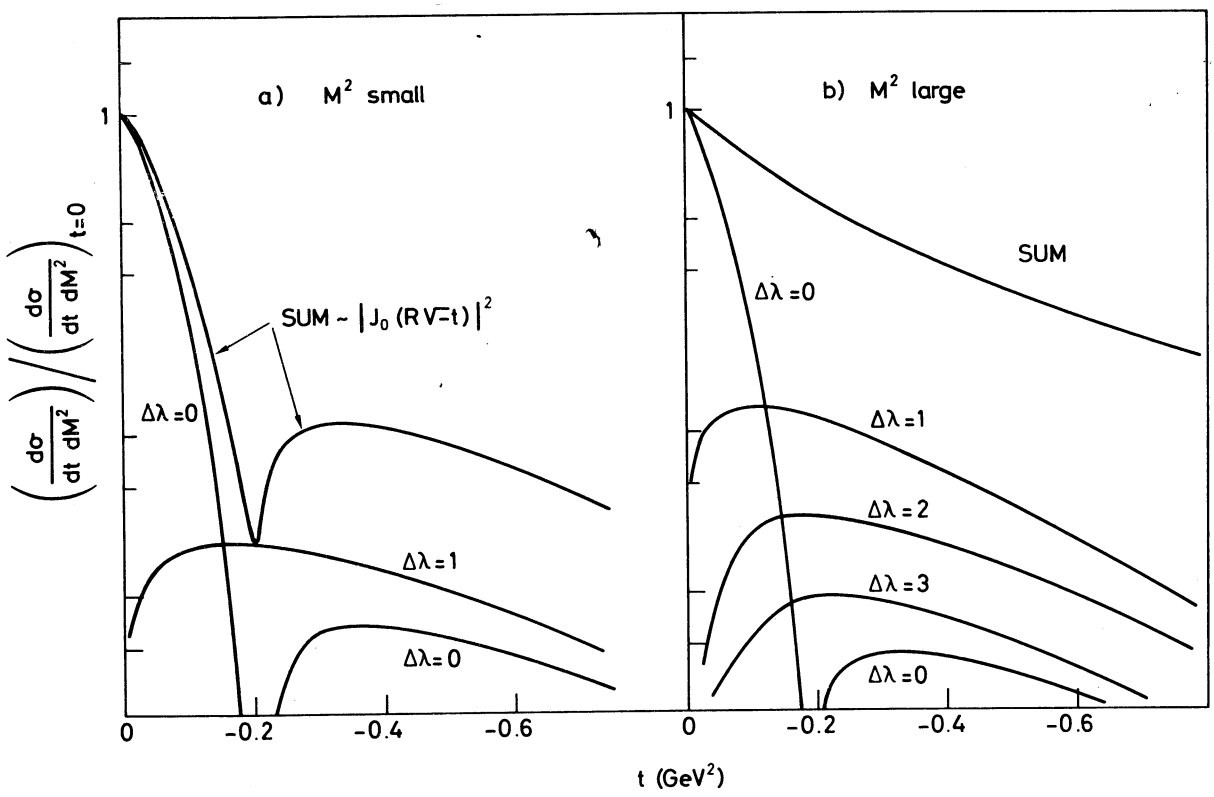

Fig. 24 Schematic illustration of the origin of the mass-slope correlation in the peripheral model of inelastic diffraction. a) M^2 small. The non-flip amplitude dominates faking a steep exponential t-dependence in the small t region. b) M^2 large. Several helicity amplitudes contribute appreciably. The differential cross-section is much flatter than in the case (a).

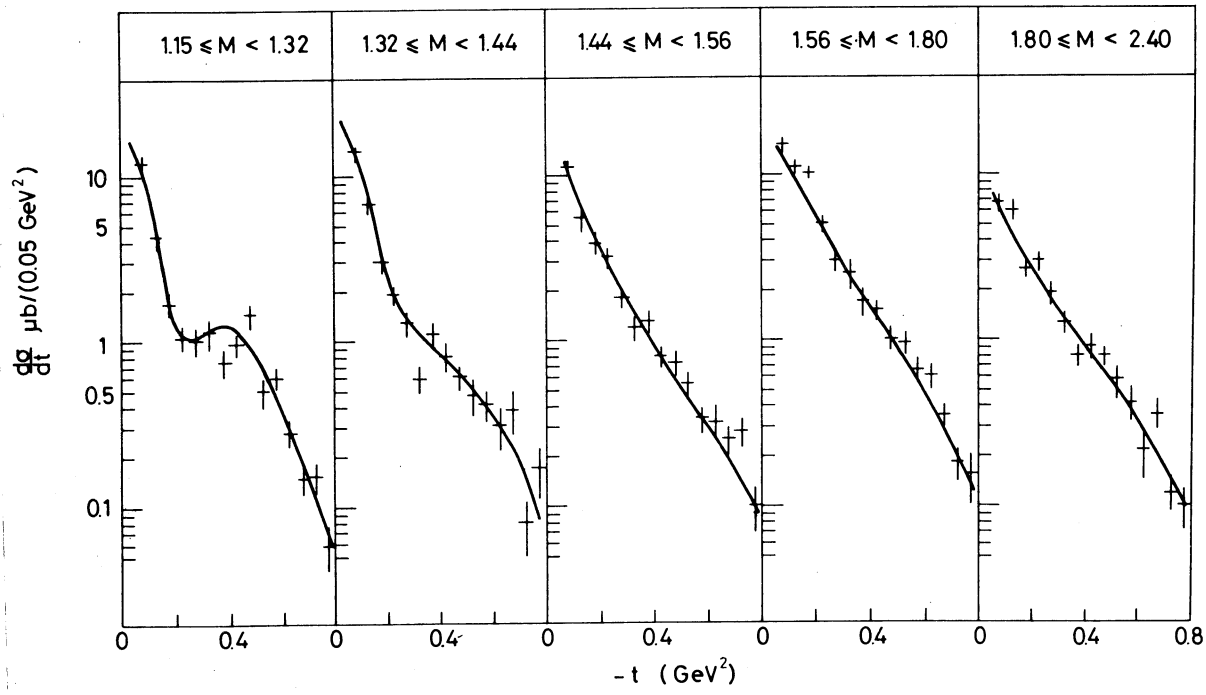

Fig. 25 Differential cross-sections $d\sigma/dt$ for the inelastic diffractive process $pp \to p(n\pi^+)$ at $s = 2809$ GeV^2 (Ref. 20). The solid curves are from a peripheral impact parameter model calculation (Ref. 70).

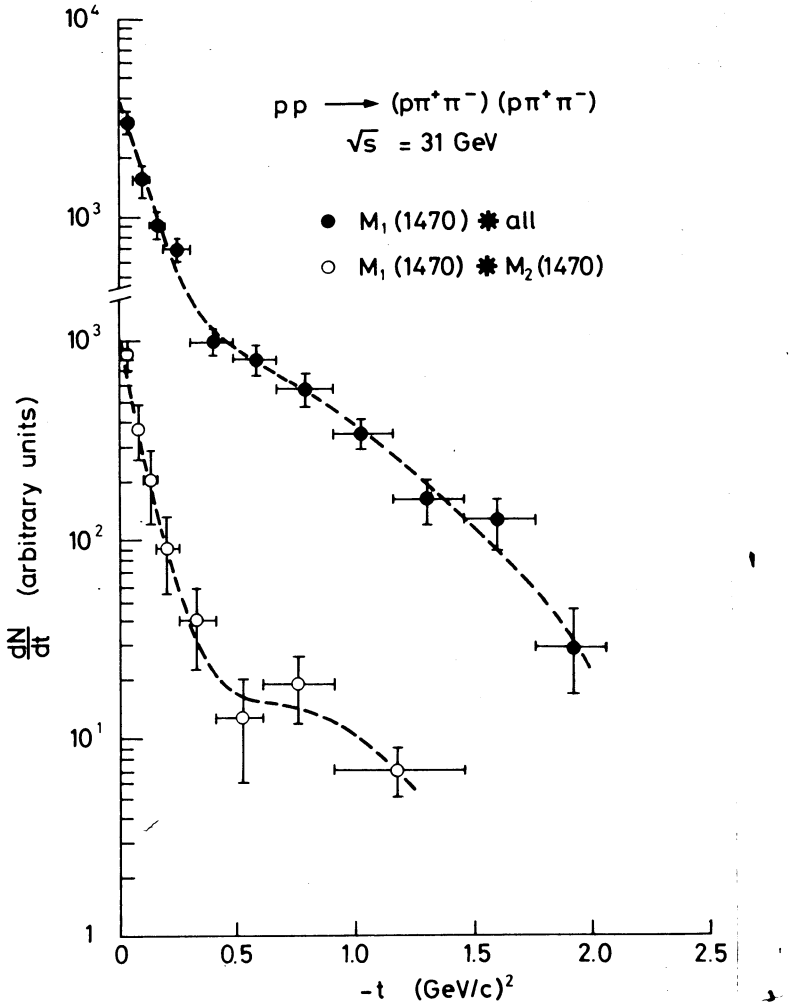

Fig. 26 Differential cross-sections for the double diffraction dissociation processes pp → "N*(1470)" $(p\pi^+\pi^-)$ and pp → "N*(1470)" "N*(1470)" (from Ref. 72)

A few remarks on the above results:

Firstly, they obviously strongly support the assumption that inelastic diffraction is peripheral in the impact parameter space. They do not, however, prove it. It is possible to describe the data also without assuming the non-flip amplitude to vanish at $t = -0.2$ GeV^2. Here are two possibilities:

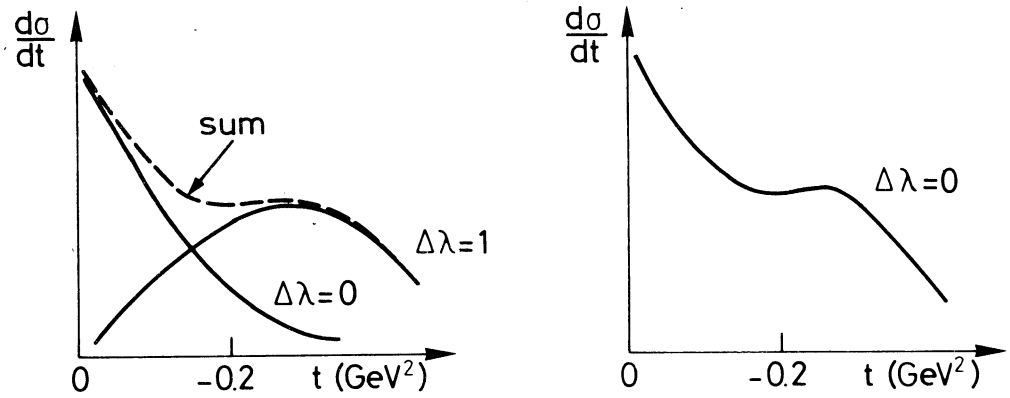

Secondly, it should be noticed that only a small fraction of the total inelastic diffractive cross-section σ_{diff} comes from the mass-range at which the $t = -0.2$ GeV^2 structures are visible. Thus, even if the peripherality explanation for them were correct, this would by no means guarantee the peripherality of the *total* profile $\sigma_{diff}(b)$.

Next, consider the mass-slope correlation. Experimentally, this phenomenon is very strong. If we ignore the spin-flip effects and make the (erroneous) assumption that the slope of $d\sigma/dt$ is proportional to the square of the interaction radius R, we conclude that R decreases by a factor of 2 when the mass of the excited system increases a few hundred MeV from the threshold! Such a rapid variation of the interaction radius is hard to understand. The peripheral picture provides us with a more appealing explanation for this phenomenon. According to this picture, the correlation is mainly caused by the peripherality of the non-flip amplitude (in the sense that the very steep slope at low masses is caused by a zero in the non-flip amplitude and not by a very large interaction radius) and by the increase of the contributions of helicity-flip amplitudes with increasing mass.

We may speculate that the mass-slope correlation phenomenon is caused by a combination of the following three effects, listed in order of decreasing importance: as the mass of the excited system, increases, a) the helicity-flip contributions increase, b) the absorption effects grow weaker, and c) the interaction radius decreases. It would be very useful to clarify the relative importance of these effects.

Finally, let me mention that the Fermilab-Northwestern-Rochester-SLAC Collaboration has obtained evidence against the simple peripheral picture. They have carried out a moment analysis of the decay of the $(p\pi^-)$ system in the process $np \to (p\pi^-)p$. Their results show that the $\langle Y_{11} \rangle$ moment in the helicity frame does not change sign around $t = -0.2$ GeV^2 but remains positive over the whole t-range $0 < |t| < 0.6$ [see T. Ferbel's talk[18]]. This moment measures the interference of a helicity non-flip amplitude with a single helicity-flip amplitude. Hence a zero in the non-flip amplitude should show up as a zero in this moment.

To conclude, we urgently need a careful s-channel amplitude analysis of the baryon dissociation processes. Such an analysis would settle the question of the b-dependence of the helicity amplitudes of these processes and thus provide us with very important information on the dynamics of diffraction dissociation.

4.2 Pumplin's bound

A very interesting and elegant result was derived by Pumplin[73]. It is well known that the s-channel unitarity equation (2.1), together with the assumption that the elastic amplitude is purely absorptive, yields the following inequality:

$$\sigma_{el}(b) \leq \tfrac{1}{2}\sigma_{tot}(b) \leq \sigma_{inel}(b) \ . \tag{4.7}$$

Here, $\sigma_i(b) = (1/2\pi)\, d\sigma_i/db^2$ and i = el, inel, tot, are the elastic, inelastic, and total cross-sections, respectively, in a collision at impact parameter b. But inelastic diffraction is a special category, resembling elastic scattering in many ways. It is therefore natural to ask: What is the proper generalization of Eq. (4.7) when inelastic diffraction is also assumed to be absorptive? Pumplin gave the following answer:

$$\sigma_{el}(b) + \sigma_{diff}(b) \leq \tfrac{1}{2}\sigma_{tot}(b) \leq \sigma_{nondiff}(b) \ . \tag{4.8}$$

Here, $\sigma_{diff}(b)$ is the total cross-section of inelastic diffraction at the impact parameter b.

The result Eq. (4.8) was proved by Pumplin in the multi-channel eikonal model approach. Other authors have shown that it holds in a variety of other models and approaches[74,75].

The physics underlying the Pumplin bound is particularly transparent in the diffraction dissociation picture of Good and Walker[76]. We shall briefly sketch a derivation of the bound in this picture.

Consider proton dissociation on a target. Ignore for simplicity the possibility that the target too may dissociate. Following Good and Walker, we expand the physical proton state $|1\rangle$ in terms of diffractive "eigenstates" ("bare particle" states) as follows:

$$|1\rangle = \sum_{k=1} U_{1k}\, |\psi_k\rangle \ . \tag{4.9}$$

The states $\{|\psi_k\rangle,\ k = 1, \ldots\}$ undergo only *elastic* diffractive scattering, i.e. the diffractive sub-section of the T-matrix is diagonal in their basis. The expansion (4.9) is illustrated below:

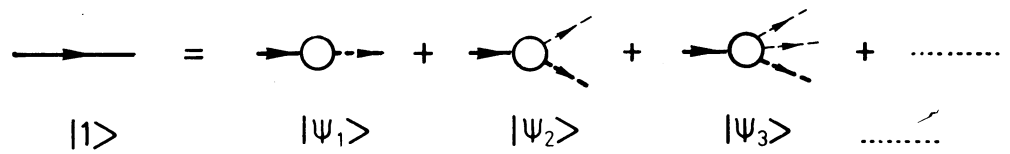

The physical inelastic diffractive states $|2\rangle$, ..., may be expanded similarly

$$|i\rangle = \sum_{k=1} U_{ik}\, |\psi_k\rangle \quad \text{where } i = 2, 3, \ldots \ . \tag{4.10}$$

Introduce the notation (where S is the S-matrix)

$$S = 1 + iT = 1 - t \ . \tag{4.11}$$

Assume that the diffractive amplitudes T_{ij}, i, j = 1, 2, ..., are purely imaginary so that t-matrix is real. The eigenvalues of this matrix represent elastic scattering of the states $|\psi_k\rangle$:

$$t_k = \langle \psi_k | t | \psi_k \rangle \quad k = 1, 2, \ldots . \tag{4.12}$$

In the following we shall work in the impact parameter representation. We impose the condition that the eigenamplitudes do not exceed the limit of maximal absorption (the "Black Disk limit"):

$$0 \leq t_k(b) \leq 1 \quad \text{for all k and b} . \tag{4.13}$$

From this it follows trivially that

$$|t_k(b)|^2 \leq t_k(b) . \tag{4.14}$$

When this inequality is written in terms of the physical cross-sections, the Pumplin bound Eq. (4.8) is obtained.

Further insight into the physical picture underlying the bound (4.8) may be obtained from the following considerations[77]. According to Eqs. (4.9) and (4.12) elastic scattering of the proton may be thought of as a three-step process: first, the physical proton decomposes to the eigenstates $|\psi_k\rangle$, the probability that it is the k'th eigenstate being $P_k = |U_{1k}|^2$, then the eigenstates scatter elastically with respective amplitudes $t_k = \langle \psi_k | t | \psi_k \rangle$, and finally, they recombine to the physical proton.

The total cross-section (= the elastic amplitude) is given by the average value of the eigenamplitudes weighted by their respective couplings to the physical proton state

$$\sigma_{tot}(b) = t_{11}(b) = \sum_{k=1} |U_{1k}|^2 \langle \psi_k | t | \psi_k \rangle \equiv \sum_{k=1} P_k t_k \equiv \langle t_k \rangle . \tag{4.15}$$

The corresponding formula for the inelastic diffractive cross-section is

$$\sigma_{diff}(b) = \tfrac{1}{2}\left[\langle t_k^2 \rangle - \langle t_k \rangle^2\right] \equiv \tfrac{1}{2} D^2(b) . \tag{4.16}$$

Thus, we see that *the total inelastic diffractive cross-section is given by the squared dispersion of the spectrum of the eigenamplitudes that couple to the two-proton state.* Equations (4.15) and (4.16) are illustrated below:

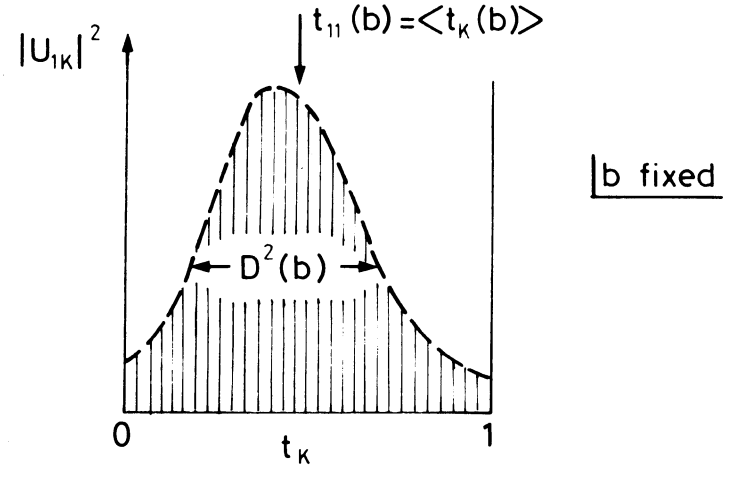

The result Eq. (4.16) expresses mathematically in a very clear way the fundamental idea of Good and Walker that diffractive dissociation processes are *regeneration processes*. In particular, we see that *if all the diffractive eigenstates ("bare particle" states in the Good-Walker language) were absorbed equally strongly, so that the eigenamplitude spectrum were a δ-peak, there would be no inelastic diffraction.* An example of such an extreme case is that of the elastic amplitude saturating the black disk limit $t_{11}(b) = t_k(b) = 1$.

We also see from Eq. (4.16) that a large cross-section for inelastic diffraction necessarily implies large variations in the opacities of the strongly coupling eigenamplitudes, and vice versa. The saturation of the Pumplin bound corresponds to a distribution that consists of two δ-peaks, one at $t_k = 0$ [weight $1 - t_{11}(b)$] and another at $t_k = 1$ [weight $t_{11}(b)$].

The phenomenological relevance of the bound was studied by Caneschi et al.[78]. If the impact profiles $\sigma_{el}(b)$ and $\sigma_{tot}(b)$ are known, Eq. (4.8) provides an upper bound for the diffractive inelastic cross-section:

$$\sigma_{diff}(b) \leq \tfrac{1}{2}\,\sigma_{tot}(b) - \sigma_{el}(b) \ . \tag{4.17}$$

This bound was applied to high-energy proton-proton scattering. Inserting the values of $\sigma_{tot}(b)$ and $\sigma_{el}(b)$ taken from an impact parameter analysis of ISR elastic scattering data[79] on the right-hand side, the bound shown in Fig. 27 was obtained.

The total inelastic diffractive cross-section in proton-proton scattering is experimentally of the same order as the elastic cross-section, i.e. between 7 and 9 mb at the FNAL-ISR energy range. One may then attempt to "squeeze" this amount of cross-section below the bound of Fig. 27. By doing this exercise one quickly convinces oneself that *$\sigma_{diff}(b)$ must be much more peripheral than $\sigma_{el}(b)$.*

In the previous section we concluded that experiments support the peripherality of inelastic diffraction. We now see that this peripherality is a direct consequence of s-channel unitarity. The constraint that elastic scattering of the diffractive *eigenstates* of the S-matrix should obey black disk limit reflects itself in the *physical* diffractive amplitudes, forcing inelastic diffraction to be peripheral, since elastic diffraction is central.

A further interesting consequence of the Pumplin bound should be mentioned. We have already noticed that this bound implies that if elastic scattering saturates the upper unitarity bound, then inelastic diffraction must vanish. Inverting this argument one concludes that *a non-vanishing $\sigma_{diff}(b)$ gives rise to an effective upper bound for the elastic amplitude below the black disk limit.* The saturation of such a bound would provide a simple explanation for the empirical observation that the value of the elastic amplitude at $b = 0$ stays nearly independent of energy over the Fermilab-ISR energy range at 75% of the black disk limit[10,74,75,77,80,81].

4.3 Rescattering effects and Pomeranchukon cuts

The theoretical status of this very active field is summarized by Dr. Schwimmer[7]. Since I have nothing to add to (or to subtract from) his excellent review, I shall simply discuss a few phenomenological applications of the new theoretical ideas.

For elastic scattering, as was discussed by Dr. Schwimmer, theory suggests very strongly that the negative rescattering cuts should be stronger than the positive AFS-type cuts. The net cut contribution is then negative. In the eikonal model and the Gribov-Reggeon calculus approaches, the rescattering cuts are actually twice as strong as the positive diffractive cuts*). Hence, in these approaches, the magnitude of the leading cut is that given by the AFS-type cuts but with its sign reversed. This cut structure is illustrated in Fig. 28. It implies, among other things, that if the non-absorbed "driving force" component (the short-range correlation component in Fig. 28) stays constant while σ_{diff} rises then the inelastic cross-section should *decrease* instead of increasing[74]. One may therefore conclude that the rise of σ_{inel} must have its origin in non-diffractive dynamics.

In the multiperipheral approach, rising total cross-sections may be described by taking the Pomeron intercept to be above one. Unitarity in the s-channel is preserved by rescattering contributions. For a limited range of energy, the average multiplicity grows as a power of s. It would be very interesting to study if this approach can provide a quantitative explanation for the 25-30% rise of the (normalized) single particle plateau height observed at the CERN ISR[82].

Snider and Wyld[83] and Crozier and Webber[84] carried out a phenomenological analysis of the influence of absorption on multiplicity distributions using the eikonal model approach. They found that in the simple versions of the model the absorptive effects were too great to be consistent with data and proposed mechanisms for their suppression. Although their analyses have shortcomings, the most important being that the effects due to inelastic diffraction were either ignored[83] or treated very crudely[84], they are extremely interesting and provide much insight into the effect of absorption on the structure of multiparticle distributions.

The influence of inelastic diffractive channels on elastic scattering was studied in Refs. 77 and 85 using the multi-channel eikonal model approach. Since not much is known about the off-diagonal transition amplitudes, inelastic diffraction was treated as a single process. Such a two-channel approximation is obviously oversimplified and, consequently, its quantitative results should be taken with caution. The qualitative features of the results, however, are more reliable and are very interesting. In Ref. 77 it was found that once inelastic rescattering effects are included in the analysis, the elastic eikonal element $\Omega_{11}(b)$ must deviate strongly from the standard Chou-Yang eikonal[86]. The Chou-Yang eikonal is determined by the overlap of two matter distributions whose shape is given by the electromagnetic form factors. Thus, the above result suggests that the proton matter and charge distributions are different. This is not particularly surprising. Results from deep inelastic electroproduction[87] imply that a large part of the proton momentum is carried by neutral constituents. There is no good reason to expect that the spatial distribution of the neutral constituents (gluons?) should be the same as that of the charged ones.

---

*) Here we simplify. The Gribov calculus cutting rules actually suggest the following decomposition: i) Positive AFS-type cuts (relative weight +1); ii) Negative absorptive corrections to the short-range amplitude (relative weight -4); iii) A positive multiparticle contribution with *double* multiplicity density (relative weight +2); the total cut contribution is then +1-4+2 = -1.

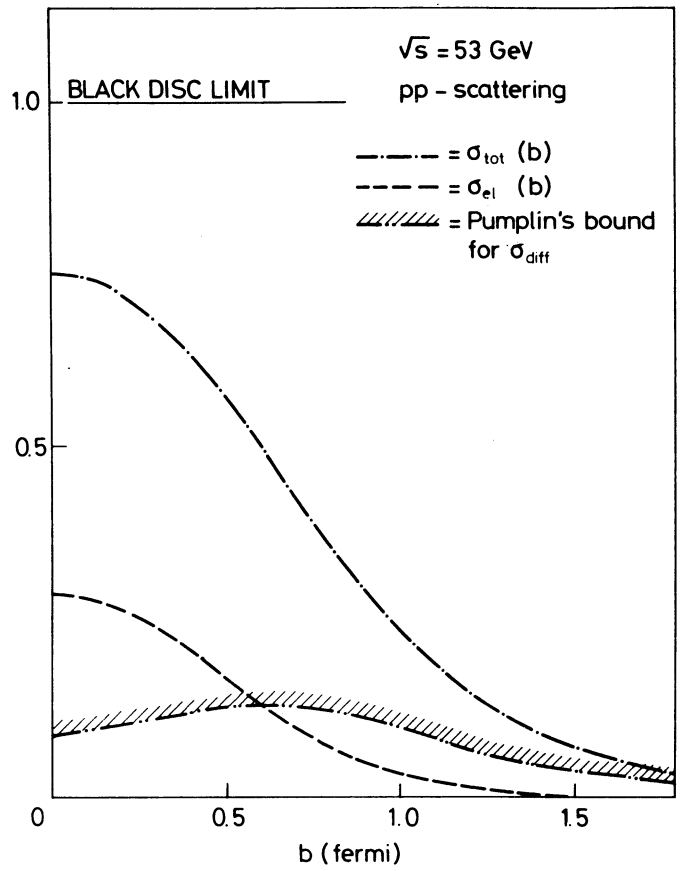

Fig. 27 Upper bound for the cross-section of inelastic diffraction $\sigma_{diff}(b)$ versus b, for pp scattering at $\sqrt{s}$ = 53 GeV (////////). Also shown are the impact parameter distributions for the pp total (— • — • —) and elastic (— — — —) cross-sections (from Ref. 78).

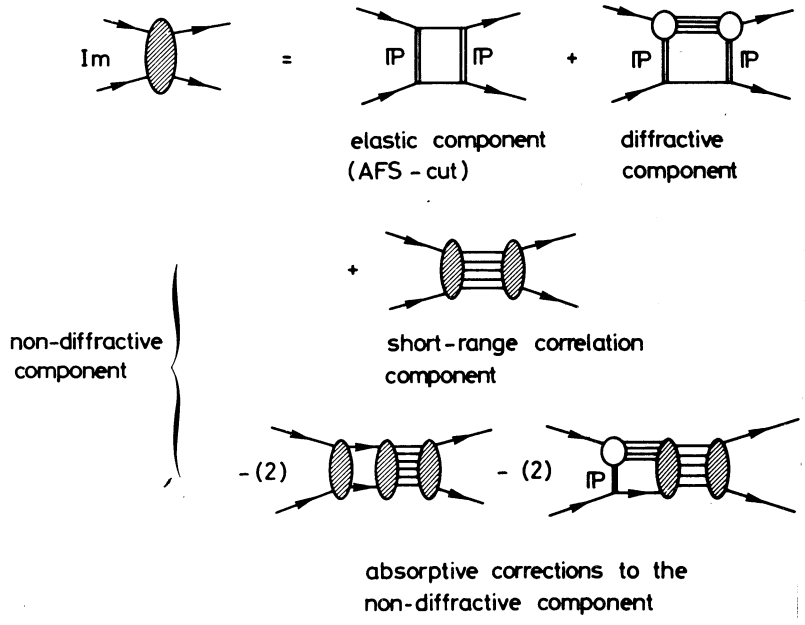

Fig. 28 Illustration of the cut-structure of the Pomeron

In inelastic diffraction, the rescattering effects are much stronger than those in elastic scattering. An analysis of the results of the previous Chapter using the eikonal model approach shows that the peripherality of $\sigma_{diff}(b)$ is caused by strong absorptive cuts. This is discussed in Refs. 77, 78, and 80. The reason why the cut-corrections to the off-diagonal amplitudes are larger than those to the diagonal ones is not particularly easy to see in the complicated (but realistic) case of large absorption and strong inelastic diffraction. In the limit of weak absorption and small $\sigma_{diff}/\sigma_{el}$ ratio, however, it can be seen as follows. Consider the two-channel eikonal model

$$\begin{pmatrix} t_{11} & t_{12} \\ t_{21} & t_{22} \end{pmatrix} = 1 - e^{-\begin{pmatrix} \Omega_{11} & \Omega_{12} \\ \Omega_{21} & \Omega_{22} \end{pmatrix}} \tag{4.18}$$

Assume that $\Omega_{12} \ll \Omega_{11} \approx \Omega_{22}$. Expand the amplitudes t_{11} and t_{12} as

$$t_{11}(b) = \Omega_{11}(b) - \frac{1}{2!}\left[\Omega_{11}^2(b) + \Omega_{12}^2(b)\right] + \ldots \tag{4.19a}$$

$$t_{12}(b) = \Omega_{12}(b) - \frac{1}{2!}\,\Omega_{12}(b)\left[\Omega_{11}(b) + \Omega_{22}(b)\right] + \ldots \,. \tag{4.19b}$$

The ratio of the leading absorption correction to the Born term is in the former case $\approx -\frac{1}{2}\Omega_{11}(b)$ and in the latter case $\approx -\Omega_{11}(b)$, i.e. the absorption is about twice as strong for inelastic diffraction as for elastic scattering.

Tsarev[88], Andrejev[89], Berger and Irving[90] and Berger and Pirilä[91] have investigated absorptive corrections to Deck-type models of low-mass excitation. From their very thorough analysis, Berger and Pirilä concluded that although absorption has a strong effect on the momentum transfer distributions, other distributions (e.g. mass, decay angles) are modified only little.

Finally, we should mention the puzzling problem of factorization. We have argued in this Section that absorptive cuts should be strong. Since Regge cuts do not factorize, one should expect to see violations of factorization. Experimentally, however, factorization works surprisingly well (for integrated quantities, the upper limit for its violation is of the order of $\lesssim 10\%$)[1-4]. A clue to the solution of this puzzle may be provided by the work of Pumplin and Kane[92]. These authors studied the breaking of factorization caused by rescattering effects, using several prescriptions to calculate the absorptive corrections. They found that even very strong cuts cause only minor violations of the factorization relations. This somewhat surprising result of "numerical factorization" is probably related to the fact that the hadrons all have about the same "size" in impact parameter.

Accurate Fermilab data on low-mass nucleon excitation using kaon and pion beams will be crucial for learning about the rescattering effects. Processes which are difficult to measure but which also would be very interesting to study are the double excitation reactions:

$$\gamma p \to \phi(n\pi^+),\ \phi(p\pi^+\pi^-) \tag{4.20a}$$

$$\gamma p \to \psi(n\pi^+),\ \psi(p\pi^+\pi^-)\ . \tag{4.20b}$$

In these processes, absorptive effects are expected to be rather weak [$\sigma_{tot}(\phi p)$ is ≈ 10 mb

and $\sigma_{tot}(\psi p)$ is only $\approx$ 1-2 mb!]. A comparison between the differential cross-sections of the above reactions and those of the corresponding hadron-initiated processes for low ($N\pi$) and ($N\pi\pi$) masses would provide very useful information on the strength of absorption effects.

5. EXCITATION OF LARGE MASSES AND THE TRIPLE-POMERON

The diffractive excitation of high mass systems was discovered two years ago at the CERN ISR. Since then, many experiments at the ISR and Fermilab have confirmed the existence of such processes, and an abundance of information on their properties has been collected. Much of the data became available last year at the time of the London Conference. The experimental situation there was summarized by Derrick[93] and Loebinger[94], and the triple-Regge phenomenology was discussed by Roy[95]. Since then, not much new data have become available. Hence I shall simply make a few phenomenological remarks. More detailed discussions on the properties of large-mass diffraction can be found in the summaries mentioned above, as well as in the talk by Dr. Goulianos[96] at this Conference and in Refs. 1 to 4.

5.1 Inclusive spectra

Let us look at the single particle inclusive process

$$p + p \to p + X \,. \tag{5.1}$$

At high energies, the invariant mass spectrum $d\sigma/dt\, d(M^2/s)$ of this process plotted versus M^2/s looks as follows:

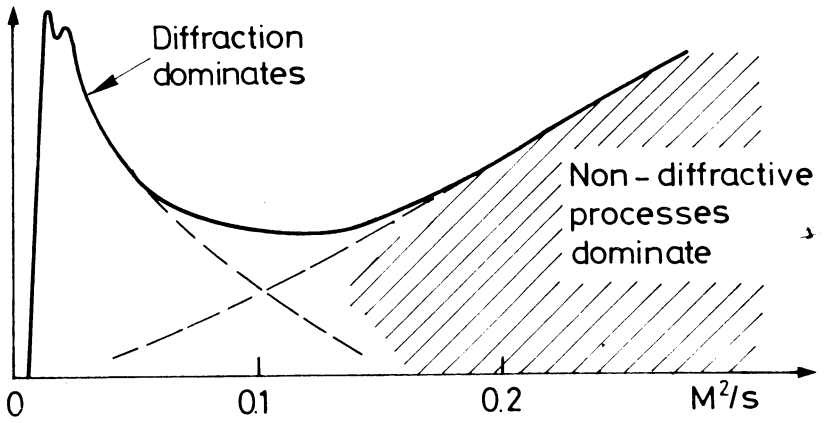

In this distribution, the peak near $M^2/s \approx 0$ [$x = 1 - (M^2/s) \approx 1$] is due to diffractive production. The region $M^2/s \gtrsim 0.1$ is dominated by non-diffractive processes. A crude separation of the two mechanisms can be obtained by applying a cut at $M^2/s = 0.1$.

The phenomenological analysis of the spectra is usually carried out using the triple-Regge formalism[97]. In this approach, diffractive excitation is described by Pomeron-Pomeron-meson (PPM) and triple-Pomeron (PPP) contributions. At small t-values, the M^2-dependence of the former component is $\sim M^{-3}$ and that of the latter one $\sim M^{-2}$. At fixed M^2/s, the PPM contribution decreases with increasing s as $\sim 1/\sqrt{s}$, whereas the PPP component

scales. In fits to the data, many other triple-Regge components are also included. They correspond to non-diffractive production (MMP, MMM, $\pi\pi$P, $\pi\pi$M, ...) and to inference between diffractive and non-diffractive production (MPM, MPP, ...).

In two contributions to this Conference, the Fermilab-Dubna-Rockefeller-Rochester Collaboration[98] has presented extensive data on the process

$$p + d \to X + d \tag{5.2}$$

for energies ranging from 50 to 400 GeV/c. In order to compare their data with previous results of the diffractive excitation of the proton, they divided their spectra by the deuteron form factor $F_d(t)$ evaluated at the appropriate t-values. Figure 29 shows a comparison between the FDRR Collaboration data and data from Fermilab[99] and ISR[100]. The agreement at low and at high values of M^2 is good, within the experimental error of $\approx 10\%$. In the region 5 GeV$^2 \leq M^2 \leq 0.05s$, the spectra show a clean M^{-2} behaviour. This shows the presence of a significant triple-Pomeron component.

Figure 30 compares spectra from the FDRR Collaboration at $t = -0.05$ GeV^2 and the three energies $s = 570$, 1045, and 1463 GeV^2 with the results obtained by the Columbia-Stony Brook Collaboration[101] and by the ANL-NAL Collaboration[102]. The spectra are multiplied by a factor $\nu/s \approx M^2/s$ to emphasize their M^{-2} dependence in the region $0.005 \lesssim M^2/s \lesssim 0.025$. While the data of the FDRR and C-SB Collaborations seem to be in good mutual agreement, the ANL-NAL data lie 60-70% above them. This discrepancy is hard to understand, since the latter data come from a bubble-chamber experiment and their normalization should be good within 10-20%.

A remark should be made here. The results of the Columbia-Stony Brook experiment were published in Physical Review Letters two months ago. In the article, the authors discuss the results of their experiment but they do not present the original data, except for some examples of them in two figures. The C-SB Collaboration data points shown in Fig. 30 are taken from one of these figures. However, in the text, the authors say that: The fall of the mass spectrum is much sharper than $1/M^2$ and typically has the form $a + c/M^\alpha$, with $\alpha = 3$-4. Thus, either the sample shown in Fig. 30 does not represent well the general behaviour of the C-SB Collaboration results or the above exponent 3-4 refers to the behaviour of the spectra in the region very near to the threshold.

The curves shown in Fig. 30 correspond to triple-Regge fits by Field and Fox[103], Roy and Roberts[104], and Roberts[105]. The analysis of Roy and Roberts was performed over a year ago. It included the ANL-NAL data and many other data not shown in Fig. 30, but not the new FDRR and C-SB Collaboration results. The new fit of Roberts uses only the FDRR Collaboration data.

In conclusion, there seems to be good experimental evidence for an important triple-Pomeron component. However, the data are partially inconsistent. Further experimental work is needed to get an accurate determination of the size of the PPP component.

Estimates for the total inelastic diffractive cross-section σ_{diff} in proton-proton scattering have been presented by many authors[106]. They have been obtained by integrating either experimental spectra of $pp \to p + X$, or triple-Regge fits to these spectra. Although the results vary considerably, they show that σ_{diff} is of the same order as the elastic

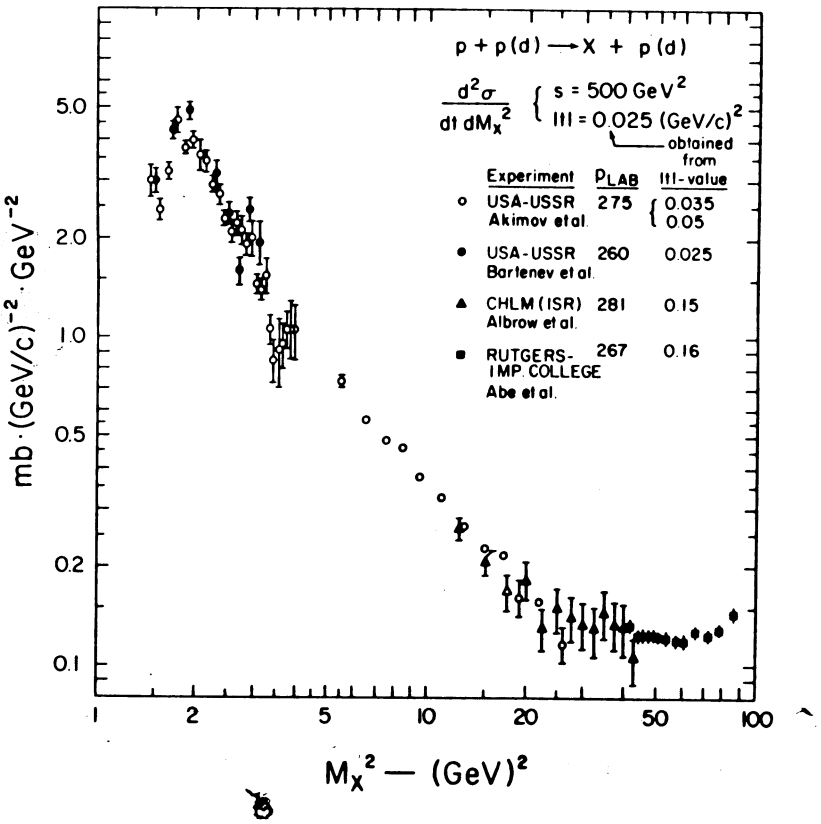

Fig. 29 Differential cross-sections for pp → Xp versus M_X^2 for $s \sim 500$ GeV^2 and $|t| = 0.025$ (GeV/c)^2, obtained from the listed $|t|$-values by extrapolation. The data points of Akimov et al. were extracted from data on p + d → X + d (from Ref. 96).

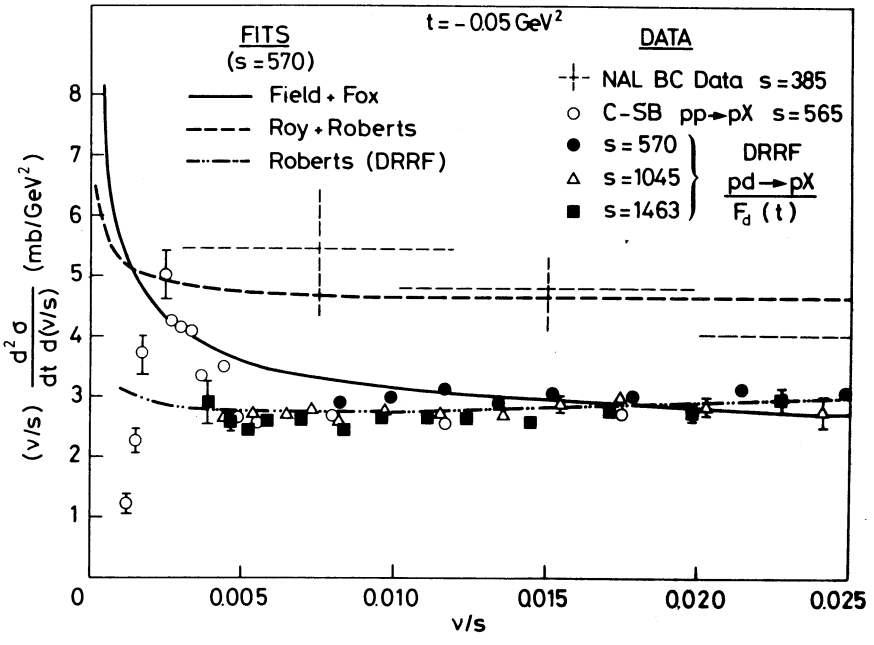

Fig. 30 Invariant mass distributions multiplied by $\nu/s \approx M^2/s$ for the process pp → p + X. The data are from Refs. 98, 101, and 102. The curves are triple-Regge fits from Refs. 103-105.

cross-section, i.e. 6-9 mb in the Fermilab-ISR energy range. The energy dependence σ_{diff} is not well determined. The presence of a large PPP component should imply that σ_{diff} rises considerably over the Fermilab-ISR energy range. In the Columbia-Stony Brook experiment, however, no rise is observed for $130 \leq E_{lab} \leq 300$ GeV. Further work is needed to clarify the question of the s-dependence of σ_{diff}.

5.2 Decay distributions

In Section 3 we analysed the dependence of the average spin of a diffractively produced system on the mass of this system by interpreting the excitation vertex as a "Pomeron-particle" scattering amplitude. This analogy raises several questions, for example: How do the average multiplicities of Pomeron-particle collisions compare with those of particle-particle collisions? The answer is well known[107] -- the multiplicities are indeed very similar. In more detail: Are the single particle distributions similar too? This question was studied by the Michigan-Rochester Collaboration[108]. Figure 31 shows the π^- inclusive distribution in the rest frame of the system X of the process (5.1) for "Pomeron-proton" ($1 \leq M^2 \leq 20$ GeV^2) and "Reggeon-proton" ($20 \leq M^2 \leq 50$ GeV^2) collisions. The solid curve shows the spectra of the on-shell process

$$\gamma + p \to \pi^- + X \tag{5.3}$$

at total energy squared $s = 18.3$ GeV^2. The three distributions are seen to be very similar. Theoretically, the similarity of Pomeron-particle and particle-particle collisions is not unexpected, and is predicted, e.g., by the multiperipheral model[109].

6. RARE DIFFRACTIVE PROCESSES: NEW RESULTS

6.1 Double excitation and Pomeron factorization

The experimental study of double diffractive excitation at accelerator energies has been hampered by two effects:

a) these processes are strongly suppressed by a kinematic t_{min} effect, and

b) the non-diffractive background is large (much larger than in the single excitation processes).

At the ISR energies both these handicaps are largely removed and the experimental study of the double diffractive processes is feasible.

Two beautiful experiments by groups at the CERN ISR have, for the first time, yielded reliable data on double dissociation processes. Although these data are not yet fully analysed, several interesting results have already been obtained.

The Aachen-UCLA-Riverside-CERN Collaboration[110] has measured the reaction

$$pp \to (p\pi^+\pi^-)_1 + X_2 \tag{6.1}$$

at energies $\sqrt{s} = 45$ and 53 GeV. They use a multiparticle spectrometer for the detection of the system $(p\pi^+\pi^-)_1$, supplemented in the opposite arm by a multiwire proportional chamber telescope, which detects decay particles from X_2. Selecting events where X_2 involves more than a single proton, the momentum spectrum of the $(p\pi^+\pi^-)_1$ system (which is equivalent to the missing mass spectrum of X_2) shows a clear peak near $p = p_{max}$. Such a peak is an unmistakable signal for the occurrence of double diffractive dissociation.

To test factorization, the authors compare the experimental rate of the process (6.1) to those of the processes

$$pp \to (p\pi^+\pi^-)_1\ p_2\ , \tag{6.2a}$$

$$pp \to p_1 X_2\ , \tag{6.2b}$$

$$pp \to p_1 p_2\ , \tag{6.2c}$$

measured in the same experiment. Geometrical cuts are applied to select events with $m(p\pi^+\pi^-) \leq 1.85$ GeV and the system X_2 having low mass. Factorization implies that the ratio of the rates of the processes (6.2b) and (6.2c) should be the same as that of the processes (6.1) and (6.2a). The results are given in the table below. They are seen to be consistent with factorization.

Table 1

Test of factorization hypothesis at $\sqrt{s}$ = 45 GeV. The quoted errors are statistical only; systematic errors are estimated to be of similar magnitude. The values of B/A should be reduced by about 5% to correct for the finite t-range.

$\lvert t\rvert$-range $(GeV)^2$	$A = \frac{(dN/dt)[p_1X_2]}{(dN/dt)[p_1p_2]}$	$B = \frac{(dN/dt)[(p\pi^+\pi^-)_1X_2]}{(dN/dt)[(p\pi^+\pi^-)_1p_2]}$	B/A
0.15 - 0.275	$(1.49 \pm 0.07) \times 10^{-2}$	$(1.76 \pm 0.18) \times 10^{-2}$	1.18 ± 0.14
0.275 - 0.40	$(3.44 \pm 0.20) \times 10^{-2}$	$(4.18 \pm 0.52) \times 10^{-2}$	1.21 ± 0.18
0.40 - 0.525	$(10.32 \pm 0.80) \times 10^{-2}$	$(10.46 \pm 1.34) \times 10^{-2}$	1.02 ± 0.15

The Pavia-Princeton Collaboration[111] has collected data on the exclusive reaction

$$pp \to (p\pi^+\pi^-)(p\pi^+\pi^-) \tag{6.3}$$

at the ISR energies $\sqrt{s}$ = 23, 31, and 53 GeV using the Split Field Magnet facility. This apparatus makes possible a measurement of the momenta of all the six particles in the above process. A clean double diffractive signal is seen.

A detailed study of the energy dependence, mass distributions and differential cross-sections of the process (6.3) was carried out. Figure 32 shows the cross-sections of the double dissociation sample of this process at the three energies (5.5 ± 1.1 μb, 5.1 ± 1.0 μb, and 4.9 ± 1.0 μb at $\sqrt{s}$ = 23, 31, and 53 GeV, respectively). Factorization predictions calculated from data on single excitation $pp \to p(p\pi^+\pi^-)$ and on elastic scattering are also shown. The agreement is impressive.

For further discussion of the results of this interesting experiment see Dr. Mantovani's talk[113].

The Saclay-Ecole Polytechnique-Rutherford Collaboration[114] studied the process

$$K^-p \to \underbrace{Q^-}_{\hookrightarrow K^{*0}\pi^-} + \underbrace{N^{*+}}_{\hookrightarrow n\pi^+} \tag{6.4}$$

ROCHESTER - MICHIGAN

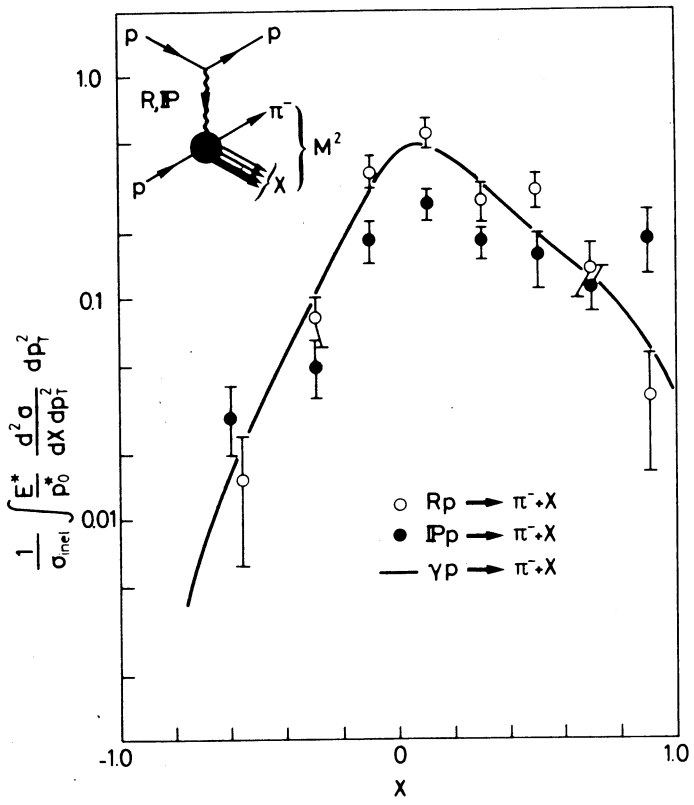

Fig. 31 Production spectra for π^- mesons produced in the virtual Reggeon-proton ($20 < M^2 < 50$ GeV^2) and Pomeron-proton ($1 < M^2 < 20$ GeV^2) collisions, at an incident proton momentum of 102 GeV/c. Positive x corresponds to π^- emission along the direction of R (IP) in the M^2 rest frame. The solid curve corresponds to the spectra for π^- mesons produced in on-mass-shell γp collisions ($s = 18.3$ GeV^2) (from Ref. 109).

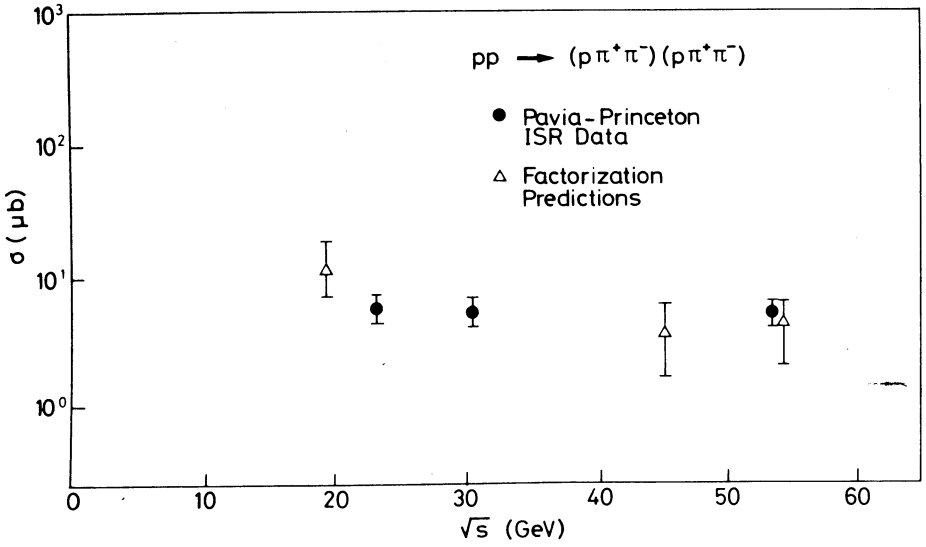

Fig. 32 Cross-section for double diffraction dissociation reaction $pp \to (p\pi^+\pi^-)(p\pi^+\pi^-)$ at c.m.s. energies 23, 31, and 53 GeV. Errors are statistical only. Factorization predictions from the data of Refs. 19 and 112 are also shown for comparison (from Ref. 111).

at 14.3 GeV/c. The cross-section for this process was found to be of the order of 10 μb, which agrees within ≈20% with what may be expected from Pomeron factorization.

6.2 Double Pomeron exchange

Multiperipheral processes with two or more Pomerons exchanged in the chain are theoretically extremely interesting. There is an abundance of literature on their expected properties and on the self-consistency problems which they raise. Experimental searches for double-Pomeron exchange (DPE) processes have provided upper limits for their cross-sections which are generally of the same order as the theoretical predictions[115-117]. No compelling evidence for the existence of DPE processes has been obtained so far.

In a paper presented to this Conference, the Aachen-Riverside-CERN-Genoa-Munich Collaboration[118] reported evidence for the observation of the DPE process

$$p + p \rightarrow p + \underbrace{X}_{\text{two charged particles}} + p \qquad (6.5)$$

at the CERN ISR. Although their results have already been summarized by Dr. Layter[119], I wish to comment briefly on them here.

The experimental set-up used by the ARCGM Collaboration is shown in Fig. 33. It consists of two separate elements: the multiwire proportional chambers located above and below the beam pipe in both arms, and the 4π counter system comprising counter groups in both arms and counters surrounding the intersection region.

For the DPE search, events were obtained at ISR beam energies of 15, 22, 26, and 31 GeV/c. The trigger used was essentially the following: A fast charged particle should be detected by the multiwire proportional chambers on each side, no particles should be seen in the "veto" counter set-ups and two charged particles should be detected by the central set-up. A momentum balance test was used to ensure that no unobserved neutral particles were present. The rapidity structure of the events accepted by the above trigger is shown in the lower half of Fig. 33.

For events satisfying the above trigger, assuming beam momentum for the leading particles, the distribution $d^2\sigma/dt_a dt_b$, $t_i = -p^2\theta_i^2$, was examined. No correlation between t_a and t_b was found. A fit to the data by the formula $d^2\sigma/dt_a dt_b = a\, e^{b(t_a+t_b)}$ yielded the value $b = 8.6 \pm 1.8\ (\text{GeV/c})^{-2}$. The values of a and the resulting DPE cross-sections are given in the table below for each ISR energy. These cross-sections are shown also in Fig. 34, together with theoretical predictions for σ_{DPE} by Chew and Chew[116] and by Roy and Roberts[117].

AACHEN - RIVERSIDE - CERN -
GENOVA - MUNICH COLLABORATION

DOUBLE POMERON SET-UP

ISR I-6:

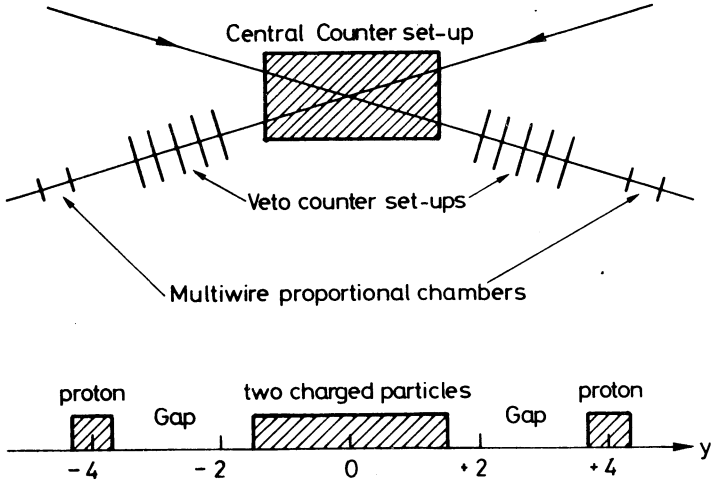

Fig. 33 Schematic view of the experimental apparatus at intersection I-6 of the CERN ISR. The drawing is not to scale. Lower figure shows rapidity distribution of events accepted by the apparatus (from Ref. 118).

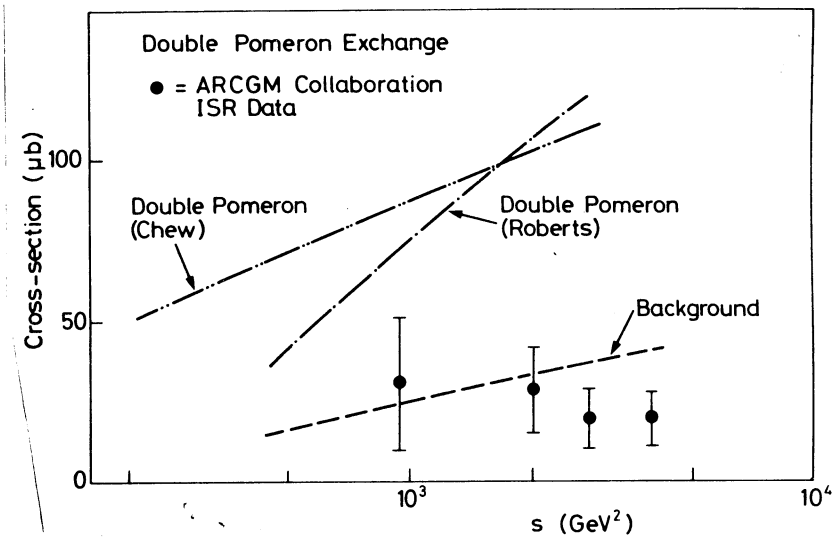

Fig. 34 Cross-section measured in the ARCGM Collaboration experiment versus energy. The upper curves are theoretical predictions for the double-Pomeron exchange to the processes $pp \to p + (2\pi) + p$ (Chew and Chew, Ref. 116) and $pp \to p + X + p$ (Roberts, Ref. 117). The lower curve is a prediction for non-diffractive "background" contribution to the latter process in the kinematical region $|x_1|, |x_2| \geq 0.9$. Since this region differs from that defined by the apparatus of Fig. 33, the curve should not be directly compared to the data.

Table 2

Accessible t-ranges, numbers of DPE and background events, and cross-sections at each ISR energy. The number of background events is estimated from a Monte Carlo calculation for a diffractively produced $p\pi^+\pi^-$ state. This contamination has been removed in the determination of the DPE cross-section.

ISR energy	15	22	26	31
t_{low}	0.0091	0.0196	0.0266	0.0364
t_{high}	0.0238	0.0549	0.0722	0.1066
SDD events	13 ± 4	24 ± 8	6 ± 2	5 ± 1
DPE events	46 ± 29	207 ± 101	62 ± 30	54 ± 22
a ($\mu b/GeV^4$)	2211 ± 1187	2048 ± 809	1390 ± 582	1434 ± 537
σ (μb)	30 ± 20	28 ± 14	19 ± 9	19 ± 8

Although the geometry of the ARCGM set-up is well-fitted for the study of double-Pomeron exchange processes and probably most of the events observed are due to the DPE mechanism, the evidence obtained cannot be regarded as conclusive, not even concerning the mere *existence* of DPE processes. The crucial point which is missing in this experiment -- as well as in all the earlier experiments -- is *signal*. Since one is dealing with very small cross-sections ($\approx$ 20 μb!) conclusions which are sensitive to theoretical background estimates should be treated with caution. To be really convinced that one is observing DPE processes one would like to see an experimental signal characteristic of DPE above a smooth background.

To emphasize the above point I have drawn in Fig. 34 a curve corresponding to the cross-section of *non-double Pomeron events which satisfy the DPE kinematical configuration and make up a background for the real DPE events*. This curve is calculated from the Mueller-Regge model using parameters obtained from fits to the single excitation process $pp \to p + X$ [117]. I am of course, not trying to claim that this background explains the cross-section measured by the ARCGM Collaboration. My only motive for showing it is to stress the need for a measurement which does not depend on theoretical background estimates.

An excellent experimental set-up for the study of the double-Pomeron exchange processes would be similar to that of the ARCGM Collaboration, but with the additional possibility of measuring the *momenta* of the particles. By plotting the density of the events in the x_1x_2-plane ($x = 2p_\parallel/\sqrt{s}$), the double-Pomeron exchange processes would show up as a peak in the corner $-x_1 \approx x_2 \approx 1$:

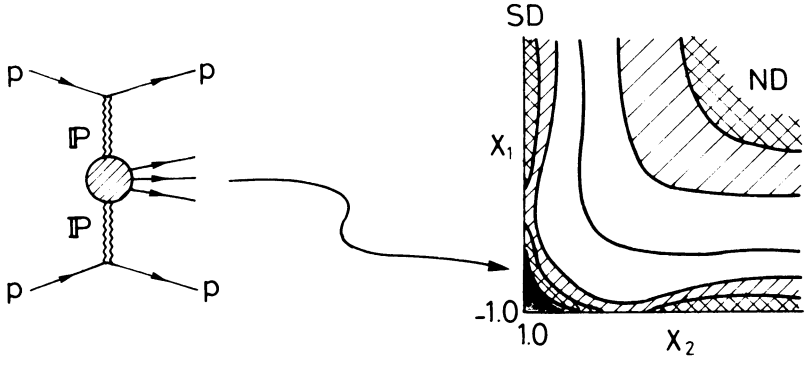

Estimates based on the triple-Regge formalism and Pomeron factorization indicate that this peak would be large and sharp enough to be clearly visible.

Double-Pomeron exchange processes are theoretically so interesting and important that -- we emphasize -- an experimental program devoted exclusively to their search and study is well worth an effort and should have a high priority on the list of future Fermilab, CERN SPS and ISR experiments.

7. CONCLUSIONS

Some of the lessons from recent data can be summarized as follows:

A) The energy dependence of low-mass diffraction dissociation processes is similar to that of elastic scattering;

B) The diffractive transitions $\pi \to (\pi\pi\pi)$ and $K \to (K\pi\pi)$ are extremely similar. This holds, not only for the mass-distributions, but for the spin structure as well;

C) The empirical systematics of the helicity conservation properties of Pomeron couplings are absolutely puzzling. No theoretical understanding of them exists;

D) The average spin of a diffractively produced system grows linearly with the mass of this system. Simple impact parameter ideas are capable of explaining this result;

E) The first partial-wave analysis of the process $pp \to p(p\pi^+\pi^-)$ was reported. The results show that the "N*(1470)" peak seen in the $(p\pi^+\pi^-)$ mass spectrum is due to a $3/2^-$S state. The "N*(1700)" peak is due to a $3/2^-$P state, but receives contributions also from the $5/2^+$ wave. The phases of these waves [relative to that of the $1/2^+P(\Delta^{++}\pi^-)$ "background" wave] do not vary with the $(p\pi^+\pi^-)$ mass;

F) Important new results on the decay of diffractively produced baryonic systems were reported. They support Deck-type models. However, large baryon exchange Deck contributions are needed to explain the data;

G) There is experimental evidence for the peripherality of low-mass diffraction dissociation in proton-proton collisions;

H) There is good experimental evidence that the triple-Pomeron coupling is large;

I) Experiment supports the bootstrap idea that Pomeron-particle collisions are similar to particle-particle collisions;

J) Detailed results on double diffractive dissociation processes at the CERN ISR were reported. Factorization seems to work well;

K) Evidence for the exclusive double-Pomeron exchange process $pp \to p + (\pi^+\pi^-) + p$ at the CERN ISR was reported. The measured cross-section is ≈ 20 μb and approximately independent of energy.

Let us attempt to list some crucial experiments that will throw light on the validity of current theoretical ideas on inelastic diffraction:

i) Analyses of the helicity conservation properties of as many diffraction dissociation processes as possible;

ii) Partial wave analyses of nucleon dissociation processes;

iii) S-channel amplitude analyses of $pp \to p(n\pi^+)$;

iv) Experiments that would yield information on the strength of absorptive effects (for example, study of the $t = -0.2$ GeV^2 dip region in nucleon dissociation);

v) Fermilab and CERN SPS data on $Kp \to K + X$, $\pi p \to \pi + X$, $Kp \to p + X$, and $\pi p \to p + X$. Detailed tests of factorization;

vi) Two domains which we have not discussed in this review, but on which accurate high-energy data would be extremely useful for learning about rescattering effects, are photoproduction (especially of ϕ mesons!) and experiments on nuclei;

vii) An experimental program for the study of double-Pomeron exchange processes.

As an over-all conclusion, it seems to me that much progress has indeed been made since the Aix Conference two years ago. However, there is a lot of work still to do before we can expect the Pomeranchuk singularity to finally reveal her ultimate secrets to us. One outstanding problem is: Theory predicts strong cut contributions to the Pomeranchuk amplitude, but experimentally the Pomeron seems to behave as a Regge pole. Why is this so?

Finally, I wish to sincerely apologise to all those authors whose work I have misrepresented or not discussed at all, or whose (often beautiful) data I have not shown. The tremendous number of new results and the short time allocated me for preparing this review, together with my limited knowledge, forced me to restrict my discussion to a few problems which interested me particularly, and to ignore many other equally important problems. Therefore, this report should be regarded as a quick survey of a few exciting developments, rather than a well-balanced review of the status of the field of inelastic diffraction.

Acknowledgements

During the last year I have benefited from the experience and advice of too many of my colleagues to name them here. I should like, however, to express my gratitude particularly to those people who have helped me in the preparation of this report: L. Caneschi, T. Ferbel, K. Fiałkowski, G. Goggi, P. Grassberger, S.A. Jackson, R.J.N. Phillips, S. Ratti, R.G. Roberts, P. Schmid, A. Schwimmer and R. Worden. The clarity of this written version of the report has been greatly improved by Dr. R. Worden's numerous suggestions.

Finally, I would like to acknowledge the support of the Herman Rosenberg Foundation and the Science Research Council of Finland.

REFERENCES

1) D.W.G.S. Leith, Diffractive processes, Lecture notes for the 1974 SLAC Summer Institute in Particle Physics, SLAC preprint SLAC-PUB-1526 (1975).

2) S.V. Mukhin and V.A. Tsarev, Recent results on nucleon diffractive dissociation, Invited paper presented at the 1974 Meeting of the Division of Particles and Fields of the American Physical Society, Williamsburg, Virginia, Fermilab preprint FERMILAB-Conf-74/97-THY-Exp (1974).

3) Ya.I. Azimov, E.M. Levin, M.G. Ryskin and V.A. Khoze, What is interesting about the region of small momentum transfers at high energies?, Proc. 9th Winter School of the Leningrad Nuclear Physics Institute on Nuclear and Elementary Particle Physics, Leningrad, 1974 (Akademiya Nauk SSSR, Leningrad, 1974), p. 5; English translation: CERN Trans. 74-8 (1974).

4) G. Goggi, Single and double diffraction dissociation at FNAL and ISR energies, Invited review talk presented at 10e Rencontre de Moriond, Méribel-lès-Allues, 1975; Pavia University preprint IFNUP/AE 02/75 (1975).

5) B.R. Webber, Progress in understanding the origin of the small Pomeron slope, Invited talk at this Conference.

6) N. Sakai, Building up Reggeons and the Pomeron from duality and unitarity, Invited talk at this Conference.

7) A. Schwimmer, Theoretical understanding of high-energy hadronic collisions with low-p_T final states, Rapporteur's talk at this Conference.

8) For an excellent review see: F. Zachariasen, Physics Reports 2C, 1 (1971).

9) An elementary introduction to the s-channel approach is given in: E.H. de Groot and H.I. Miettinen, Shadow approach to diffraction scattering, Proc. 8e Rencontre de Moriond, Méribel-lès-Allues, 1973 (ed. J. Tran Thanh Van)(CNRS, Orsay, 1973), Vol. II, p. 193.

10) H.I. Miettinen, Impact structure of diffraction scattering, Proc. 9e Rencontre de Moriond, Méribel-lès-Allues, 1974 (ed. J. Tran Thanh Van)(CNRS, Orsay, 1974), Vol. I.

11) A. Białas and N. Sakai, Phys. Letters 55B, 81 (1975).

12) R. Baier, Short-range correlations and cluster production, Invited talk at this Conference.

13) N. McCubbin, Correlations in multi-particle final states, Rapporteur's talk at this Conference.

14) G. Ranft et al., Leipzig-Dubna Collaboration, Preprint KMU-HEP 7410 (1974).
C.M. Bromberg et al., Phys. Rev. D 9, 1864 (1974); Rochester-Michigan preprint UR-485, COO-3065-82 (1974).
T. Ferbel, Contribution to the 5th Internat. Symposium on Many Particle Hadrodynamics, Leipzig-Eisenach, 1974; Rochester preprint UR-500/COO-3065-91 (1974).
K. Eggert et al., Angular correlations between the charged particles produced in pp collisions at ISR energies, CERN preprint (1974).

15) P.D.B. Collins, F.D. Gault and A. Martin, Nuclear Phys. B80, 135 (1974).

16) P. Grassberger, C. Michael and H.I. Miettinen, Phys. Letters 52B, 60 (1974).
P. Grassberger and H.I. Miettinen, Nuclear Phys. B92, 309 (1975).
A. Krzywicki and D. Weingarten, Phys. Letters 50B, 265 (1974).
D. Weingarten, Phys. Rev. D 11, 1924 (1975).
A. Krzywicki, Nuclear Phys. B86, 296 (1975).

17) T.T. Chou and C.N. Yang, *in* High energy physics and nuclear structure (ed. G. Alexander) (North-Holland Publishing Co., Amsterdam, 1967), p. 348.
L. Durand III and R. Lipes, Phys. Rev. Letters 20, 637 (1968).
T.T. Chou and C.N. Yang, Phys. Rev. 170, 1591 (1968); Phys. Rev. Letters 20, 1213 (1968).

18) J. Biel et al., Fermilab-Northwestern-Rochester-SLAC Collaboration, Diffraction dissociation of neutrons in np collisions at Fermilab energies, Paper No. G3-14 submitted to this Conference, and Decay properties of $p\pi^-$ systems produced in neutron dissociation at Fermilab energies, Paper No. L-04 submitted to this Conference.
T. Ferbel, Studies of neutron dissociation at Fermilab energies, Invited talk at this Conference.

19) R. Webb et al., Aachen-UCLA-Riverside-CERN Collaboration, Phys. Letters 55B, 331 (1975). Figure 7 of the present review is taken from the preprint version of this paper (CERN preprint, 1974).

20) E. Nagy et al., CERN-Hamburg-Orsay-Vienna Collaboration, Experimental results on inelastic diffraction scattering in proton-proton collisions at the ISR, Contributed paper to the 17th Internat. Conf. on High Energy Physics, London, 1974.

21) CERN-Hamburg-Orsay-Vienna Collaboration, private communication.

22) A. Wetherell, Elastic and total cross-sections and implications, Rapporteur's talk at this Conference.

23) B.Y. Oh and W.D. Walker, Phys. Letters 28B, 564 (1969).
H. Satz, Phys. Letters 32B, 380 (1970).
S. Pokorski and H. Satz, Nuclear Phys. B19, 113 (1970).
L. Caneschi, Nuovo Cimento Letters 2, 122 (1969).

24) H.I. Miettinen and P. Pirilä, Phys. Letters 40B, 127 (1972).
See also: Athens-CERN-Demokritos-Liverpool-Vienna Collaboration, A study of $dN/dt_{pp}dm_{K^*\pi}$ distributions in the reactions $K^-p \to \bar{K}^{*0}(890)\pi^-p$ and $K^+p \to K^{*0}(890)\pi^+p$ at $p_{lab} = 8.25$ GeV/c, Paper No. G2-21 submitted to this Conference.

25) A. Martin, Nuclear Phys. B77, 226 (1974).

26) V. Barger, J. Luthe and R.J.N. Phillips, Tests of geometrical scaling and generalizations, University of Wisconsin preprint (1975).

27) P. Kobe et al., Bonn-Hamburg-Munich Collaboration, Nuclear Phys. B52, 109 (1973).

28) E. Dahl-Jensen et al., Scandinavian Bubble Chamber Collaboration, Exchange mechanisms and energy dependence of isospin amplitudes for the reaction $pN \to NN\pi$ in the energy range 5-1480 GeV, Stockholm University preprint (1974), and references given therein.

29) P. Bosetti et al., Aachen-Berlin-Bonn-CERN-Heidelberg-London-Vienna Collaboration, A comparison of $\pi\pi\pi$, $\bar{K}\pi\pi$, $\pi K\bar{K}$, $\bar{K}K\bar{K}$ systems produced in the reactions meson + p → → 3 mesons + p, Paper No. G3-30 submitted to this Conference; also CERN preprint CERN/D.Ph.II/PHYS 75-28 (1975).

30) R. Carlitz, M.B. Green and A. Zee, Phys. Rev. Letters 26, 1515 (1971) and Phys. Rev. D 4, 3439 (1971).

31) T. Inami, Tensor dominated Pomeron, Invited talk at this Conference.

32) J. Pumplin and G.L. Kane, Does the Pomeron have vacuum quantum numbers?, University of Michigan preprint (1975).

33) Yu.M. Antipov et al., CERN-IHEP Collaboration, Nuclear Phys. B63, 153 (1973).

34) G. Otter et al., Aachen-Berlin-Bonn-CERN-Heidelberg Collaboration, Nuclear Phys. B80, 1 (1974).

35) P. Dennery and A. Krzywicki, Phys. Rev. 136, 3839 (1964).

36) M.G. Bowler, M.A.V. Game, I.J.R. Aitchison and J.B. Dainton, Diffraction dissociation, the Deck mechanism and diffractive resonance production, to be published in Nuclear Phys. B.

37) S.D. Drell and K. Hiida, Phys. Rev. Letters 7, 199 (1961).
R.T. Deck, Phys. Rev. Letters 13, 199 (1964).
M. Ross and Y.Y. Yam, Phys. Rev. Letters 19, 546 (1967).

38) E.L. Berger, A critique of the Reggeized Deck model, Argonne preprint ANL-HEP-PR-75-06 (1975).

39) P. Schmid, New results on meson diffraction dissociation, Invited talk at this Conference.

40) H.M. Chan, H.I. Miettinen and R.G. Roberts, Nuclear Phys. B54, 411 (1973).

41) R.G. Roberts, Proc. 14th Scottish Universities Summer School in Physics, Middleton Hall, 1973 (eds. R.L. Crawford and R. Jennings), p. 201, and references given therein.

42) G. Ascoli et al., Phys. Rev. Letters 25, 962 (1971) and 26, 929 (1971); Phys. Rev. D 7, 669 (1973).

43) J.D. Hansen, G.T. Jones, G. Otter and G. Rudolph, Nuclear Phys. B81, 403 (1974).

44) B.R. French, Mesons - 1975, Rapporteur's talk at this Conference.

45) G. Otter et al., Aachen-Berlin-CERN-London-Vienna Collaboration, Evidence for different polarization properties of the ρK and K*(890)π states of the 1^+ wave in the Q region, Paper No. G3-34 submitted to this Conference; also CERN preprint CERN/D.Ph.II/PHYS 75-6 (1975).

46) Amsterdam-CERN-Nijmegen-Oxford Collaboration, Analysis of the $(\bar{K}\pi\pi)^0$ system produced in the reaction $K^-p \to (\bar{K}\pi\pi)$ at 4.2 GeV/c, Paper No. F1-15 submitted to this Conference; also CERN preprint CERN/D.Ph.II/PHYS 75-24 (1975).

47) D. Burland et al., Mons-Paris-Saclay-Brussels Collaboration, Study of the reaction $K^+d \to K^+\pi^+\pi^-d$ at 8.25 GeV/c, Paper No. F1-19 submitted to this Conference.

48) S.N. Tovey et al., Rutherford-Ecole Polytechnique-Saclay Collaboration, Partial wave analysis of the Q region in the reactions $K^-p \to K^-\pi^+\pi^-p$ and $K^-p \to \bar{K}^0\pi^-\pi^0p$ at 14.3 GeV/c, Paper No. F1-27 submitted to this Conference.

49) G. Otter et al., Aachen-Berlin-CERN-London-Vienna Collaboration, Partial wave analysis of the $(\bar{K}^0\pi^-\pi^0)$-system produced in the Q-mass region in $K^-p \to (\bar{K}^0\pi^-\pi^0)p$ at 10 and 16 GeV/c, Paper No. F1-28 submitted to this Conference; also CERN preprint CERN/D.Ph.II/PHYS 75-14 (1975).

50) G. Otter et al., Aachen-Berlin-CERN-London-Vienna Collaboration, Nuclear Phys. B89, 201 (1975).

51) G. Otter et al., Aachen-Berlin-Bonn-CERN-Heidelberg Collaboration, Investigation of the low mass $(\pi K\bar{K})$-system in the reactions $\pi^\pm p \to (\pi^\pm K^+K^-)p$ at 16 GeV/c, Paper No. G3-33 submitted to this Conference.

52) A. Eskreys, Exclusive experiments -- recent results, Rapporteur's talk at the 6th Internat. Colloquium on Multiparticle Reactions, Oxford, 1975, to be published in the Proceedings.

53) K. Kölbig and B. Margolis, Nuclear Phys. B6, 85 (1968).

54) C. Bemporad et al., Nuclear Phys. B33, 397 (1971) and B42, 627 (1972).
P. Mühlemann et al., Nuclear Phys. B59, 106 (1973).
R.M. Edelstein et al., Carnegie-Mellon-Northwestern-Rochester Collaboration, Measurement of the coherent dissociation reaction $p + A \to p\pi^+\pi^- + A$ at 15 and 23 GeV/c, Paper No. 710 submitted to the 17th Internat. Conf. on High Energy Physics, London, 1974.
W.C. Carithers et al., Rochester-BNL Collaboration, Diffractive production of $p\pi^-$ systems on nuclei and determination of the unstable $p\pi^-$ nucleon total cross-section, Paper No. 454 submitted to the 17th Internat. Conf. on High Energy Physics, London, 1974.

55) W. Beusch et al., CERN-ETH Zürich-Imperial College London-Milano Collaboration, Phys. Letters 55B, 97 (1975).

56) For a review see: G. Otter, Proc. 12th Cracow School of Theoretical Physics, 1972, Acta Phys. Polon. B3, 809 (1973). For references to recent work see Refs. 1 and 2.

57) G. Otter et al., Aachen-Berlin-Bonn-CERN-Heidelberg-London-Vienna Collaboration, Nuclear Phys. B87, 189 (1975).

58) Similar ideas have often been applied to particle-particle scattering. For a pedagogical discussion see: H. Harari, Ann. Phys. 63, 432 (1971).

59) V. Blobel et al., Bonn-Hamburg-Munich Collaboration, Partial wave analysis of the low mass $(\pi^+\pi^-p)$ system produced in the reaction $pp \to p(\pi^+\pi^-p)$ at 12 and 24 GeV/c, Paper No. L-23 submitted to this Conference; also Max Planck Institute preprint MPI PAE Exp El 49 (1975).

60) A. Kotanski, Partial wave analysis of the three-particle proton dissociation, Jagellonian University preprint TPJU 20/74 (1974), to be published in Acta. Phys. Polon. B.

61) V. Blobel et al., Bonn-Hamburg-Munich Collaboration, Nuclear Phys. B69, 454 (1974), and references given therein.

62) K. Boesebeck et al., Aachen-Berlin-Bonn-CERN-Heidelberg-London-Vienna Collaboration, Nuclear Phys. B33, 445 (1971).

63) Particle Data Group, Review of particle properties, Phys. Letters 50B, 1 (1974).

64) A.H. Rosenfeld, D.J. Herndon, R. Longacre, L.R. Miller, G. Smadja, P. Söding, R.J. Cashmore, D.W.G.S. Leith, G.P. Gopal, R.A. Stevens, V. Taylor and A. White, Phys. Letters 55B, 486 (1975).
P.J. Litchfield, Proc. 17th Internat. Conf. on High Energy Physics, London, 1974 (Science Research Council, Didcot, 1974), p. II-65.

65) See Ref. 34 and references given therein.

66) E.L. Berger, Systematics of cross-over effects in inelastic diffraction, Paper No. G3-29 submitted to this Conference; also Argonne preprint ANL/HEP 7464 (1974).

67) H. Satz and K. Schilling, Nuovo Cimento Letters 1, 351 (1971).

68) Aachen-Berlin-Bonn-CERN-Heidelberg Collaboration, Study of the cross-over effect in $\pi^\pm p \to \pi^\pm(\pi^-\Delta^{++})$ at 16 GeV/c, Paper No. L-21 submitted to this Conference.

69) G.L. Kane, Proc. 12th Cracow School of Theoretical Physics, 1972, Acta Phys. Polon. B3, 845 (1973).

70) S. Humble, Nuclear Phys. B76, 137 (1974) and B86, 285 (1975).

71) See Ref. 28 and Fig. 10 of Ref. 10.

72) These data are discussed in Ref. 111. I thank Dr. G. Goggi for providing me with Fig. 26.

73) J. Pumplin, Phys. Rev. D 8, 2899 (1973).

74) R. Blankenbecler, Phys. Rev. Letters 31, 964 (1973).
R. Blankenbecler, J.R. Fulco and R.L. Sugar, Phys. Rev. D 9, 736 (1974).

75) J.A.J. Skard and J.R. Fulco, Phys. Rev. D 8, 312 (1973).
H.M. Fried and K.S. Soh, Phys. Rev. D 10, 636 (1974).
S.J. Chang and T.M. Yan, Phys. Rev. D 10, 1531 (1974).
See also: J.G. Schaffner, P.J. Camillo, P.M. Fishbane and J.S. Trefil, to be published in ~~Phys~~. Rev. D, and references therein.

76) M.L. Good and W.D. Walker, Phys. Rev. 120, 1857 (1960).
E.L. Feinberg and I.Ia. Pomeranchuk, Suppl. Nuovo Cimento III, 652 (1956).

77) K. Fiałkowski and H.I. Miettinen, Semi-transparent hadrons from multi-channel absorption effects, CERN preprint TH.2057 (1975), to be published; Absorption effects in elastic and inelastic diffraction, Invited talk at the 6th Internat. Colloquium on Multiparticle Reactions, Oxford, 1975. CERN preprint TH.2062 (1975), to be published.

78) L. Caneschi, P. Grassberger, H.I. Miettinen and F. Henyey, Phys. Letters 56B, 359 (1975).

79) P. Pirilä, P.V. Ruuskanen and H.I. Miettinen, in preparation. Some preliminary results of this analysis are given in Ref. 10.

80) G. Cohen-Tannoudji and U. Maor, Phys. Letters 57B, 253 (1975).
U. Maor, Comments on the systematics of Pomeron exchange reactions, Invited talk at the 10e Rencontre de Moriond, Méribel-lès-Allues, 1975. Saclay preprint (1975).

81) H.I. Miettinen, Geometrical description of hadronic collisions, Invited talk at the 5th Internat. Symposium on Many Particle Hadrodynamics, Leipzig-Eisenach, 1974 (Karl-Marx Universität, Leipzig, 1974); CERN preprint TH.1906 (1974), to be published in Acta Phys. Polon.

82) H. Böggild, B.G. Duff, A. Duane, M. Gibson, K. Guettler, S. Henning, G. Jarlskog, R. Little, O. Leistam, H. Newman, H. Ogren, M. Prentice, T. Sanford, S. Sharrock and S.L. Wu, Inclusive particle production at large angles and small transverse momenta, measured at the CERN ISR, Paper No. L-03 submitted to this Conference.

83) D.R. Snider and H.W. Wyld, Jr., Phys. Rev. D11, 2538 (1975).

84) P.J. Crozier and B.R. Webber, Eikonal model studies of multiparticle production, Paper No. G4-48 submitted to this Conference.

85) P.J. Crozier and B.R. Webber, Eikonal model studies of elastic scattering and diffractive dissociation, Paper No. G3-25 submitted to this Conference.

86) See Ref. 17. For recent applications of the Chou-Yang model to proton-proton scattering, see: B. Carreras and J.N.J. White, Nuclear Phys. B32, 319 (1971) and B42, 95 (1972).
J.N.J. White, Nuclear Phys. B51, 23 (1973).
M. Kac, Nuclear Phys. B62, 402 (1974).

87) G. Miller et al., Phys. Rev. D 5, 528 (1972).

88) V.A. Tsarev, Phys. Rev. D 11, 1864 and 1875 (1975).

89) I.V. Andrejev, Lebedev Institute preprint N 59 (1975), to be published in Yadernaya Fizika. I thank Prof. E.L. Feinberg for bringing Dr. Andrejev's work to my attention.

90) E.L. Berger and A.C. Irving, Absorptive corrections to the pion exchange Deck amplitude, Argonne preprint ANL-HEP-PR-75-19 (1975).

91) E.L. Berger and P. Pirilä, Absorptive effects in exclusive diffraction dissociation, Argonne preprint ANL-HEP-PR-75-27 (1975).

92) J. Pumplin and G.L. Kane, Phys. Rev. Letters 32, 963 (1974).
See also: A. Schwimmer and F. Zachariasen, The radius of the Pomeron and absorptive cuts, Paper No. G3-09 submitted to this Conference; also Caltech preprint CALT 68-490 (1975).

93) M. Derrick, Proc. 17th Internat. Conf. on High Energy Physics, London, 1974 (Science Research Council, Didcot, 1974), p. I-3.

94) F.K. Loebinger, Proc. 17th Internat. Conf. on High Energy Physics, London, 1974 (Science Research Council, Didcot, 1974), p. I-71.

95) D.P. Roy, Proc. 17th Internat. Conf. on High Energy Physics, London, 1974 (Science Research Council, Didcot, 1974), p. I-80.

96) K. Goulianos, High energy pd → Xd and pp → Xp diffraction dissociation, Invited talk at this Conference.

97) C.E. DeTar, C.E. Jones, F.W. Low, Chung-I Tan, J.M. Weis and J.E. Young, Phys. Rev. Letters 26, 675 (1971).
For phenomenological applications of the triple-Regge theory, see: Refs. 40, 96, 103, 104 and references given therein.

98) Y. Akimov et al., Fermilab-Dubna-Rockefeller-Rochester Collaboration, Diffraction dissociation of high energy protons in p-d interactions, Paper No. G3-06 submitted to this Conference; also Fermilab preprint FERMILAB PUB 75/2-EXP (1975); Excitation of high energy protons into low-mass states in p-d interactions, Paper No. G3-49 submitted to this Conference; also Fermilab preprint FERMILAB PUB 75/26-EXP (1975).

99) V. Bartenev et al., Moscow-Fermilab-Rochester-Rockefeller Collaboration, Phys. Letters 51B, 299 (1974).
K. Abe et al., Rutgers-Imperial College-Illinois Collaboration, Phys. Rev. Letters 31, 1527 (1973).

100) M.G. Albrow et al., CERN-Holland-Lancaster-Manchester Collaboration, Nuclear Phys. B72, 376 (1974).

101) S. Childress et al., Columbia-Stony Brook Collaboration, Phys. Rev. Letters 32, 389 (1974).
R.D. Schamberger, Jr., et al., Columbia-Stony Brook Collaboration, Phys. Rev. Letters 34, 1121 (1975).

102) S.J. Barish et al., ANL-NAL Collaboration, Phys. Rev. Letters 31, 1080 (1973).

103) R.D. Field and G.C. Fox, Nuclear Phys. B80, 367 (1974).

104) D.P. Roy and R.G. Roberts, Nuclear Phys. B77, 240 (1974).

105) R.G. Roberts, unpublished calculations.

106) For a compilation of data and references see Ref. 77.

107) For discussions and references see: J. Whitmore, Phys. Reports 10 C, 273 (1974).

108) J.P. DeBrion et al., Michigan-Rochester Collaboration, Phys. Letters 52B, 477 (1974).

109) A. Morel and B. Petersson, Nuclear Phys. B91, 109 (1975) and references given therein.
See also: R.J. Yaes, Bootstrap model with a bare Pomeron, Paper No. G3-44 submitted to this Conference and references given therein.

110) R. Webb et al., Aachen-UCLA-Riverside-CERN Collaboration, Phys. Letters 55B, 336 (1975).
L. Baksay et al., Aachen-UCLA-Riverside-CERN Collaboration, Phys. Letters 55B, 491 (1975).

111) M. Cavalli-Sforza et al., Pavia-Princeton Collaboration, Energy dependence of the exclusive reaction $pp \to (p\pi^+\pi^-)(p\pi^+\pi^-)$ in the range 23 GeV $\leq \sqrt{s} \leq$ 53 GeV studied with the Split Field Magnet detector at the CERN ISR, Paper No. G3-19 submitted to this Conference; Mass spectra in the exclusive reaction $pp \to (p\pi^+\pi^-)(p\pi^+\pi^-)$ studied in the range 23 GeV $\leq \sqrt{s} \leq$ 53 GeV with the Split Field Magnet detector at the CERN ISR, Paper No. G3-20 submitted to this Conference; t-dependence of the double diffraction dissociation $pp \to (p\pi^+\pi^-)(p\pi^+\pi^-)$ at ISR energies and test of cross-section factorization, Paper No. G3-21 submitted to this Conference.

112) M. Derrick, B. Musgrave, P. Schreiner and H. Yuta, Phys. Rev. Letters 32, 1880 (1975).

113) G.C. Mantovani, Double diffraction dissociation at ISR energies, Invited talk at this Conference.

114) D. Denegri et al., Saclay-Ecole Polytechnique-Rutherford Collaboration, Double dissociation in the reaction $K^-p \to K^-\pi^+\pi^-n\pi^+$ at 14.3 GeV/c and Pomeron factorization, Paper No. G3-22 submitted to this Conference.

115) J.G. Rushbrooke and B.R. Webber, Proc. 3rd Internat. Colloquium on Multiparticle Reactions, Zakopane, 1972 (Inst. Nuclear Research, Warsaw, 1972. Report No. NR 1421/VI/PH), p. 441; Cambridge University preprint HEP 74/11 (1974).
R. Shankar, Nuclear Phys. B70, 168 (1974).
D.M. Chew, Nuclear Phys. B82, 422 (1974).
U. Idschok et al., Bonn-Hamburg-Munich Collaboration, Nuclear Phys. B53, 282 (1973).
M. Derrick, B. Musgrave, P. Schreiner and H. Yuta, Phys. Rev. Letters 32, 80 (1974).
D.M. Chew et al., LBL-NAL Collaboration, Search for Pomeron-Pomeron-2π events in 205 GeV/c π^-p interactions, Berkeley preprint LBL-2106 (1973).
P. Grassberger, Double Pomeranchon exchange, Notes of the 11th ISR Discussion Meeting between Experimentalists and Theorists (unpublished).
D. Denegri et al., France-Soviet Union Collaboration, Double Pomeron exchange and diffractive dissociation in the reaction $pp \to pp\pi^+\pi^-$ at 69 GeV/c, CERN preprint DPh PE 75-04, M17 (1975).

116) D.M. Chew and G.F. Chew, Phys. Letters 53B, 191 (1974).

117) D.P. Roy and R.G. Roberts, Proc. 5th Internat. Symposium on Many Particle Hadrodynamics, Leipzig-Eisenach, 1974 (Karl-Marx-Universität, Leipzig, 1974), p. 887.
R.G. Roberts, private communication.

118) L. Baksay et al., Aachen-Riverside-CERN-Genoa-Munich Collaboration, A search for double Pomeron exchange interactions at the CERN-ISR, Paper No. G3-03 submitted to this Conference.

119) J. Layter, A search for double Pomeron exchange interactions at the CERN ISR, Invited talk at this Conference.